UNIVERSITAT DE BARCELONA

Modulating Immune Cell Fate and Inflammation through CRISPR-mediated DNA Methylation Editing

Gemma Valcárcel Ximenis

Universitat de Barcelona, Facultat de Medicina

Programa de Doctoral de Biomedicina

Modulating Immune Cell Fate and Inflammation through CRISPR-mediated DNA Methylation Editing

Gemma Valcárcel Ximenis

Supervisor de la tesi:

Dr. José Luis Sardina Ortega

Tutor de la tesi:

Dr. Joan Gil Santano

Insitut de Recerca Contra la Leucèmia Josep Carreras

TABLE OF CONTENT

TABLE OF CONTENT **1**

LIST OF ABBREVIATIONS **5**

ABSTRACT **9**

INTRODUCTION **13**

1. CELL FATE DECISIONS IN THE IMMUNE SYSTEM **14**

1.1 Hematopoietic system 14
1.2. Lineage-determining transcription factors 15
1.2.1 Experimentally induced cell fate conversion 16
1.3 Role of myeloid cells in innate immunity 18
1.3.1 Origin and diversity of macrophages 19
1.3.2 Activation of macrophages during inflammation 20
1.3.3 In vitro polarization of human monocytes 21

2. INTERLEUKIN-1 (IL-1) PATHWAY AND ITS ROLE IN INFLAMMATION **22**

2.1 Receptor agonists: IL-1β 23
2.2 Endogenous IL-1 inhibitors: IL-1 receptor antagonist 23
2.3 Dysregulation of the IL-1 pathway 25
2.3.1 Myeloid malignancies 25
2.3.2 Autoinflammatory syndromes 26
2.3.2.1 CAPS: Cryopyrin-associated periodic syndromes 26
2.3.2.2 DIRA: genetic IL1RN deficiency 27

3. EPIGENETIC REGULATION OF GENE EXPRESSION **28**

3.1 Histone post-translational modifications (PTMs) 28
3.1.2 PTMs impact on transcription regulation 29
3.2 DNA methylation 30
3.2.1 The writers and erasers 31
3.2.2 Genomic distribution of epigenetic marks in the context of gene regulation 32
3.2.3 Biological mechanisms of DNAm during early development 35
3.2.4 DNMT and TET activities during development 36
3.2.4.1 DNMT and TET activities during myeloid differentiation 38
3.2.5. DNA methylation in disease 39

4. EPIGENOME MANIPULATION **40**

4.1 Non-specific methods: epidrugs 41
4.2 Targeted methods 42

4.2.1 Genome engineering: ZFN, TALENS 42
4.2.2 CRISPR/Cas9: discovery and applications 43
4.2.3 CRISPR-MEDIATED EPIGENOME-EDITING 45
4.2.3.1 Targeted transcriptional regulation 46
4.2.3.2. Multiplex epigenome editing 48
4.2.3.3 Targeted histone modification 49
4.2.3.4 DNA methylation editing 50
4.2.3.4.1 DNAm editing on gene regulation 51
4.2.3.4.2 DNAm editing in the hematopoietic system 53
4.2.3.4.3 DNAm editing therapies 55
4.2.3.5 Recent advances in clinical applications 57

OBJECTIVES 61

MATERIALS AND METHODS 65

RESULTS 83

CHAPTER 1: GENOME-WIDE CORRELATION STUDIES BETWEEN DNA METHYLATION AND TRANSCRIPTION DURING HUMAN MYELOID COMMITMENT 84
1. Whole-genome Bisulfite Sequencing reveals DNA methylation reshaping during human B-cell to macrophage TD 84
2. Interplay between DNA demethylation and chromatin accessibility at GREs during transdifferentiation. 87
3. Macrophage gene regulatory regions lose methylation during transdifferentiation 89
4. Integrative analyses reveal the IL1RN promoter as a top event showing a DNA methylation-expression correlation 92
CHAPTER 2: EMPLOYING DCAS9-METHYLATION EDITING TOOLS TO MODIFY THE DNA METHYLATION STATUS OF THE IL1RN PROMOTER 94
1. dCas9-TET1-mediated demethylation of the IL1RN promoter is sufficient for its gene reactivation 94
2. dCas9-DNMT3A binding specificity during TD 98
3. dCas9-DNMT3A specifically hypermethylates the IL1RN promoter, leading to its downregulation. 100
CHAPTER 3: DCAS9-DNMT3A-MEDIATED HYPERMETHYLATION OF THE IL1RN PROMOTER LEADS TO IMPAIRED HUMAN MYELOID CELL FATE ACQUISITION 102
1. IL1RN epigenome editing alters transcriptional dynamics and phagocytic capacity during transdifferentiation 102
2. shRNAs-mediated validation of IL1RN involvement in myeloid cell fate acquisition and phagocytic activity. 107
3. C/EBPα binds to GREs of IL1 pathway genes during the acquisition of the myeloid cell fate. 109

CHAPTER 4. IL1RN DNAm EDITING AFFECTS NFKB AND IFN EARLY TRANSCRIPTION UPON IL-1B TREATMENT 112
1. dCas9-DNMT3A IL1RN DNAm editing sensitizes iMacs to IL-1β treatment .. 112
2. IL1RN DNAm editing leads to enhanced p65/NF-kB and diminished interferon pathway activation upon IL1β treatment 113
3. IL1RN-editing leads to altered transcriptional kinetics in response to IL-1β treatment 115
4. Single-cell RNA-seq analyses identified an ISG-monocyte signature in the IL1RN-downregulated genes 118
CHAPTER 5. IL1RN PROMOTER DNAm ALTERS THE MACROPHAGE CAPACITY TO SUPPORT CANCER GROWTH 120

DISCUSSION 124

CHAPTER 1: GENOME-WIDE CORRELATION STUDIES BETWEEN DNAm AND TRANSCRIPTION DURING HUMAN MYELOID COMMITMENT 125
1. WGBS-seq reveals a DNAm reshaping during transdifferentiation 125
2. Interleukin 1 Receptor Antagonist (IL1RN) promoter as the top event showing DNA methylation-expression correlation 129
CHAPTER 2: EMPLOYING DCAS9-METHYLATION EDITING TOOLS TO MODIFY THE DNA METHYLATION STATUS OF THE IL1RN PROMOTER 131
1. dCas9-TET1-mediated demethylation of the IL1RN promoter is sufficient for altering B cell fate 131
2. Validation of dCas9-DNMT3A editing specificity at IL1RN promoter 133
CHAPTER 3: DCAS9-DNMT3A-MEDIATED HYPERMETHYLATION OF THE IL1RN PROMOTER LEADS TO IMPAIRED HUMAN MYELOID CELL FATE ACQUISITION 135
1. IL1RN epigenome editing alters transcriptional dynamics and phagocytic capacity during transdifferentiation 135
2. C/EBPα binds IL-1-pathway GREs during physiological myeloid cell fate 137
CHAPTER 4. IL1RN DNAm EDITING INCREASES THE RESPONSIVENESS OF IMACS TO IL-1B TREATMENT 138
CHAPTER 5. IL1RN PROMOTER DNAm ALTERS THE MACROPHAGE CAPACITY TO SUPPORT CANCER GROWTH 140
How do we apply IL1RN DNAm editing to in vivo therapeutic applications? 142

CONCLUSIONS 145

APPENDIX 149

REFERENCES 156

LIST OF ABBREVIATIONS

5hmC: 5-hydroxymethylcytosine

5mC: 5-methylcytosine

AAV: adeno-associated viruses

AML: acute myeloid leukemia

AP-1: protein activator 1

ATAC: Assay for Transposase-Accessible Chromatin

B-ALL: B-cell acute lymphoblastic leukemia

BM: bone marrow

bp: base pair

BP: biological process

C/EBPα: CCAAT/enhancer-binding protein-α

CAPS: cryopyrin associated periodic syndromes

CFSE: Carboxyfluorescein Succinimidyl Ester

CGI: CpG islands

ChIP-seq: Chromatin immunoprecipitation sequencing

ChrX: chromosome X

CLP: common lymphoid progenitor

CMP: common myeloid progenitor

CpG: CpG site

CRISPR: clustered regularly interspaced short palindromic repeats

CRISPRa: clustered regularly interspaced short palindromic repeats activation

CRISPRi: clustered regularly interspaced short palindromic repeats interference

CTCF: CCCTC-binding factor

CTRL: control

DC: dendritic cells

dCas9: catalytically dead Cas9

DEG: differential expressed genes

DIRA: Deficiency of the Interleukin-1-Receptor Antagonist

DMR: differential methylated region

DNAm: DNA methylation

DNMT: DNA methyltransferase

DNMT3A: DNA methyltransferase 3A

DoRothEA: Discriminant Regulon Expression Analysis

E2: β-estradiol

ESCs: embryonic stem cells

ETR: engineered transcriptional repressors

EZH2: Enhancer of zeste homolog 2

FACS: fluorescence-activated cell sorting

FDA: Food and Drug Administration

FDR: false discovery rate

FMF: familial Mediterranean fever

FXS: fragile X syndrome

GM-CSF: granulocyte macrophage-colony stimulating factor

GMP: granulocyte-monocyte progenitor

GO: gene ontology

GP: granulocyte progenitors

GRE: gene regulatory element

gRNA: guide RNA

GSEA: Gene Set Enrichment Analysis

HAT: histone acetylases

HDAC: histone deacetylases

HDACi: Histone deacetylase inhibitors

HMA: hypomethylating agents

HMT: histone methyltransferases

HSC: hematopoietic stem cells

ICR: imprinting control regions

IFN: interferon

IL-1: interleukin-1

IL-1R: Interleukin-1 receptor

IL1RN: IL-1 receptor antagonist

IL-1α: Interleukin-1 alpha

IL-1β: Interleukin-1 beta

iMac: induce macrophage

iPSC: induced pluripotent stem cells

IRAK: interleukin-1 receptor-associated kinase 1

ISG: interferon stimulated genes

Kb: kilobase

KRAB: krüppel-associated box

LNP: lipid nanoparticles

LPS: lipopolysaccharide

Mac: macrophage

M-CSF: macrophage colony-stimulating factor

MEP: megakaryocyte-erythrocyte progenitors

MFI: mean fluorescence intensity

MK: megakaryocytes

MoMac: monocytes and macrophages

Mon: monocytes

MPP: multipotent progenitors

NF-kB: nuclear factor kappa-light-chain-enhancer of activated B cells

NG2: neuron-glial antigen-2

NK: natural killer

PAM: protospacer adjacent motif

PCA: principal component analysis

PDX: patient derived xenograft

PE: proximal enhancer

PRC2: polycomb repressive complex 2

PTM: post translational modifications

RNA-seq: RNA Sequencing

RNP: ribonucleoprotein

RT-qPCR: Reverse transcription polymerase chain reaction

RTT: Rett syndrome

SAM: synergistic activation mediators

scFv: single chain fragment variables

ScRNA-seq: single-cell RNA sequencing

ShRNA: small hairpin RNAs

SPN: supernatant

TALEN: transcription activator-like effector nucleases

TAM: tumor-associated macrophages

TD: transdifferentiation

TE: transposable element

TET: ten-eleven translocation

TF: transcription factor

TLR4: toll-like receptor 4

TSS: transcription start site

UMAP: uniform manifold approximation and projection

VP16: herpes simplex viral protein 16

VP64: tetramer of herpes simplex virus 16

WGBS-seq: whole-genome bisulfite sequencing

XCI: X chromosome inactivation

Xi: inactive X chromosom

ZFN: zinc finger nucleases

ABSTRACT

Immune cell differentiation and activation are associated with widespread DNA methylation changes; however, the causal relationship between these changes and their impact in shaping cell fate decisions still needs to be fully elucidated. Here, we conducted a genome-wide analysis to investigate the relationship between DNA methylation and gene expression at gene regulatory regions in human immune cells. By utilizing CRISPR/dCas9-TET1 and -DNMT3A epigenome editing tools, we successfully established a cause-and-effect relationship between the DNA methylation levels of the promoter of the Interleukin1-receptor antagonist (*IL1RN*) gene and its expression. Most importantly, we observed that modifying the DNA methylation status of the *IL1RN* promoter is sufficient to alter human myeloid cell fate and change the cellular response to inflammatory stimuli, resulting in pro-inflammatory cytokine release and a distinctive capacity to support cancer growth. Collectively, our findings demonstrate the potential of targeting specific DNA methylation events to directly modulate immune and inflammatory responses, providing a proof-of-principle for intervening in a broad range of inflammation-related diseases.

RESUMEN

La diferenciación y activación de las células inmunes se asocian con cambios en la metilación del ADN; sin embargo, la relación causal entre estos cambios y su impacto en las decisiones sobre la identidad celular aún se desconoce. En esta tesis, hemos realizado un análisis de todo el genoma para investigar la relación entre la metilación del ADN y la expresión génica en las regiones reguladoras de los genes en células inmunes. Para eso, hemos utilizado herramientas de edición epigenómica CRISPR/dCas9-TET1 y -DNMT3A, y hemos establecido una relación de causa y efecto entre los niveles de metilación del ADN del promotor del gen antagonista del receptor de interleucina 1 (IL1RN) y su expresión. Hemos observado que al modificar el estado de metilación del ADN del promotor de *IL1RN* es suficiente para alterar la identidad de las células mieloides humanas. Además, al cambiar la respuesta celular a los estímulos inflamatorios, promoviendo como resultado la liberación de citoquinas proinflamatorias y una capacidad distinta en la modulación del crecimiento del cáncer. En conclusión, nuestros hallazgos demuestran el potencial de modificar la metilación del ADN en zonas específicas del genoma para modular directamente la respuesta inmune e inflamatoria, proporcionando vías alternativas para el tratamiento de enfermedades relacionadas con la inflamación.

RESUM

La diferenciació i activació de les cèl·lules immunes s'associen amb canvis en la metilació de l'ADN; no obstant, la relació causal entre aquests canvis i el seu impacte en les decisions sobre la identitat cel·lular encara no se saben. En aquesta tesi, hem fet una anàlisi de tot el genoma per investigar la relació entre la metilació de l'ADN i l'expressió gènica a les regions reguladores dels gens en cél·lules immunes. Per això, hem utilitzat eines d'edició epigenòmica CRISPR/dCas9-TET1 i -DNMT3A, i hem establert una relació de causa i conseqüència entre els nivells de metilació de l'ADN del promotor del gen antagonista del receptor d'interleucina 1 (IL1RN) i la seva expressió. Hem observat que al modificar l'estat de metilació de l'ADN del promotor *d'IL1RN* és suficient per alterar la identitat de cèl·lules humanes mieloides. A més a més, hem canviat la resposta cel·lular als estímuls inflamatoris, promovent com a resultat l'alliberació de citocines proinflamatòries i una capacitat diferencial en la modulació del creixement del càncer. En conclusió, la nostra investigació demostra el potencial de modificar la metilació de l'ADN en zones específiques del genoma per modular directament la resposta immune i pro-inflamatòria, proporcionant vies alternatives pel tractament de malalties relacionades amb la inflamació.

INTRODUCTION

INTRODUCTION

1. Cell fate decisions in the immune system

1.1 Hematopoietic system

The human body is composed of multiple cell types, each of which has a specific function that contributes to the correct physiology, such as oxygen transport and immune defence. However, these differentiated cells lack self-renewal potential, have a limited lifespan, and need to be replaced to sustain the regular function of different tissues and organs. Therefore, the balance between differentiation and self-renewal needs to be highly regulated.

Hematopoietic stem cells (HSCs) are undifferentiated cells that maintain tissue homeostasis by originating stem cells or newly committed progenitors (Pinho and Frenette 2019). HSCs reside in the bone marrow (BM) and are characterized by their self-renewal capacity and ability to generate different mature blood cells in a tightly regulated manner.

In the classical model of hematopoiesis, the first step of lineage decision at the HSC level consists of the bifurcation in the lymphoid and myeloid fates. HSCs can differentiate into multipotent progenitors (MPPs). Secondly, common lymphoid progenitors (CLPs) with decreasing pluripotency, in turn, differentiate into lymphoid cells such as B and T lymphocytes or natural killers (NKs). Alternatively, HSCs can differentiate into common myeloid progenitors (CMPs), which further differentiate into the megakaryocyte-erythrocyte progenitors (MEPs) or the granulocyte-monocyte progenitor (GMPs) (Jacobsen and Nerlov 2019). MEPs will finally generate erythrocytes and megakaryocytes (MKs), which are the precursors of platelets. On the other branch,

myeloid cells come from GMPs that differentiate into monocytes, the precursors of macrophages, osteoclasts and dendritic cells (DC), and granulocyte progenitors (GPs), which differentiate into the different kinds of granulocytes: neutrophils, basophils, eosinophils and mast cells (**Figure 1**).

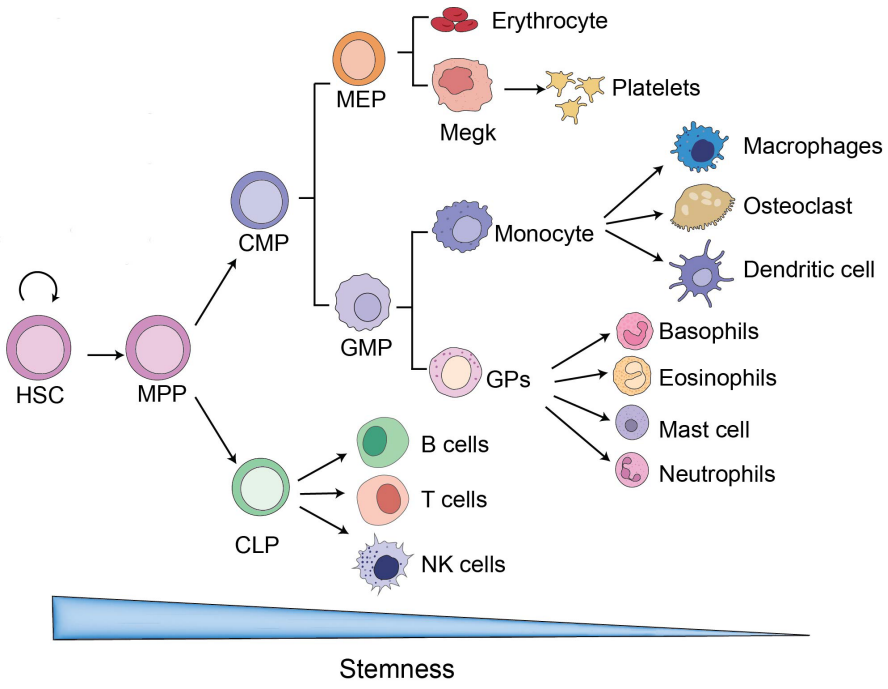

Figure 1. Hematopoietic differentiation. *Schematic representation of the hierarchical tree model of blood cells. Hematopoietic stem cells (HSCs) in the bone marrow divide and differentiate, generating other immature progenitor cells that will generate committed mature cells. The hematopoietic differentiation is concomitant with a loss of self-renewal capacity. Adapted from* (Rieger and Schroeder 2012) *(*(Jacobsen and Nerlov 2019).

1.2. Lineage-determining transcription factors

To maintain this balanced equilibrium, stem cells are influenced by intrinsic signals such as transcription factors (TFs) and the surrounding microenvironment. Therefore, much research has been

done to identify signalling molecules that can result in the activation of transcription factors (TFs) that will determine lineage identity (Robb 2007). For example, B-cell commitment is primarily directed by interactions between early B-cell factor 1 (EBF1), Pax5, and PU-1. On the other hand, transcription regulation in myeloid cells is mainly characterized by the expression of PU-1, C/EBPα, and RUNX1 (Dahl et al. 2003). Furthermore, TF's precise control relies on the expression level rather than an all-or-none response. For example, high PU-1 expression is required for myeloid lineage commitment, while low levels are required in the lymphoid lineage (Iwasaki et al. 2005).

1.2.1 Experimentally induced cell fate conversion

The classical model of cell differentiation was considered a "one-way street". One of the most comprehensive representations of this concept is the "epigenetic landscape" proposed by Conrad Waddington. In this metaphor, he describes a ball representing a stem cell rolling down a hill, with the final valley symbolizing the differentiated state (Waddington 2012).

Nonetheless, a new paradigm emerged when Davis, Weintraub and Lassar in 1986 showed that fibroblasts were able to switch lineages into contracting muscle cells through the forced expression of the MyoD TF (Davis et al. 1987). Multiple groups subsequently succeeded in switching the identity of differentiated cells after the ectopic expression of defined transcription factors by direct cell conversion without passing through a precursor state. These processes of experimentally induced cell fate conversion are known as transdifferentiation (TD) (**Figure 2**) (reviewed in (Graf 2011)). Several models of TD have been set

up in the hematopoietic system. For example, GATA-1 overexpression in myeloblasts induced the formation of erythroblasts, platelet precursors and eosinophils (Kulessa et al. 1995).

In 2004, Xie and co-workers demonstrated that the ectopic expression of CCAAT/enhancer-binding protein-α (C/EBPα) or C/EBPβ triggers the conversion of mouse pre-B lymphocytes into macrophages (Xie et al.). It is important to explain that C/EBPα in hematopoiesis is almost exclusively expressed in myeloid cells. Remarkably, *Cebpa* knockout causes the failure of hematopoietic progenitors to generate GMPs (Zhang et al. 2004).

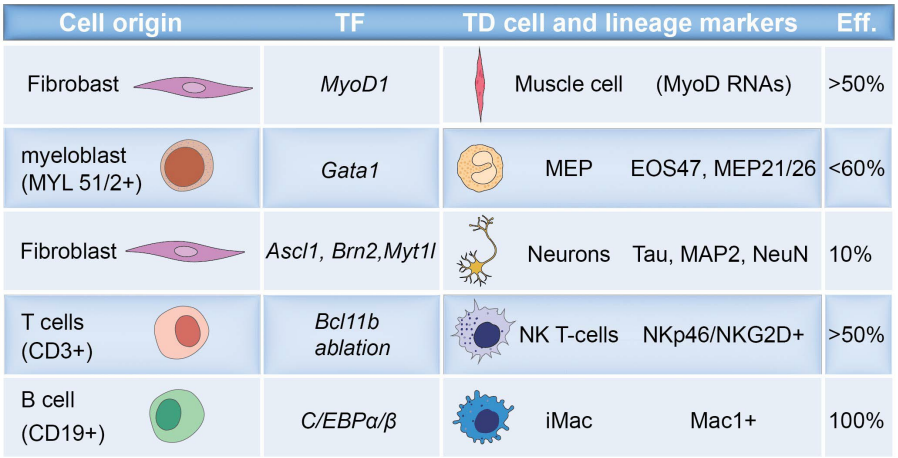

Figure 2. Examples of cell transdifferentiation (TD) induced by transcription factors (TF). *Protein markers for cell identity and efficiency (Eff.) of each cell conversion used in each study are indicated. Adapted from* (Davis et al. 1987) (Kulessa et al. 1995) (Li et al. 2007) (Xie et al.) (Graf 2011).

Inspired by this efficient system, Rapino and colleagues in the Graf's lab (Bussmann et al. 2009) developed a C/EBPα-induced transdifferentiation system from human leukemic B cells into macrophages. Of note, C/EBPα induction impaired cell tumorigenicity after transplantation into immunodeficient mice (Rapino et al. 2013).

Therefore, this unique cellular model can be used to study gene regulatory events that occur during the cellular switch and determine the drivers of the loss of tumorigenic capacity.

1.3 Role of myeloid cells in innate immunity

As mentioned before, the coordinated action of lineage-determining transcription factors (TF) allows the establishment of immune cells, which orchestrate the immune response. The immune system comprises cells, chemicals, and processes that function to protect the host from infectious agents, such as bacteria, fungi, or viruses. The recognition of these pathogens' signals leads to the activation of different types of immune cells that can be classified into two branches: innate and adaptive (Vivier and Malissen 2005; Chaplin 2010).

The first defence barrier against infections is coordinated by the innate immune system and is mediated by distinct types of myeloid cells (such as monocytes, macrophages and DCs) or lymphoid cells (NK). It acts as a rapid and non-specific response by recognizing general pathogen-associated molecular patterns (PAMPs). The second phase is mediated by the adaptive immune system, primarily by T and B lymphocytes. It is highly specific for antigens and triggers the activation and clonal expansion of lymphocytes that will fight against the pathogen (Marshall et al. 2018). As myeloid cells are the focus of this doctoral thesis, the next chapter will elaborate on these cells, particularly macrophages.

1.3.1 Origin and diversity of macrophages

Macrophages (Mac) are a heterogeneous population of mononuclear phagocytic cells ubiquitously expressed, essential for tissue homeostasis and host defence. For instance, during infection or tissue damage, circulating monocytes differentiate into macrophages, which, together with tissue-resident macrophages, participate in the inflammatory response (Gordon and Taylor 2005).

Tissue macrophages are derived from embryonic or adult HSCs in homeostatic conditions. During embryonic development, macrophage precursors arise from the fetal yolk sac or the fetal liver progenitors (**Figure 3**).

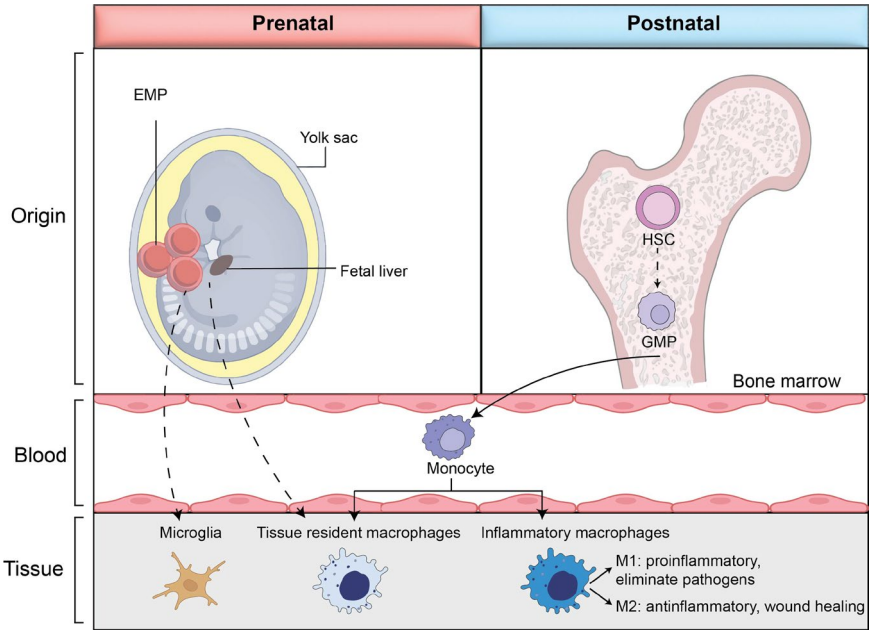

Figure 3. Ontogeny and differentiation of phagocytes. *Myeloid cells are derived from the yolk sac and fetal liver during the developing embryo (prenatal origin) or from the hematopoietic stem cells (HSCs) in the bone marrow during the postnatal stage and adulthood. In the yolk sac, erythro-myeloid progenitors (EMPs) give rise to macrophages and monocytes that can differentiate into tissue-resident macrophages. In the bone marrow, monocytes develop from a granulocyte-monocyte progenitor (GMP), which gives rise to monocytes in the blood. In homeostatic conditions, monocytes will*

differentiate into tissue-resident macrophages. However, in response to inflammation, monocytes are recruited from the blood to the tissue and differentiate into inflammatory macrophages that can polarize into specific phenotypes such as M1 or M2. Exceptions include microglial cells, which arise from the yolk sac-derived macrophages. Adapted from (Lawrence and Natoli 2011) (Ginhoux and Jung 2014).

For some tissues, such as microglia, these embryonic precursors will proliferate and give rise to tissue-resident adult macrophages that will never be replaced. Still, other tissues, such as cardiac or alveolar, can harbour both embryonic-derived macrophages and monocytes-derived ones. On the other hand, in tissues such as the intestine or skin, there is a high dependence on monocytes as a source for macrophages to maintain tissue homeostasis (Davis et al. 1987; Mosser et al. 2021).

1.3.2 Activation of macrophages during inflammation

Under inflammatory conditions, monocytes extravasate from the BM into the circulation and differentiate into functional phagocytic macrophages. In doing so, they can remove and recycle dead cells and tissue debris (Metchnikoff 1893). In macrophages, the pseudopod structures allow for the detection of surrounding microorganisms, forming a vesicle called a phagosome. Next, the phagosome fuses with the lysosome, where the microorganism is degraded.

Depending on environmental factors, these cells exhibit plasticity and change their phenotype. This biological process is known as macrophage polarization and has been classically divided into pro-inflammatory (M1) and anti-inflammatory (M2) states (**Figure 3**).

Microbial products or pro-inflammatory cytokines such as IFN-γ or LPS induce M1 macrophage polarization. The binding of each ligand to its pattern recognition receptor (PRR) triggers a signalling cascade

with different gene expression responses. Specifically, IFN-γ activates the JAK-STAT1 pathway that initiates the expression of major histocompatibility complex (MHC) II, IL-12, IL-23 and nitric oxide synthase 2 (NOS2) (Lawrence and Natoli 2011). Alternatively, LPS and microbial ligands bind the Toll-like receptor 4 (TLR4) that triggers the activation of three key signalling molecules: protein activator 1 (AP-1), interferon responsive factor 3 (IRF3) and the nuclear factor kappa-B (NF-kB) pathway (p65 and p50). As a result, high levels of proinflammatory cytokines and chemokines are expressed (Chen et al. 2023).

The initiation of M2 polarization occurs when IL-4 and IL-13 cytokines bind to IL-4Rα and trigger the activation of STAT6 TF to modulate interferon genes that mediate antiviral responses. As a result, arginase 1 (ARG 1), IL-10, CCL17 and C206 (mannose receptor 1, MRC1) are expressed. Eventually, these products contribute to tissue remodelling, wound healing, tissue fibrosis and regulation of tumor environment (Mantovani 2012)

The balance between M1/M2 populations is controlled by the cytokine composition (paracrine and autocrine signals) during inflammation. Recent advancements, such as scRNA-seq technologies, have revealed that the M1 or M2 dichotomy is an oversimplification and that a wide range of intermediate identities and activation states exists(Blériot et al. 2020; Sanin et al. 2022).

1.3.3 *In vitro* polarization of human monocytes

In the tumor microenvironment, the ratio of M1/M2-like tumor-associated macrophages (TAMs) is crucial for regulating immune therapy responses. For instance, M2-like TAMs upregulate

immunosuppressive genes such as PD-L1, IL-10, TGFβ and IL-4, which weakens the ability of T cells to suppress tumor growth (Wang 2024) (DeNardo and Ruffell 2019). Therefore, there is a need to develop models to study the underlying mechanism of myeloid differentiation. When culturing monocytes in the presence of GM-CSF (granulocyte-macrophage colony-stimulating factor), LPS, and TNF-α, the cells differentiate into M1-like macrophages. Conversely, when monocytes are cultured with M-CSF (macrophage colony-stimulating factor), IL-4, and IL-10, they become M2-like macrophages. This demonstrates the dependency of cell type identity on cytokines(Lacey et al. 2012; Rodriguez et al. 2019).

2. Interleukin-1 (IL-1) pathway and its role in inflammation

Interleukin-1 (IL-1) was originally described in 1974 as a fever-inducing substance released by activated leukocytes called “pyrexin” (Dinarello et al. 1974). Significant members of the IL-1 family include 2 cytokines that bind the same receptor: IL-1α and IL-1β (Sims et al. 1988). However, the IL-1 family comprises 11 members that are usually classified as pro-inflammatory or anti-inflammatory. Overall, there are 7 cytokines with agonist activity (IL-1α, IL-1β, IL-18, IL-33 and IL-36a/b/g), 3 receptor antagonists (IL1RN, IL-36Ra, IL-38), and an anti-inflammatory cytokine (IL-37) (Garlanda and Mantovani 2021) (Dinarello 2019). Given its relevance on inflammatory response in myeloid cells we will focus on IL-1β and IL1RN cytokines in the next chapter.

2.1 Receptor agonists: IL-1β

IL-β, a pro-inflammatory cytokine, is mainly produced by activated monocytes and macrophages via TLR activation and the cytosolic inflammasome complex (Elliott and Sutterwala 2016). Signalling from the inflammasome activates caspase-I, which cleaves the inactive precursor peptide pro-IL-1β to generate the mature forms that are secreted. After secretion, IL-1β binds to IL-1 receptor type 1 (IL-1R1) and the co-receptor IL-1 receptor 3 (IL-1R3) (**Figure 4a**). Upon binding, a conformation change in the receptor occurs and enables the recruitment of an IL1RN accessory protein (IL-1RAcP). Next, it initiates the activation of TLRs, that recruit myeloid differentiation factor 88 (MYD88), which starts a kinase-derived phosphorylation cascade called IL-1R-associated kinases (IRAKs), followed by the phosphorylation of IkB Kinase B (IKKB), IKB and nuclear factor kappa-light-chain-enhancer of activated B cells (NF-kB) translocation to the nuclei (Miller et al. 2006). Then, the signalling complex triggers the activation of p38, c-Jun N-terminal kinases (JNKs), extracellular signal-regulated kinases (ERKs) and mitogen-activated protein kinases (MAPKs).

Finally, proinflammatory cytokines and chemokines are expressed and act in local or systemic inflammation. Thus, protecting against infections (Gabay et al. 2010).

2.2 Endogenous IL-1 inhibitors: IL-1 receptor antagonist

The existence of natural IL-1 inhibitors is fundamental to avoid excessive inflammatory responses. IL-1 receptor antagonist (IL1RN) is a natural antagonist that blocks the proinflammatory activity of IL-1β and IL-1α by competitively binding to IL-1 receptors (Arend et al. 1985) (**Figure 4b**). Upon binding, it triggers a conformational change that

impedes the recruitment of IL-1R3, halting the signalling cascade. Consequently, NF-kB activation via the IL-1 pathway is abrogated, preventing the transcription of pro-inflammatory genes.

Remarkably, the importance of IL1RN in regulating the effects of IL-1 has been demonstrated in knockout mice deficient in *Il1rn*, which exhibit excessive inflammatory responses. These animals present signs of polyarthritis, vasculitis or skin inflammation (Gabay and Palmer 2009).

Recent studies indicate that IL1RN may regulate the inflammatory response to RNA vaccines by reducing excessive pro-inflammatory cytokine release (Tahtinen et al. 2022). Interestingly, clinical use of recombinant IL1RN (anakinra) can be effective for the treatment of COVID-19 (Cauchois et al. 2020; Huet et al. 2020; Kyriazopoulou et al. 2021). Thus, the balance between IL-1 agonists and IL1RN is critical in pathogenic immune responses.

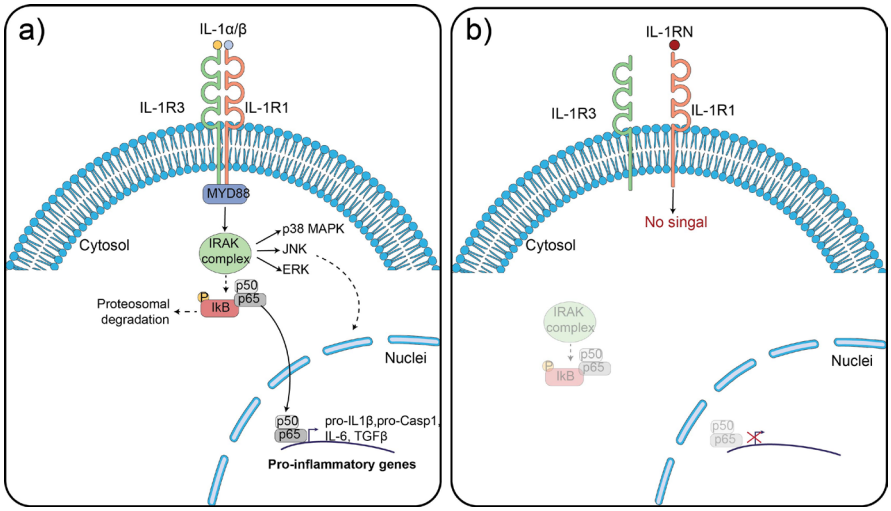

Figure 4. IL-1 signalling pathway. a) *Schematic activation of IL-1 receptor 1 (IL-1R3) and the co-receptor IL-1R3 by IL-1α and IL-1β cytokines. Upon binding, both receptors undergo a conformation change that leads to the recruitment of myeloid differentiation*

factor 88 (MYOD88) adaptor and the initiation of a proinflammatory signalling pathway. In brief, IL-1 associated kinases (IRAK) complex will activate mitogen-activated protein kinases p38 (MAPK), c-Jun N-terminal kinases (JNK) and extracellular signal-regulated kinases (ERKs). Next, IRAK will phosphorylate IkB Kinase β (IKKβ) that will be degraded in the proteasome triggering the translocation into the nuclei of nuclear factor kappa - light-chain-enhancer of activated B cells (NF-kB) resulting in transcription of proinflammatory genes. ***b)*** *Schematic inactivation by IL-1 receptor antagonist (IL1RN). When IL-1RN binds to IL-1R1 it causes a different conformational change that blocks the recruitment of IL-1R3. Therefore, NFKB does not translocate to the nuclei and no pro-inflammatory signalling occurs. Adapted from* (Dinarello 2019) (Gabay et al. 2010).

2.3 Dysregulation of the IL-1 pathway

2.3.1 Myeloid malignancies

Aberrant expression of IL-1 signalling is described in different myeloid malignancies (Caiado et al. 2023). Hence, targeting IL-1 in cancer represents a potent therapeutic strategy. Importantly, increased IL-1β levels are associated with poor prognosis in patients with BCR-ABL chronic myeloid leukemia (CML) and acute myeloid leukemia (AML) (Ren 2005). Both hematological malignancies are characterized by a block in cellular differentiation that results in an accumulation of myeloid blast cells in peripheral blood and BM (Zhang et al. 2012).

Currently, in the clinical setting, IL-1β blocking strategies with monoclonal antibodies (such as canakinumab) are being tested in Phase II clinical trials to treat low and intermediate risk of CML (NTC04239157). Interestingly, another strategy is to use the IL-1 antagonist to balance the IL-1β dysregulated levels. For instance, the use of IL1RN in combination with nilotinib, a BCR-ABL tyrosine kinase inhibitor, has been shown to reduce leukemic cells and enhance the self-renewal potential of leukemic stem cells in mouse models of CML (Ågerstam et al. 2015).

However, IL1RN can also have a role in disease pathogenesis. In fact, low *IL1RN* expression correlates with a negative survival prognosis in AML, specifically in M4-M5 patients. Moreover, loss of *IL1RN in vivo* biases HSC differentiation into the myeloid lineage through IL-1β overexpression (Villatoro et al. 2023).

2.3.2 Autoinflammatory syndromes

Excessive IL-1 signalling is directly linked to pathogenesis in autoinflammatory syndromes(Broderick and Hoffman 2022). These syndromes are monogenic inherited disorders whose main clinical features are characterized by fever and excessive inflammation affecting multiple organs. Examples of these disorders are cryopyrin-associated periodic syndromes (CAPS), familial Mediterranean fever (FMF), tumor necrosis factor receptor-associated periodic syndrome (TRAPS), and the deficiency of IL1RN (DIRA), among others. Notably, anakinra (commercialized as Kineret) is FDA-approved in clinics for treating CAPS, DIRA and rheumatoid arthritis.

2.3.2.1 CAPS: Cryopyrin-associated periodic syndromes

Autoinflammatory diseases caused by mutations in the NLR family pyrin domain containing 3 (NLRP3) are termed cryopyrin-associated periodic syndromes (CAPS), also known as cryopyrinopathies (Hoffman et al. 2001). This group of inherited disorders includes four clinical variants from the mildest to the most severe: familial cold autoinflammatory syndrome (FCAS), cutaneous and articular syndrome (CINCA), Muckle-Wells syndrome, neonatal-

onset multisystem inflammatory disease (NOMID). These patients develop fever and systemic symptoms.

The NLRP3 is involved in the inflammasome assembly, which is responsible for the production and secretion of IL-1β through caspase I activation (Agostini et al. 2004). Consequently, gain-of-function mutations in CAPS patients lead to chronic inflammation because of constitutive activation and hypersecretion of IL-1β.

As a proof-of-concept study, blocking IL-1R1 with anakinra rapidly attenuated the symptoms and prevented organ damage in CAPS patients (Hoffman et al. 2001) (Hawkins et al. 2003). Using a similar approach, forced *IL1RN* expression in HSCs rescued multi-tissue inflammation in a CAPS mouse model (Colantuoni et al. 2023).

2.3.2.2 DIRA: genetic IL1RN deficiency

DIRA (deficiency of *IL1RN*) syndrome is a rare disease caused by the homozygous loss-of-function mutation of *IL1RN,* leading to a lack of *IL1RN* production that begins around birth. These infants have several clinical manifestations, including systemic inflammation of the skin, joints, and bone with many infiltrating neutrophils and high levels of IL-17, a cytokine involved in autoimmune disorders (Aksentijevich et al. 2009).

Because of the *IL1RN* mutation, the resulting protein is truncated. Consequently, there is no secretion of IL1RN, which results in a hypersecretion of inflammatory cytokines. When patients are treated daily with anakinra by subcutaneous injection, a rapid remission occurs with normal levels of C-reactive protein (an early marker of inflammation) and blood cell counts (Aksentijevich et al. 2009; Pillai et al. 2024).

3. Epigenetic regulation of gene expression

Epigenetics was first introduced by Conrad Hal Waddington in 1942 to name “the causal interactions between genes and their products, which bring the phenotype” (Waddington 2012). Epigenetic modifications are critical for regulating gene and noncoding RNA expression. These mechanisms specifically involve adding chemical modifications to the DNA and the histone proteins without altering the underlying DNA sequence itself. This process defines the cell's epigenetic landscape (Goldberg et al. 2007).

3.1 Histone post-translational modifications (PTMs)

The most diverse epigenetic modifications are post-translational modifications (PTMs) on histone proteins. To pack the large size of the human genome, histone proteins are associated with the DNA molecules to conform the nucleosome, which is the fundamental unit of the chromatin.

The nucleosome is a tightly regulated structure that consists of a central histone octamer that coats the DNA forming the nucleosome core particles, which is composed of two copies each of four histone proteins (H2A, H2B, H3 and H4) with approximately 150 bp of DNA. Based on the level of compaction, chromatin can be either heterochromatic (tightly packed) or euchromatic (lightly packed). In this last chromatin state, the DNA is more accessible for the cellular machinery and regulate key processes like transcription, replication, or DNA repair (Millán-Zambrano et al. 2022).

The most thoroughly researched PTMs are found on the N-terminal 'tail' of histones, which protrude from the nucleosome, making them readily accessible. Interestingly, these amino-terminal regions can undergo methylation at arginine (R) residues and acetylation,

methylation, ADP-ribosylation, ubiquitylation, phosphorylation, citrullination or sumoylation at lysine (K) residues (Falkenberg and Johnstone 2014). In this thesis, we will briefly describe histone tail modifications by methylation or acetylation for their role in gene expression.

3.1.2 PTMs impact on transcription regulation

Histone methyltransferases (HMTs) and demethylases (HDMs) are enzymes that methylate or demethylate lysine residues on histone H3 and H4 tails. This lysine residues can be mono-, di-, or tri-methylated, having different effects on gene expression regulation. Additionally, the HMT CARM1 can methylate arginine (R) residues, which is typically linked with active transcription (Bauer et al. 2002) (**Figure 5a**).

On the other hand, histone acetylases (HATs) and deacetylases (HDACs) add or remove acetyl groups at histone H3 and H4. Examples of these PTMs are H3K27ac and H4K16ac (**Figure 5b**). Of note, the location of this modifications is tightly regulated and is crucial for its effect on transcription (Li et al. 2007).

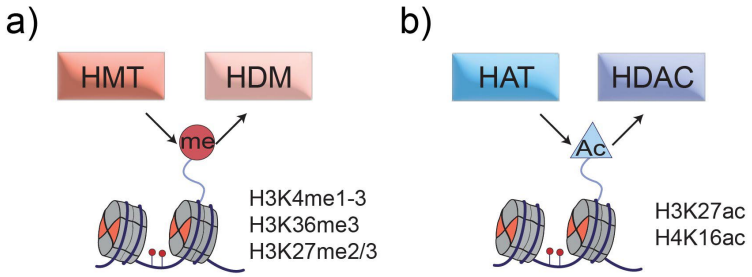

Figure 5. Histone modifications overview. *Schematic of histone post-translational modifications.* ***a)*** *Methyl groups are added by histone methyltransferases (HMT) and erased by histone demethylases (HDM).* ***b)*** *On the other hand, acetyl marks on histones can be deposited by histone acetyltransferases (HAT) and removed by histone*

deacetylases (HDAC. Selection of common histone modifications are shown. Adapted from (Li et al. 2007).

Genome-wide approaches such as chromatin immunoprecipitation followed by sequencing (ChIP-seq) allow the profile of specific histone marks and uncover their association with particular genomic features. For instance, H3K4me3 is usually associated with active promoters, whereas H3K27me3 is enriched in Polycomb-associated repressive chromatin in developmental genes (Boyer et al. 2006). Interestingly, both these marks can be found in the same region referred to as bivalent chromatin in 'poised' genes (Bernstein et al. 2006). Notably, in cis-regulatory elements, active enhancers are often defined with H3K4me1/2 and H3K27ac marks. In contrast, poised enhancers are marked with H3K4me1/2 and the repressive mark H3K27me3. Although the presence of histone modifications is important in defining active enhancers, the binding of transcription factors and co-regulators in the region is essential to their complete activation (Vavouri and Lehner 2012; Heinz et al. 2015).

3.2 DNA methylation

DNA methylation (DNAm) was first discovered in *Mycobacterium tuberculosis* in 1925. However, its biological importance in gene regulation was not elucidated for decades. In mammals, 5-methylcytosine (5mC) was discovered to be distributed in the DNA, specifically in the cytosine residues linked to guanine via a phosphate group on the same strand, called CpG dinucleotides. This non-random distribution suggested a possible biological function (Bird 2002).

3.2.1 The writers and erasers

The deposition and maintenance of DNAm is mediated by 3 major DNA methyltransferases (DNMTs). DNA methyltransferases (DNMT3A and DNMT3B) are responsible for the *de novo* DNA methylation process by adding a methyl group to the fifth carbon of cytosines (5-methylcytosine (5mC)) at CpG dinucleotides (Li et al. 1992; Okano et al. 1999). DNMT1 maintains the pre-existing DNA methylation patterns by copying the information from the parental DNA strand into the nascent DNA strand during DNA replication (**Figure 6**). There is also a catalytically inactive DNMT, DNMT3L, which interacts with DNMT3A and acts as an accessory protein involved in DNA methylation establishment during embryonic development (Wienholz et al. 2010).

Conversely, DNAm can be removed by dilution after each cell division in a process termed passive DNA demethylation. Alternatively, 5mC can be actively removed from the DNA in a dynamic multi-step process initiated by the Ten-Eleven Translocation (TET) enzymes. The TET family consists of three paralogues (TET1, TET2, and TET3) that oxidize 5mC into 5-hydroxymethylcytosine (5hmC) and then to 5-formylcytosine (5fC) and 5-carboxylcytosine (5caC) (Tahiliani et al. 2009; Ito et al. 2011). Interestingly, all oxidized forms can enhance DNA demethylation during replication, as no maintenance activity like DNMT1 for 5mC has been found for them. In the case of 5fC and 5caC, demethylation can also occur through the thymine DNA glycosylase (TDG) and the base excision repair (BER) machinery activities (**Figure. 6**) (Bird 2002; He et al. 2011; Ito et al. 2011).

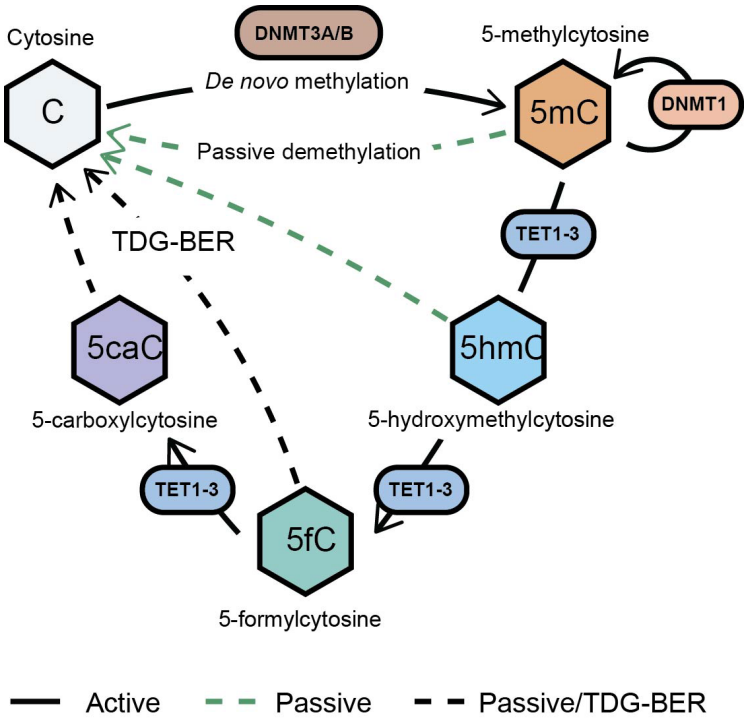

Figure 6. Schematic representation of the DNA methylation and the demethylation processes. *De novo methylation of cytosines (C) is carried out by DNMT3A/B enzymes, resulting in a 5-methylcytosine (5mC) mark, which is maintained during replication by the DNMT1 enzyme. 5mC can be reverted to C through active or passive demethylation. In the active demethylation, TET enzymes catalyse the sequential oxidation of 5mC to 5-hydroxymethylcytosine (5hmC) and 5-formylcytosine (5fC) to 5-carboxylcytosine (5aC). Thymine DNA glycosylase coupled with the base excision repair (TDG-BER) will convert either 5fC or 5caC to unmethylated cytosine (C). When DNA methylation is not maintained during replication, 5mC is converted into unmethylated cytosine (C) in a process known as passive demethylation. Adapted from* (Wu and Zhang 2017).

3.2.2 Genomic distribution of epigenetic marks in the context of gene regulation

The advance of high-throughput technologies has enabled the analysis of genome-wide DNA mapping, thus helping to improve the interpretation of each DNA modification's biological function depending on its genomic context (Jones 2012; Allis and Jenuwein 2016).

Of note, when observing the mammalian genome, more than half of the genes contain short (approximately 1 kb) CpG-rich regions known as CpG islands (CGIs). CGIs are characterized by CpG density, where 1 out of every 10 dinucleotides is a CpG (Bird 1986). Interestingly, most gene promoters, all the housekeeping genes and 50% of the tissue-specific genes, are covered by CGIs that tend to be demethylated (Bird 2002). In addition, their nearby CGI shores (the region within 2 kb of the islands) also tend to remain unmethylated (Doi et al. 2009).

Gene promoters with CGIs at their TSS typically show H3K4me3, lack DNAm, and have active transcription (**Figure 7a**) (Kelly et al. 2010). TET enzymes frequently bound at CpG-rich promoters are responsible for maintaining their unmethylated state (Jones 2012). Moreover, H3K4me3 has been shown to block *de novo* DNA methylation by preventing the binding to chromatin of DNMT3 enzymes (Ooi et al. 2007; Zhang et al. 2010). However, CpG-poor promoters can be repressed by various mechanisms, such as de novo DNA methylation or through Polycomb complexes (**Figure 7b**). For example, during embryonic development, *PAX6* is suppressed in embryonic stem cells (ESCs) by the deposition of H3K27me3. In contrast to active promoters, **gene bodies** of actively transcribed genes are enriched with DNAm. Moreover, changes in gene body methylation have been correlated with the usage of alternative promoters, suggesting a more complex function

that is cell-type specific(Rideout et al. 1990; Maunakea et al. 2010; Greenberg and Bourc'his 2019).

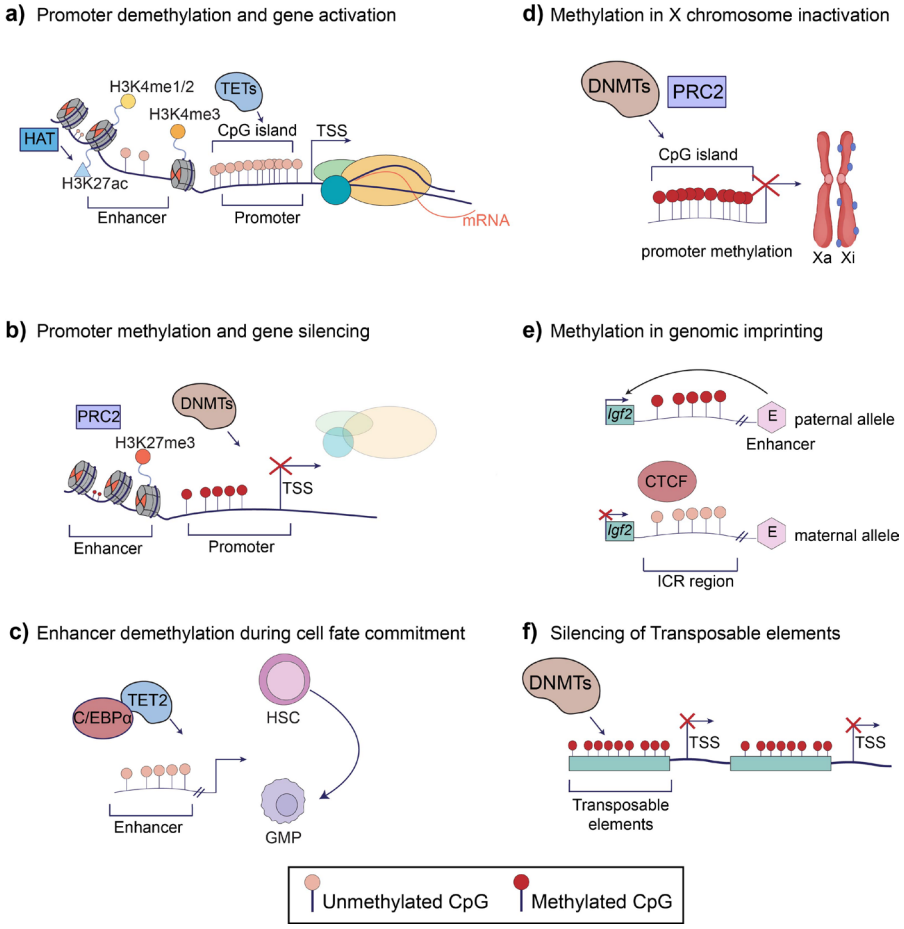

Figure 7. Cellular functions of DNA methylation and its role in gene expression. a) *Representative mechanism of TET-mediated DNA demethylation activating transcription process in CpG island promoter. On the left, an active enhancer region marked with H3K4me3 and H3K27ac.* ***b)*** *Schematics of gene silencing by DNMT-mediated DNA methylation in a promoter region. Inactive enhancers are usually associated with the recruitment of Polycomb repressive complex 2 (PRC2) and the deposition of trimethylation of H3 at lysine 27 (H3K27me3).* ***c)*** *TET2 is recruited by C/EBPα to induce DNA demethylation and enhancer activation during myeloid differentiation of hematopoietic stem cells (HSCs) to granulocyte-monocyte progenitors (GMPs).* ***d)*** *Schematics of X-linked gene inactivation through PRC2 complex and DNA methylation.* ***e)*** *Schematics of genomic imprinting process exemplified by Igf2 where DNA methylation is asymmetrically deposited in the parental allele in regions*

known as imprinting control regions (ICR), leading to differences in gene expression. DNAm in the paternal allele prevents CTCF binding and, therefore, allows the downstream enhancer to activate Igf2 expression. ***f)*** *DNA methylation is required for the silencing of transposable elements. Adapted from* (Sardina et al. 2018; Greenberg and Bourc'his 2019).

Recent studies have suggested a novel class of CGIs named "orphan" CGIs which are not associated with TSS and can be found within gene bodies (intragenic) or between annotated genes (intergenic). Moreover, orphan CGI can act as alternative promoters were when found at poised enhancers, facilitating their interaction with long-range distal genes (Pachano et al. 2021).

3.2.3 Biological mechanisms of DNAm during early development

The balance between DNMTs and TETs is crucial for epigenetic reprogramming at first stages during development. At the phase of germ cell specification, there is a loss of DNAm, which provides a 'blank slate' for establishing cell type-specific methylation patterns (Monk et al. 1987; Sasaki and Matsui 2008; Reik and Surani 2015). Additionally, DNA methylation is involved in transcriptional silencing during mammalian development. One mechanism in which DNA methylation can contribute to gene silencing is by inhibiting TF binding or through methyl-CpG-binding domain (MBD) proteins (Kaluscha et al. 2022). MBD proteins known as "readers" can recognize 5mC marks and recruit corepressor complexes, leading to gene repression (Bogdanović and Veenstra 2009). Here, we will briefly describe some long-term silencing process where DNA methylation participates.

X-chromosome inactivation (XCI). XCI begins when XIST, a long non-coding RNA, spreads across the future inactive X

chromosome (Xi) and recruits Polycomb repressive complexes (PRCs). Next, heterochromatic marks such as H3K27me3 are deposited, resulting in gene silencing (Forsyth et al. 2024) (**Figure 7d**). As a final layer of regulation, promoters and enhancers gain DNAm that will be maintained in each cell division (Lock Cell 1987).

Genomic imprinting. In this process, DNAm is unequally added in the parental germlines in DNA sequences known as imprinting control regions (ICRs). The involvement of imprinting in gene regulation is exemplified by the role of CTCF, a TF that can insulate a promoter from a remote enhancer, in the *Igf2* locus (**Figure 7e**). The maternal allele is methylation-free, allowing CTCF binding and insulation. However, the ICR at the paternal allele is methylated, preventing CTCF binding and, therefore, allowing the downstream enhancer to activate *Igf2* expression. Importantly, disrupting imprinting leads to neurological and metabolic disorders (Fitzpatrick et al. 2002).

Genome stability. DNAm is involved in the transcriptional repression of genomic repetitive elements such as transposable elements (TE) which is crucial for genomic stability (**Figure 7f)** (Walsh et al. 1998). Subsequently, when TEs promoters like LINE-1 are hypomethylated, it leads to the activation of these mobile genetic elements causing genomic instability (Shukla et al. 2013; Babaian et al. 2016).

3.2.4 DNMT and TET activities during development

Many studies have reported the role of methylation loss in gene activation and its relevance in development. Previous work in zebrafish has demonstrated TET-mediated active demethylation of enhancers is

key for vertebrate development (Bogdanović et al. 2016). Additionally, losing the three Tet enzymes in embryonic stem cells leads to increased promoter hypermethylation in genes implicated in embryonic development, causing impaired differentiation (Dawlaty et al. 2014). In another study, it was observed that conditional deletions of Tet enzymes lead to gastrulation failure (Dai et al. 2016). Thus, highlighting the crucial roles of DNA methylation in various stages of mammalian development.

Parallel research has also explored the effects of DNA methylation loss on the molecular level. Interestingly, *Tet2* deficiency results in DNA hypermethylation and loss of 5hmC at enhancers regions, which finally leads to reduced gene expression (Hon et al. 2014a). Indeed, these enhancer regions are directly bound by TET2, which lacks DNA binding domain. Therefore, this enzyme needs to be recruited by TF to gene regulatory elements (GREs) for active demethylation which might result in active transcription (Wang et al. 2018).

Interestingly, DNAm can modulate the physical access of TFs to the DNA. In fact, several TFs show methyl-cytosine binding sensitivity. Therefore, the recruitment of some TFs into a particular region depends on the presence of DNA methylation marks at their recognition sites (Yin et al. 2017). In particular, TF can recognize methylated sequences during cell reprogramming and interact with methylation enzymes to regulate gene expression during cell fate transitions. In the case of myeloid cell fate establishment, Sardina and co-workers showed that C/EBPα and KLF4 transcription factors can recruit *Tet2* to myeloid enhancers, leading to their demethylation and activation (**Figure 7c**)

(Sardina et al. 2018). Otherwise, DNA methylation at enhancers can restrict TF binding.

On the other hand, *Dnmt* loss during endodermal differentiation led to a global reduction of DNAm and embryonic lethality (Okano et al. 1999). Moreover, *Dnmt3a* null HSCs contribute to upregulating multipotent genes, resulting in a block of hematopoietic stem cell differentiation (Challen et al. 2012; Liao et al. 2015). Overall, DNA methylation enzymes are essential during normal development and cell fate transitions.

3.2.4.1 DNMT and TET activities during myeloid differentiation

The differentiation from progenitors to fully mature myeloid cells necessitate the timely involvement of epigenetic mechanisms to regulate immune cell gene expression (Geissmann et al. 2010). During neutrophil commitment, DNAm levels first increase as CMPs transition to GMPs, followed by a decrease as GMPs mature. Remarkably, these changes in DNAm are correlated with changes in gene expression (Rönnerblad et al. 2014). This dynamic epigenetic control, together with lineage-specific transcription factors such as PU.1, C/EBPα and GATA1, is essential to determine myeloid cell identity (Roy et al. 2021).

Interestingly, several studies have shown that active DNA demethylation occurs during the *in vitro* differentiation of primary human monocytes into macrophages. Klug and co-workers identified a loss of methylation during differentiation, accompanied by a TET2-driven rise in 5hmC (Klug et al. 2013). Another study found TET2-dependent demethylation occurred during the in vitro differentiation of monocytes to DCs. Vitamin C treatment, a TET enzyme cofactor, similarly enhanced DNA demethylation, which correlated with gene

upregulation and increased proinflammatory cytokine production in DC (Morante-Palacios et al. 2022b).

3.2.5. DNA methylation in disease

Nowadays, it is well known that hypermethylation of CpG islands located at promoter regions of tumor suppressor genes leads to their repression in a wide range of cancers (Jones and Baylin, 2002; Esteller and Berdasco, 2019). Examples of these hypermethylated genes include the DNA repair gene *MGMT* in colorectal cancer and the cyclin-dependent kinase inhibitor 2A/B (*CDKN2A/B*), which regulate cell cycle progression and are repressed in different types of hematological malignancies.

Alterations in genes encoding regulators of DNA methylation such as DNMT3A and TET enzymes are frequent in a wide range of diseases, such as neurodegeneration, immunodeficiency and haematological cancers.

Alterations of DNMTs. Heterozygous mutations in the *DNMT1* gene are present in patients with neurodegenerative disorders characterized by dementia and hearing loss (Kernohan 2016). Mutations in the *DNMT3B* catalytic domain have been described in patients with immunodeficiency, centromeric instability, and facial anomalies (ICF1) syndrome. In acute myeloid leukemia (AML) aberrant DNAm is considered a hallmark of the disease (Huang and Figueroa 2021). Importantly, mutations in *DNMT3A* gene are found in around 20-25% of patients (Challen et al. 2012; Patel et al. 2012). Most of these are missense mutations localized at the arginine 882 (R882) in the catalytic domain. Remarkably, these patients show a hypomethylation state,

especially at CpG islands, shores, and promoters (Russler-Germain et al. 2014; Yang et al. 2016; Spencer et al. 2017).

Alterations of TETs. *TET2* loss of function mutations are frequently observed in hematological malignancies such as acute myeloid leukemia (AML), myelodysplastic syndromes (MDS) and myeloproliferative neoplasms (MPN). In contrast to *DNMT3A* mutations, *TET2* mutations result in genome-wide hypermethylation and decreased 5hmC levels. Moreover, *Tet2* depletion in mouse hematopoietic precursors leads to myeloid bias (Figueroa et al. 2010; Ko et al. 2010; Li et al. 2011; Moran-Crusio et al. 2011). Interestingly, high frequencies of *TET2* mutations are present in individuals with clonal hematopoiesis of indeterminate potential (CHIP), a preleukemic condition associated with aging(Xie et al. 2014; Tulstrup et al. 2021). Recent studies show that *TET2*-associated hypermethylation occurs at enhancers associated with myeloid differentiation in CHIP and AML patients (Li et al. 2011; Rasmussen et al. 2019; Ostrander et al. 2020).

Thus, understanding the mechanistic role of DNAm in a disease context has helped us to interpret its role in gene regulation and the development of effective therapeutics (Greenberg and Bourc'his 2019).

4. Epigenome manipulation

Given the broad importance of epigenetic modifications in pathogenesis many efforts have been made to perturb the epigenome and therefore understand the function of each modification. Early studies relied on genetic manipulation techniques such as gene knockouts, point mutations, domain deletions, or targeted knockdowns of a transcript (Holtzman and Gersbach 2018). In recent years,

numerous epigenetic editing technologies have allowed targeted modifications to study cellular phenotypes and accurately replicate disease mechanisms.

4.1 Non-specific methods: epidrugs

Recently, interest in epigenetic drugs for cancer treatment has surged. These drugs, known as “epidrugs,” represent an alternative to traditional chemotherapy agents. Precisely, epidrugs are small chemical molecules that inhibit the enzymes necessary for the maintenance or establishment of histone or DNA modifications therefore acting to restore a “normal” epigenetic landscape. They can be classified as altering:

DNA methylation: hypomethylating agents (HMAs), like 5-azacitidine, work by inhibiting DNA methyltransferases, leading to gene demethylation. Of note, 5-azacitidine is FDA-approved for the treatment of myeloid malignancies. It demethylates aberrantly hypermethylated genes such as cyclin-dependent kinase inhibitor 2B (CDKN2B), which leads to its gene reactivation (Toyota et al. 2001).

Histone PTMs: Histone deacetylase (HDACi) inhibitors have been FDA-approved to treat T-cell malignancies. Other HDACi have been approved by the FDA for the treatment of multiple myeloma, offering an alternative for drug-resistant patients (Prince et al. 2009).

Although small inhibitors are valuable options to treat disease, they cause irreversible and global effects since they lack specificity for a particular tissue or genomic target. Moreover, it remains a major challenge to reduce their off-target effects and predict which genes will be activated unspecifically because of these treatments (Baylin and

Jones 2016; Berdasco and Esteller 2019). Consequently, there is an unmet need for precise tools for epigenetic therapy purposes.

4.2 Targeted methods

DNA-binding-based technology has emerged as a precise, flexible, and locus-specific technique to alter the epigenome. Therefore, it allows us to establish a causal link between epigenetic changes and gene regulation. The diversity of epigenome editing approaches presents a wide range of biological applications, from gene regulation, high-throughput screenings, perturbations of noncoding regulatory elements, manipulation of 3D genome and disease perturbations, among others (Nakamura et al. 2021).

4.2.1 Genome engineering: ZFN, TALENS

Genome editing technology has emerged in research to study the genetic basis of cell function and disease by inducing specific modifications to the DNA.

Early work in gene editing began with DNA-binding proteins such as zinc finger nucleases (ZFNs) (Klug and Rhodes 1987) and transcription activator-like effector nucleases (TALENs) (Sanjana et al. 2012). ZFNs and TALENs are constructed by fusing several DNA binding modules with endonucleases linked to a DNA cleavage domain. Therefore, these constructed array enables the recognition of long DNA sequences and increases target specificity.

ZFNs: are one of the most common DNA binding motifs found in eukaryotes. Multiple ZF domains are combined for genome

engineering to recognize sequences (3-4 bp) via DNA-protein interaction.

TALENs: are derived from bacteria. In a similar way, each peptide domain recognizes a specific nucleotide and can be assembled in series to recognize a target sequence.

Moreover, ZFNs and TALENs can be fused with epigenetic enzymes to induce site-specific chromatin modifications (Perez-Pinera et al. 2012). One example is the fusion of ZF with histone methyltransferases (HMT) or histone acetyltransferases (HAT) (Coates et al. 2005), this last approach was applied to restore neuroprotection mechanisms in a Parkinson model by activating a neurotrophic factor on glial neurons (Laganiere et al. 2010). In a similar way, TALENs have been used for transcriptional activation (Polstein et al. 2015) and for visualizing the architecture of endogenous repetitive sequences by fusing them with fluorescent proteins (Miyanari et al. 2013).

However, these strategies are laborious and intensive as each repetitive domain recognizes a particular DNA base in the target sequence. In addition, engineering a different ZF or TALE domain for each target region is time-consuming and challenging for multiplexing approaches.

4.2.2 CRISPR/Cas9: discovery and applications

A major discovery in genome editing came from the advent of the CRISPR/Cas9 system. Thanks to its high efficiency, specificity, and flexibility, the targeting platform has become the most widely used genome-engineering tool.

There are several subtypes that have been classified in two classes depending on the protein complex. Class 1 includes (types I, III, and IV and is characterized by multiple subunits of Cas protein complexes, whereas class 2 systems (types II, V, and VI) comprise a single unit of Cas9 effector protein (Makarova et al. 2015). Interestingly, this mechanism was discovered in prokaryotes, where CRISR/Cas plays a role in the adaptative immune system against foreign nucleic acids (Mojica et al. 2009).

The mechanism of action in type II systems is usually divided into three stages. First, clustered regularly interspaced short palindromic repeats (CRISPR) systems and Cas9 endonuclease formed the ribonucleoprotein (RNP) complex. Second, CRISPR RNA (crRNA) and trans-activating RNA (tracRNA) are fused to produce a single guide RNA (gRNA), that undergoes complementary base pairing (protospacer) that is adjacent to a protospacer adjacent motif (PAM) (Gilbert et al. 2013). Finally, Cas9 RNP binds to the PAM, it cleaves the DNA strand by generating a blunt double-strand break (DSB) that will be repaired by non-homologous end-joining (NHEJ) and homology-directed repair (HDR) pathways (Hussmann et al. 2021).

Consequently, for genome editing, CRISPR/Cas system has been widely used to cut dsDNA by generating DSB for targeted deletions, gene knock-out, and gene knock-in by exploiting cellular phenotypes (Jinek et al. 2012). Many efforts have been made to improve CRISPR/Cas properties, such as specificity and efficacy. For instance, initial CRISPR technologies focused on Cas9 orthologues from Streptococcus pyogens (SpCas9). However, new effectors have been identified with reduced Cas9 size and less restrictive PAM requirements (Chatterjee et al. 2018). Besides Cas9, other RNA-guided

programmable nucleases, including Cas12 (Zetsche et al. 2015) and Cas13 (Abudayyeh et al. 2016) from type V and VI CRISPR systems have been discovered and characterized (Jiang and Doudna 2017) (**Figure 8**).

Nowadays, CRISPR's applications have expanded far beyond inducing double-strand breaks. The toolbox includes single base pair modification, fluorescent tagging of genomic loci, and regulation of gene expression (Mali et al. 2013). Notably, CRISPR gene editing has been incorporated in several clinical trials to treat diverse diseases (Villiger et al. 2024a). Recently, Anzalone and co-workers developed the so-called prime editing, a novel strategy for introducing small to medium-sized targeted insertions, deletions, and nucleotide replacement. Here, a Cas9 variant is fused with a reverse transcriptase, which, together with a prime editor, guides RNA (pegRNA) that serves as a primer for the reverse transcription (Anzalone et al. 2019). This novel strategy offers huge flexibility and precision as it does not introduce DSB, leading to fewer errors and less off-target effect. Notably, CRISPR gene editing has been incorporated in several clinical trials to treat diverse diseases (Villiger et al. 2024a).

Here, we focus on the recent advances of CRISPR-based tools for epigenome engineering in the context of gene expression regulation and therapeutic applications.

4.2.3 CRISPR-mediated epigenome-editing

Epigenome editing has emerged as a precise approach to modify epigenetic marks. In CRISPR-based systems, Cas9's catalytic domain is mutated, making it an inactive “dead” Cas9 (dCas9).

To edit the epigenome, dCas9 is fused to epigenetic effector (epi-dCas9) domains to target any genomic locus using a gRNA complementary to the target sequence (Gilbert et al. 2013)(**Figure 8**). Therefore, this tool allows us to directly test each individual epigenetic mark's causal function in gene expression and chromatin structure. Additionally, this aids in studying biological processes and diseases where these modifications are altered.

4.2.3.1 Targeted transcriptional regulation

Transcriptional modulators can act by transiently recruiting chromatin remodelling complexes or chromatin-modifying enzymes that produce chromatin compaction (CRISPRi) or decompaction (CRISPRa). This strategy offers an alternative to transgene overexpression or knock-down-mediated gene repression(Pulecio et al. 2017). In the following sections, we will describe each modification and the composition of the epigenome editing tool.

CRISPR interference **(CRISPRi).** Early work in generating CRISPR-based repressors relied on fusions of dCas9 with the repressive chromatin modifier Krüppel-associated box (KRAB) domain (Gilbert et al. 2013). Once KRAB binds to the target region, it recruits co-repressors (KAPI and HP1 proteins) that induce heterochromatinization to rapidly silence transcription. Of note, CRISPRi has become an alternative strategy to traditional RNA interference methods. Moreover, since CRISPRi does not interact with the endogenous microRNA machinery, like traditional RNA interference methods, it can target non-coding elements (Gilbert et al. 2014).

CRISPR activation **(CRISPRa):** It is based in the fusion of dCas9 with transactivation domains. The most common one is the herpes virus transcription factor VP16 (or 4 copies of VP16, named VP64). CRISPRa promotes transcription by recruiting co-activators and the transcriptional machinery to the target gene (Perez-Pinera et al. 2012). For instance, dCas9-VP64-mediated gene activation was sufficient to induce changes in neuronal cellular identity (Joshua Black CSC 2016). However, in most cases, the activation level driven by CRISPRa is unstable. Therefore, next-generation CRISPRa uses multiple effector fusions such as VPR (VP64, p65, and Rta), SAM, and the SunTag system (Chavez et al. 2015).

-**The SunTag system:** was developed to enhance transcriptional activation by recruiting multiple VP64 domains to a single molecule of dCas9. For this, single-chain variable fragments (scFv) antibodies were fused with multiple copies of GCNA peptide and VP64 (Tanenbaum et al. 2014) (**Figure 8**). Konnerman and co-workers engineered different combinations of synthetic transactivating domains, showing that synergistic activation mediator (SAM) was the optimal tool for high on-target specificity and transcription activation (Konermann et al. 2015). However, these tools act as scaffolds and do not enzymatically modulate the chromatin state directly.

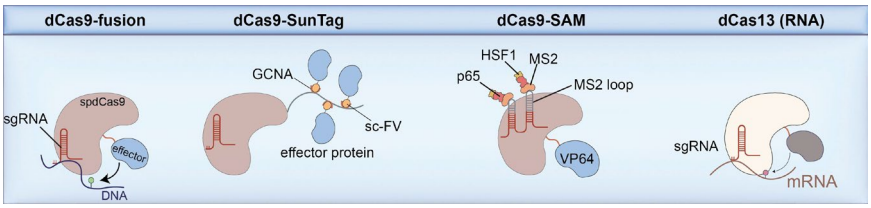

Figure 8. Schematic of CRISPR-dCas epigenome editors constructs. dCas9-fusion *is constituted by the Streptococcus pyogens catalytically dead Cas9 (spdCas9) fused with different effector domains to modify chromatin marks or modulate transcription in the presence of a single guide RNA (sgRNA) complementary to DNA.* ***dCas9-SunTag*** *is formed of SpdCas9 fused with tandem repeats of GCNA binding motif, which recruits effector proteins coupled with small-chain variable fragment (scFV) domain.* ***dCas9-SAM*** *is formed by SpdCas9 enzyme fused to the transcriptional activator VP64. The gRNA is modified to include two RNA aptamers for binding with engineered MS2 bacteriophage coat proteins, which recruit two transcriptional activators, p65 and HSF1.* ***dCas13*** *(catalytically dead Cas13) enzyme fused with an effector domain allows precise editing of different RNA base modifications. Adapted from* (Policarpi et al. 2021; McCutcheon et al. 2024).

4.2.3.2. Multiplex epigenome editing

Given the potential role of dCas9-based tools in unveiling biological mechanisms, strategies to combine these tools have been developed to simultaneously target multiple regions or induce a more lasting effect (McCutcheon et al. 2024). Another key consideration is to decipher how the combination of chromatin marks influences gene regulation to understand sophisticated regulatory circuits (Policarpi et al. 2021).

Policarpi and co-workers engineered a dCas9-SunTag system fused with 9 key chromatin modifiers that deposit H3K4me3 (Prdm9-CD), H3K27ac (p300-CD), H3K79me2 (Dot1l-CD), H3K9me2 (G9a-CD), H3K36me3 (Setd2-CD), DNA methylation (Dnmt3a/3l-CD), H2AK119ub

(Ring1b-CD) and full-length (FL) enzymes that write H3K27me3 (Ezh2-FL) and H4K20me3 (Kmt5c-FL). Moreover, this toolkit is coupled with a single-cell transcriptomic readout. They observed robust gene activation by H3K4me3 deposition, even in genes that are never active. In addition, they showed that DNAm induced silencing was not as strong as the repression associated with other epigenetic marks, such as H2AK119ub or H3K9me2/3 (Policarpi et al. 2024).

Multiplex strategies can also be applied to shed light on disease-associated epigenetic mechanisms. For instance, Nuñez and co-workers (Nuñez et al. 2021) used a highly specific genome-wide approach targeting thousands of different loci in human cells, highlighting the potential utility in therapeutic screening. They specifically used a CRISPRoff tool, based in the fusion of dCas9 with the effectors KRAB, DNMT3A and DNMT3L together, and a sgRNA library. Notably, the gene silencing obtained was maintained after cell division and differentiation. Moreover, it could be reverted with a CRISPRon tool (an optimized version of dCas9-TET1 with transactivator domains) (Nuñez et al. 2021).

4.2.3.3 Targeted histone modification

Another approach for epigenome editing has explored fusing dCas9 with histone modifiers enzymes to deposit or erase PTMs in a specific locus to better understand the exact role of histone marks in gene regulation or chromatin architecture (Pulecio et al. 2017). Depending on the PTM deposited or erased, this editing system can be classified as activating (dCas9-p300) or repressive (dCas9-EZH2) (Roth).

Editing H3K27ac (dCas9-p300): Hilton et al. fused dCas9 with the catalytic histone acetyltransferase (HAT) core domain p300. As expected, enhancers and promoters targeted with dCas9-p300 were decorated with H3K27 (Hilton et al. 2015). Interestingly, their associated genes became activated, highlighting a causal relationship between histone acetylation and gene expression. Additionally, targeted acetylation of the *Oct4* promoter and enhancer has been described as sufficient to initiate iPSC reprogramming (Liu et al. 2018a).

Editing H3K27me (dCas9-EZH2): A study showed long-term gene repression by H3K27me3 deposition using dCas9 fused with a catalytic subunit of PRC2 Enhancer of Zeste Homolog 2 (EZH2)(O'Geen et al. 2019)(**Figure 9**). Interestingly, the silencing obtained was enhanced with *de novo* DNA methyltransferase (DNMT3A) and its ortholog DNMT3L, suggesting that histone and DNAm interaction are important for epigenetic memory (O'Geen et al. 2019, 2022).

Collectively, histone epigenome editing has been applied in CRISPR screens, allowing the discovery and validation of coding and noncoding regulatory elements impacting cellular phenotypes. Thus, offering a new avenue of applications for different therapies (Konermann et al. 2015; Klann et al. 2017; Tarjan et al. 2019).

4.2.3.4 DNA methylation editing

For many decades, comparative genomic analysis between DNAm, TF and chromatin modifications have been used to infer the functions of DNAm in the context of gene regulation. These studies relied on non-specific approaches like insertion of TF binding motifs with different methylation states, pharmacological inhibition with 5-

azacytidine, or genetic perturbations (Stadler et al. 2011; Maurano et al. 2015). However, these techniques only provide correlative information and lead to broad transcriptional changes resulting in pleiotropic off-target effects. Thus, targeted methylation editing tools enable precise manipulation of local regions and study the direct impact on gene regulation.

4.2.3.4.1 DNAm editing on gene regulation

To study DNAm in the context of gene expression, several groups have fused dCas9 with the catalytic domain of DNMT3A or TET1 to trigger DNA methylation or demethylation, respectively (Liu et al. 2016a) (**Figure 9**).

Editing DNA demethylation (dCas9-TET1): As a proof of concept, targeted demethylation of the myogenic TD (MyoD) enhancer region by dCas9-TET1 resulted in gene activation and facilitated muscle cell differentiation (Liu et al. 2016a). Moreover, dCas9-TET1-mediated demethylation has been employed to perturb differentially methylated regions (DMRs) located in imprinting genes (Kojima et al. 2022).

Editing DNA de novo methylation (dCas9-DNMT3A): To study how methylation affects DNA loops, dCas9-DNMT3A was employed to methylate CTCF binding sites. Notably, CTCF TF binding was altered when methylation was deposited. Thus, confirming CTCF methylation-sensitivity and highlighting the importance of 5mC mark in genome architecture (Liu et al. 2016a). Nevertheless, genome-wide analysis of these methylation editing tools has shown potential off-target effects (Liu et al. 2018a). Of note, when measuring dCas9-DNMT3A

methylation activity in cells depleted from the endogenous methylation machinery high global off-target effect occurred. Importantly, the unspecific editing was independent of sgRNAs (Galonska et al. 2018). On the contrary, other works have achieved specific effects and less off-target methylation when compared with dCas9-DNMT3A when using a modular SunTag-DNMT3A system (Pflueger et al. 2018).

To gain mechanistic insights, recent studies have investigated the interplay between hypermethylated CGI promoters and H3K27me3 repressive marks during exit from naïve pluripotency. Additionally, by using SunTag-TET1 they have shown that precision erasure of DNAm at the imprinted *Zdbf2* locus results in increased CTCF binding and failure to completely activate gene expression during differentiation (Monteagudo-Sánchez et al. 2024).

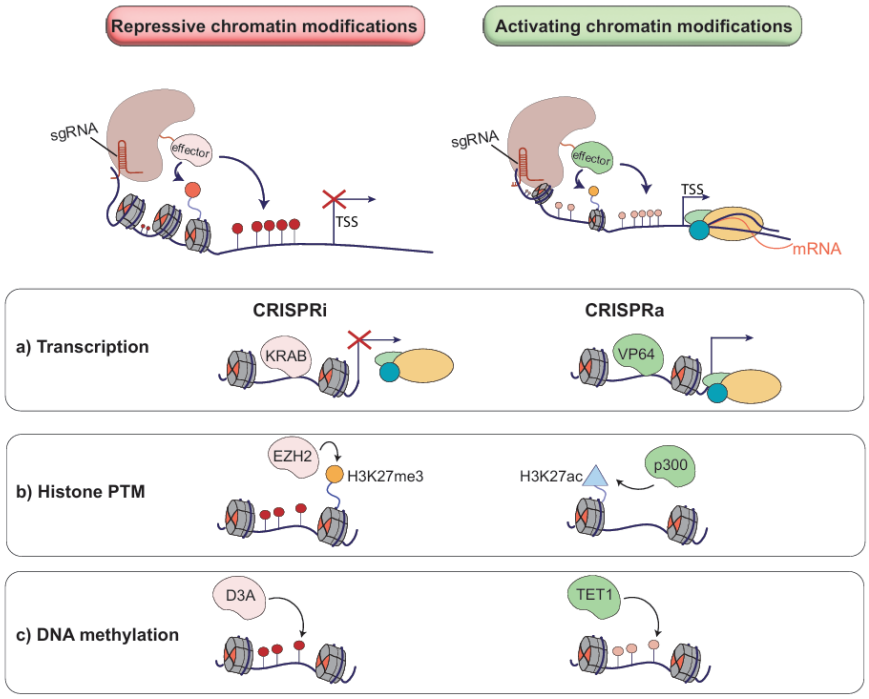

Figure 9. Epigenome editing technologies for gene regulation. a) *On the left, repressive dCas9 epigenome modifications at the transcription (dCas9-KRAB) also referred as CRISPR inactivation (CRISPRi) which impedes the binding of RNA polymerase II. On the right, activating modifications at the transcription (dCas9-VP64) also referred as CRISPR activation (CRISPRa) which recruits RNA polymerase II.* ***b)*** *Left: at the histone level (dCas9-EZH2) deposit a repressive histone mark. Right: at the histone level (dCas9-p300) deposit active histone mark.* ***c)*** *Left: at the DNA methylation (DNAm) level dCas9 fused with DNMT3A (dCas9-D3A) will add methylation to a particular region on the DNA which is usually associated with gene silencing. Right: at the DNAm level dCas9 fused with TET1 (dCas9-TET1) will remove cytosine methylation in a particular region which is usually associated with gene activation. Adapted from*(McCutcheon et al. 2024; Roth et al. 2024).

4.2.3.4.2 DNAm editing in the hematopoietic system

Alterations of the DNAm landscape in the hematopoietic system are present in a wide range of disease phenotypes (Liu et al. 2023). Therefore, many efforts have been made to target therapeutically relevant cells, such as HSCs, and to overcome immunological barriers.

Moreover, the introduction of epigenetic editing tools and the maintenance of editing is challenging due to the large size of Cas9 protein, which results in low lentiviral transduction rates. Also, primary cells have a limited culture duration which makes difficult to address long-term effects upon editing (McCutcheon et al. 2024). To address this issue, Amabile and co-workers co-delivered a CRISPR-based repressive complex, achieving the first stable epigenetic gene repression (effective silence was monitored for more than 50 days). Notably, a transient delivery of the named engineered transcriptional repressors (ETRs) combination composed of the effector domains KRAB, DNMT3A, and DNMT3L led to the silencing of endogenous genes in primary T lymphocytes (Amabile et al. 2016).

Despite these advances in achieving long-term repression, additional research is needed to apply epigenome editing for *in vivo* cell therapy in the immune system. To this end, Saunderson and co-workers recently targeted the p15 promoter (usually hypermethylated in AML) in primary human CD34+ cells with dCas9-DNMT3A-DNMT3L, leading to gene downregulation (Saunderson et al. 2023). Moreover, when p15-edited cells were injected into immunodeficient mice, its DNA hypermethylation was inherited and maintained through lymphoid and myeloid lineages. Thus, demonstrating that DNAm editing can be used to study the biological contribution of epigenetic mechanisms in cancer (Saunderson et al. 2023).

4.2.3.4.3 DNAm editing therapies

Methylation editing can be applied to investigate the causality of disease-associated DNAm events, such as X-linked, imprinting-related disorders and cancer.

X-linked disorders: DNAm editing has recently been explored as a potential therapeutic tool to treat X-linked neurodevelopmental disorders, including fragile X syndrome (FXS) and Rett syndrome (RTT):

- **FXS** is caused by the silencing of the *FMR1* gene during brain development (Liu et al. 2018a). In FXS, the *FMR1* promoter region, containing an expansion of trinucleotide (CGG) repeats, is hypermethylated. Liu and co-workers used the dCas9-TET1 tool to reverse the methylation of the CGG repeats favouring the reactivation of the *FMR1* gene and remarkably rescuing the normal cellular electrophysiology. Moreover, the reactivation of the *FMR1* gene was also observed in the mouse brain when the editing tool was delivered by adeno-associated viruses (AAVs) (Liu et al. 2018a).

- **RTT** is caused by inactivating mutations in the methyl CpG-binding protein 2 (*MECP2*), a DNA methylation reader, on the X chromosome. In a recent study, Qian an co-workers targeted the *MECP2* promoter located at the Xi chromosome with dCas9-TET1 and observed its gene reactivation (Qian et al. 2023a). In addition, to reach a more stable reactivation, the authors developed another editing strategy targeting the chromatin boundaries. Precisely, inactive Cpf1 (a smaller than Cas9 RNA-guided endonuclease) was fused with CTCF and delivered along with dCas9-Tet1. Importantly,

using this multiple editing approach, authors obtained a complete rescue in the neuronal activity by reaching a more efficient reactivation(Qian et al. 2023a).

Imprinting-related disorders: Other studies have focused on imprinting disorders in which DNAm status differs between maternal and paternal alleles at ICRs. For instance, DNA demethylation editing was used in Prader-Willi Syndrome (PWS) cells to reactivate the maternal allele-specific gene *SNRPN* that persists during neuronal differentiation (Rohm et al. 2024).

Cancer: Epigenome editing has also been used in several cancer models. For example, SunTag dCas9-TET1 leads to demethylation and gene activation in cancer cell lines (Morita et al. 2016). In addition, dCas9-TET targeted hydroxymethylation leads to gene activation in models of *in vivo* kidney fibrosis*,* and colorectal cancer cell lines at *the BRCA1* promoter (usually hypermethylated in breast and ovarian cancers) (Choudhury et al. 2016; Xu et al. 2016; Tejedor et al. 2023).

- In a recent collaborative study (Lopez-Millan et al. 2024), we have applied dCas9-DNA methylation editing tools to decipher whether the *neuron-glial antigen-2 (NG2*) gene, a direct target of MLL-AF4 fusion protein in B-cell acute lymphoblastic leukemia (B-ALL), is epigenetically regulated. A differentially methylated region (DMR) between MLL-AF4 B-ALL patient's cells and normal B cell progenitors was previously detected at this gene (including residues CpG066 and CpG1)(Tejedor et al. 2021). Interestingly, its methylation status was detected as negatively correlated with the *NG2* expression. To investigate causality in this association, we

delivered the dCas9-DNMT3A tool (d93A WT) and gRNAs targeting the relevant CpGs in an MLL-AF4 B-ALL cellular model (SEM cells). dCas9-DNMT3A-mediated editing led to efficient hypermethylation of both CpGs analyzed (066 and C1) and to *NG2* downregulation (**Figure 10**). Therefore, we conclude that *NG2* expression is controlled by the methylation status of this regulatory region (Lopez-Millan et al. 2024). Given that NG2 levels are associated with brain invasiveness (Prieto et al. 2018), we might be able to directly impact cancer by regulating the methylation of this region.

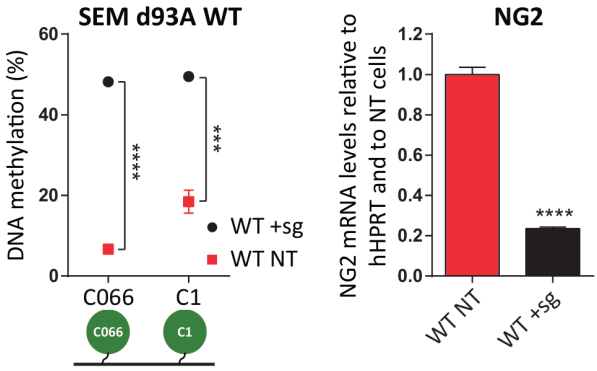

Figure 10. dCas9-DNMT3A targeting NG2 regulatory region. *Left panel. DNA methylation levels at the indicated CpG residues (C066 and C1) in dCas9-DNMT3A WT-targeted SEM cells (WT+sg) and non-targeted SEM cells (WT NT) (left panel). Right panel shows NG2 expression by qPCR in dCas9-DNMT3AWT-targeted and non-targeted SEM cells. Data from* (Lopez-Millan et al. 2024) .

4.2.3.5 Recent advances in clinical applications

For years, delivering methylation editors *in vivo* has been the primary challenge in developing epigenome editing-based therapies due to the vector sizes exceeding the delivery capacity of AAVs. To circumvent this

limitation, a recent study has shown long-term silencing of *Pcsk9* in the mouse liver by delivering methylation editors via lipid nanoparticles (LNPs) (Cappelluti et al. 2024a). Precisely, in hypercholesterolemia, *PCSK9* plays a crucial role in regulating cholesterol levels by controlling the degradation of low-density lipoprotein (LDL) receptor. Therefore, strategies to inhibit Pcsk9 are being explored to reduce cardiovascular risk. To this end, Cappeluttii and co-workers transiently deliver the ZFP-ETRs complexes (introduced in **4.2.3.4.2** section) targeting *Pcsk9* as an mRNA packed into LNPs (Cappelluti et al. 2024a).

In a similar way, other studies have used CRISPRa and CRISPR-mediated gene silencing administered with AAVs to treat diseases in mouse models such as Duchenne muscular dystrophy (DMD) (Liao et al. 2017), obesity (Matharu et al. 2019), neuropathologies (Moreno et al. 2021) and hypercholesterolemia (Thakore et al. 2018). Alternatively, generation of transgenic Cre-inducible epigenome editing mouse lines: dCas9-p300 for gene activation and dCas9-KRAB for gene repression (Gemberling et al. 2021). Thus, these preliminary works highlight great potential to use epigenome editing tools for therapeutic applications *in vivo* (McCutcheon et al. 2024).

CRISPR-based approaches for cell therapy involving *ex vivo* engineering of cells, such as CAR-T cells, and *in vivo* gene correction are currently in clinical trials. Importantly, this year, the first FDA-approved clinical trial using prime editing technology to treat chronic granulomatous disease (CGD) will start (Kohn et al. 2020). Moreover, at the end of 2023 the first-in-class ex vivo CRISPR-Cas9 gene therapy (Casgevy) was approved by the FDA and the MHRA for treating sickle cell disease (SCD) and transfusion-dependent β-thalassemia (Newby et al. 2021). Future improvements in safety, specificity, delivery

technologies, and durability might help incorporate next-generation CRISPR epigenome editors into clinical use.

OBJECTIVES

HYPOTHESIS AND OBJECTIVES

DNA methylation (DNAm) is an epigenetic modification that critically regulates gene expression in mammalian cells and thus has pivotal roles in determining cellular identity and function (Jones and Baylin 2002). Although DNAm has been extensively studied, using small inhibitor drugs leads to global alterations of the methylome. Also, they are not specific and, therefore, present a challenge to distinguish between direct or indirect effects on gene expression (Holtzman and Gersbach 2018; Greve et al. 2023).

Recent epigenome studies have offered valuable insights into the relationship between DNAm, transcription and immune identity (Álvarez-Errico et al. 2015). However, there is an urgent need for a more comprehensive understanding of the molecular mechanisms that drive changes in immune identity in response to DNAm alterations. The use of CRISPR/dCas9 DNA methylation editing tools that allow precise addition or removal of DNAm marks can help to better understand DNAm role in immune cell fate (McCutcheon et al. 2024).

In this thesis, we have investigated the potential of targeting specific DNA methylation events to alter myeloid cell fate and modulate the immune and inflammatory responses.

This main objective was achieved by the establishment of the following specific aims:

1. Dissect gene regulatory regions controlled by dynamic DNA methylation events during the C/EBPα-driven transdifferentiation (TD) of human leukemic B cells into induced macrophages (iMacs).

2. Study the causal relationship between DNA methylation and gene expression and its biological relevance through CRISPR/dCas9 DNA methylation editing.

3. To explore the consequences of DNAm editing by dCas9-DNMT3A at particular regions during human myeloid cell fate acquisition.

4. Interrogate the differential inflammatory response of DNA methylation-edited macrophages and their immune modulation capacity.

MATERIALS AND METHODS

METHODS

Cell lines and cell culture

BLaER cells are derived from a human B-cell precursor leukemia cell line (RCH-ACV) that stably expresses the myeloid transcription factor C/EBPα fused with the estrogen receptor (ER) and labeled with GFP(Rapino et al. 2013). BlaER cells and subclones were grown in suspension in RPMI 1640 (GIBCO) supplemented with 10% heat-inactivated FBS (GIBCO), 1X Penicillin-Streptomycin (GIBCO), 1X L-glutamine (GIBCO) and 0,1X β-mercaptoethanol (GIBCO). Culture medium was replaced every 2-3 days upon counting in a hemocytometer and using trypan blue exclusion dye to discriminate between live and dead cells. Then, cells were seeded at $2x10^5$ cells per ml into an appropriate tissue culture flask.

HEK-293T cells were grown in Dulbecco's Modified Eagle's Medium (DMEM) (+) D-glucose supplemented with 10% heat-inactivated FBS, 1X L-glutamine, and 1X Penicillin-Streptomycin. They were passed when confluent cultures were observed under the microscope (usually every 2-3 days). To pass the cells, medium was removed, and cells were washed once with 1X PBS to remove residual FBS that might interfere with the subsequent reaction. Next, pre-warmed trypsin-EDTA (GIBCO) solution was added to de-attach cells and after a brief incubation it was inactivated by adding fresh medium. Finally, cells were seeded at the desired density for lentiviral production.

For optimal growth, all cell lines were kept in a 5% CO2 humidified atmosphere at 37 ºC. Cells were checked for mycoplasma infection every month and tested negative.

Thawing and cryopreservation of cells

Frozen vials were rapidly thawed for 1 min at 37 ºC and were washed 2 times with PBS at 300 x g for 5 minutes to remove residual cryopreservative (DMSO) and were cultured with their expansion medium. For cryopreservation, cells were counted as previously described and then were frozen using a FBS 10% DMSO freezing solution. Vials were frozen in Mr. Frosty container at -80 ºC, this recipient allow the temperature to slow decrease at 1 ºC/min rate.

Transdifferentiation of human B cells into macrophages

To induce transdifferentiation of human leukemic B cells (B cells) into induced macrophages (iMacs), $2x10^5$ BLaER cells were seeded in a 12-well plate. To activate C/EBPα, 100 nM 17-beta estradiol (E2) (Sigma Aldrich), human IL-3 (10 ng per ml) (PeproTech) and human M-CSF (10 ng per ml) (PeproTech) were added to the medium to favor the conversion. Specifically, E2 induces C/EBPα-ER to shuttle from the cytoplasm to the cell nucleus where this factor develops its transcriptional activity. Additionally, human IL-3 and human M-CSF cytokines favor the conversion by mimicking stromal secreted cytokines. In overall, the whole process takes 7 days and not further addition of medium or cytokines is required (Rapino, et al 2013).

Cells were harvested at the indicated time points and processed for FACS analysis, RNA, DNA and phagocytosis assays.

Lentiviral production and cellular transduction with the DNA methylation editing tools

To transduce B cells with the DNA methylation editing tools, low-passaged HEK293T cells were seeded for transfection. Lentiviruses were produced in these cells by co-transfecting them with lentiviral plasmids VSV-G, psPAX2, and a transfer vector (Fuw-dCas9-DNMT3A-P2A-tagBFP -Addgene #84569-; Fuw-dCas9-TET1-P2A-tagBFP -Addgene #108245- and pLV GG hUBC-dsRED -Addgene #85034-) using calcium phosphate. Briefly, calcium phosphate-DNA preciptates were prepared by mixing the three plasmids in a 2.5M CaCl2 aqueous solution. While vertexing, one volume of the calcium phosphate-DNA solution was added dropwise to an equal volume of HBS 2X (HEPES-buffered saline solution pH = 7.05, 280 mM NaCl, 0.05 M HEPES and 1.5 mM Na2HPO4). The mixture was incubated for 15 minutes at room temperature and added dropwise to HEK-293T cells onto 150 mm dishes. After 14-16 hours of incubation at 37ºC, the transfection medium was replaced with f16 ml of pre-warmed DMEM. Supernatants containing lentiviral particles were collected and filtered through 0.45 µm strainers at 48- and 96-hours post-transfection. Lentiviral particles were then concentrated by centrifugation at 70.000 x g for 2 h at 10 ºC (AVANTI High-Speed Centrifuge - Beckman Coulter). The supernatant was properly discarded and 100 µl of PBS were added to resuspend the viral pellet. For that, tubes containing the concentrated lentivirus were incubated for 1h at 4 ºC while shaking.

BLaER or SEM cells were then spin-infected (1000 x g; 32 ºC for 90 min) with the concentrated viruses. Next, cells were cultured as described above and single-cell sorting of the BFP+ population was performed to generate stable dCas9-DNMT3A-P2A-BFP (hereafter dCas9-DNMT3A) or dCas9-TET1-P2A-BFP (hereafter dCas9-TET1) clones. Single sorted cells were then grown at 37ºC in 20% FBS-RPMI medium for 14-20 days to generate individual clones containing the dCas9-DNMT3A or the dCas9-TET1 epigenome editing tool.

To modify the methylation status, dCas9-DNMT3A and dCas9-TET1 clones were selected (based on their dCas9/BFP expression and protein levels). Next, selected clones were infected with lentiviruses harboring simultaneously 4 sgRNAs targeting the *IL1RN* gene promoter (sgIL1RN) and scramble regions (sgCTRL).

Guide RNA design

The design of the single guide RNAs (sgRNAs) targeting the *IL1RN* promoter (chr2:113,127,440-113,127,701) and CTRL regions was performed using Benchling sgRNAs design tool for CRISPR (https://www.benchling.com/crispr). sgRNAs close to a protospacer adjacent motif (PAM) with 5'-NGG-3' were selected with the best on-target and off-target scores. Multiplex sgRNA-dsRED (pVL GG hUBC-dsRED plasmid -Addgene # 84034-) construct was cloned using a two-step protocol as described by Engler and coworkers(Engler et al. 2008; Kabadi et al. 2014). Briefly, each protospacer was first annealed and cloned into the desired expression vector [phH1-gRNA (Addgene # 53186); ph7SK-gRNA (Addgene #53189); pmU6-gRNA (Addgene # 53187), and phU6-gRNA (Addgene #53188)] using a BbsI restriction

enzyme site. Next, four promoter-gRNA cassettes were cloned into the lentiviral destination vector GG hUBC-dsRED using Golden Gate assembly(Engler and Marillonnet 2014). Plasmids were sequenced using the M13 Reverse primer. Single gRNA sequences are listed in **Table 2.**

CSFE proliferation assay in cancer cells

To assess cell proliferation, dCas9-DNMT3A CTRL and sgIL1RN iMacs were treated for 24h with IL-1β (1ng per ml). Then, 2 million HCT-116 or Cal-12t cancer cells were stained with CFSE (Invitrogen Cat #C34570) following the manufacturer's instructions. Next, cancer cells were seeded at 10,000 cells per ml and grown with the supernatant collected from CTRL or sgIL1RN iMacs. Cells were analyzed for CFSE levels using a FACS Canto II flow cytometer. Data was analyzed with FlowJo software.

Immunocytochemistry and microscopy for p65

To assess p65 cellular localization, dCas9-DNMT3A CTRL and sgIL1RN iMacs were seeded at $0.8x10^6$ cells per ml on poly-lysine coated coverslips. After 2 days, iMacs were treated with IL-1β (1ng per ml) for 3h. Next, cells were fixed with 4% paraformaldehyde (in PBS) for 20 min and permeabilized with PBS + Triton X-100 0.5% for 10 min. Coverslips were washed twice with PBS, blocked with blocking solution (PBS + BSA 4% + 0.025% Tween 20) and incubated with an anti-p65 antibody (1:200 Abcam Cat #ab16502) overnight at 4ºC. After washing, cells were incubated with an anti-rabbit Alexa Fluor 647 (1:300

Invitrogen Cat #A21245) for 1 h at room temperature. After four washes with PBS, cells were stained with DAPI 2 µg per ml and mounted into slides using Vectashield (Vector Laboratories Cat # H-5700-60). Images were obtained with a Leica TCS-SL confocal microscope. ImageJ was used to quantify the mean intensity of the nucleus/cytoplasm ratio for p65 signal. 20 cells were counted for each sample.

shRNA-mediated IL1RN silencing

For constitutive shRNA-mediated gene silencing, oligonucleotide pairs encoding *IL1RN* shRNAs were annealed and cloned into pSICOR-PGK-puro (Addgene #12084). pSicoOligomaker 1.5 (https://venturalaboratory.com) was used to select and design oligos. The following shRNAs were used:

Luciferase shRNA (shLuc): CCTAAGGTTAAGTCGCCCTCG

IL1RN shRNA_1 (sh1): GCGTCATGGTCACCAAATT

IL1RN shRNA_2 (sh2): GTACTATGTTAGCCCCATA

BlaER cells were transduced with shLuc or shIL1RN lentiviruses and selected with puromycin (1 µg per ml) for 2 days.

Phagocytosis assay

Phagocytosis assays were performed using dCas9-DNMT3A CTRL and sgIL1RN iMacs. The assays were also performed in iMacs containing shRNA (shLuc and shIL1RN_1/2). In both cases, cells were seeded at $0.5x10^6$ cells per ml in DMEM media. Next, Fluoresbrite

carboxyl bright blue beads (1 µm, Polysciences Cat # 17458-10) were added to the media (300 beads per cell) and incubated for 24h before FACS analysis. Data was analyzed with FlowJo software.

Surface markers profiling

Stainings for CD14 and CD11b were conducted in dCas9-DNMT3A CTRL and sgIL1RN iMacs, as well as in iMacs with shRNAs (shLuc and shIL1RN_1/2). Briefly, cells were collected and incubated with Human FcR Binding Inhibitor (eBiosciences Cat #16916173) to avoid unspecific staining. Next, cells were stained against the macrophage marker CD11b (1:200 of CD11b-APC BD Pharmingen Cat #550019) and CD14 (1:200 of CD14-APC BD Pharmigen Cat #561383) and resuspended in PBS containing 7-AAD as a viability marker.

Western Blotting

Cells were harvested and centrifuged at 300 x g during 5 min and the supernatant was discarded. For protein extraction pellet cells were resuspended with lysis buffer (50mM Tris-HCl pH=7.4 1% Triton X-100 0.1% SDS Cocktail protease inhibitors) and incubated 1 hour on ice. Then, samples were centrifuged at 12.000 x g for 15 min and the supernatant was stored at -20ºC. For protein quantification Bradford Buffer (Bio-Rad) method was used and Bovine serum albumin was used as a standard. Assays were performed in 96-well plates in triplicated and measurement at 595 nm wavelength.

Next, 60 µg of sample were mixed with 4X Laemmli sample buffer (8% SDS, 40% glycine, 20% β-mercaptoethanol, 0,250 M Tris pH 6.8, 0,008% bromophenol blue) and boiled for 5 min at 95ºC. Protein

extracts were separated by electrophoresis and transferred to a nitrocellulose membrane. Membranes were blocked with 5% non-fat milk or 5% BSA for 1 hour at RT. Then, membranes were incubated overnight at 4ºC (while shaking) with the following primary antibodies: goat anti-IL1RN (RD Systems Cat # AF280NA) in 1:1000 in blocking solution and mouse anti-β actin (MERCK Cat # A1978) and rabbit anti-vinculin (Cell Signaling Cat #18799) 1:5000 in blocking solution. Membranes were washed 3 times in TBS-Tween before incubation with a secondary antibody anti-mouse IgG Alexa Fluor 790 nm (Invitrogen Cat #A11375), anti-goat IgG Alexa Fluor 800 nm (Invitrogen Cat# A32930) or anti-rabbit IgG Alexa Fluor 680 nm (Invitrogen Cat # A-21109) 1:5000 in blocking solution for 1 hour at RT. Finally, membranes were developed in an Odyssey CLx system. Image Studio Lite 5.2 (Li-COR) was used for visualization and quantification analysis.

Cytokine measurements

The LEGENDplex™ Human M1/M2 Macrophage Panel (10-plex) (BioLegend Cat# 740508) was used to quantify proinflammatory (IL-12p70, TNF-α, IL-6, IL-1β, IL-12p40, IL-23 and IP-10) and anti-inflammatory (IL-10, TARC, and IL-1RA) cytokines in the supernatant of dCas9-DNMT3A CTRL and sgIL1RN iMacs treated with IL1β for 24h. The recommended filter plate method was used, and all steps were followed per the manufacturer's protocol. Samples were acquired in a FACS Canto II flow cytometer, and LEGENDplex™ Data Analysis Software (BioLegend) was used for data analysis according to the manufacturer's recommendations. Samples were run in triplicates and included technical duplicates.

Real-time quantitative Polymerase Chain Reaction (RT-qPCR)

For total RNA extraction, 1 million cells were harvested and lysed in Trizol (eBioscences) reagent. Then, chloroform (Sigma Aldrich) was added and cells were centrifuged at 12.000 x g for 10 min at 4 ºC. After, the homogenate was separated into a clear upper aqueous phase (containing RNA) that was precipitated using isopropanol. RNA concentration and purity of the samples was determined in a Nano-Drop Spectrophotometer.

For retrotranscription, 500 ng of total RNA were converted into cDNA using the RNA to cDNA kit (Applied Biosystems) following the manufacturer's instructions. Real-time quantitative PCR reactions were performed using SYBR Green reagent and analyzed using QuantStudio 5 System (Applied Biosystems). *HPRT and B2M* were used as housekeeping genes. Unpaired student's t-test was used to determine statistical differences in gene expression among the different samples tested (t-test, ***p<0.001). Normality and homogeneity in variance were assumed for RT-qPCR experiments with biological triplicates.

To ensure primer specificity and avoid primer dimers, RT-qPCR primers were tested by standard curve method and checked for melting curves, standard curve and amplification plot parameters. Primer sequences are listed in **Table 3.**

RNA-seq

For the transdifferentiation experiment, approximately 1–2x10^6 dCas9-DNMT3A CTRL or sgIL1RN cells were collected in duplicates at 0, 3 and 7 days after C/EBPα induction. For the IL-1β

treatment experiment, dCas9-DNMT3A CTRL or sgIL1RN iMacs were collected in duplicates at 0, 3 and 16h after IL-1β (1 ng per ml) treatment. Total RNA was extracted with the RNeasy Mini Kit (QIAGEN Cat#74104) according to manufacturer's instructions and quantified with NanoDrop spectrophotometer. 0.2-0.5ug of RNA was used for mRNA sequencing with poly-A enrichment. Briefly, quality control with Fragment analyzer (Agilent) was performed before library preparation to ensure proper RNA integrity (RIN>7). A DNABSEQ Eukaryotic Strand-specific mRNA library protocol was used for library preparation. Then, libraries were sequenced in a DNABSEQ-G400 sequencer using a pair-end 150-bp protocol. More than 35 million reads were obtained for each sequenced sample.

Bisulfite conversion (BS) and pyrosequencing

Sample DNA methylation status was assessed by bisulfite pyrosequencing. Briefly, 1 ug of genomic DNA was bisulfite (BS)-converted using the EZ DNA Methylation Gold Kit (Zymo Research Cat# D5006) following the manufacturer's instructions. BS-treated DNA was PCR-amplified using the IMMOLASE DNA polymerase Kit (Bioline). Primers used for the PCR were designed with PyroMark Assay Design 2.0 software (QIAGEN) and listed in **Table 4**. PCR products were pyrosequenced with the Pyromark Q48 system (QIAGEN) according to the manufacturer's protocol and analyzed with PyroMark Q48 Autoprep (QIAGEN).

Whole Genome Bisulfite-seq (WGBS-seq)

Genomic DNA was extracted from 1 million cells at 0, 24, 96, and 168 hours of transdifferentiation using the DNeasy Blood & Tissue kit (QIAGEN Cat #69504) following the manufacturer's instructions and quantified using Qubit dsDNA (Invitrogen Cat #Q32851). Cytosine conversion, library preparation and sequencing were done by the provider of the sequencing services. Briefly, genomic DNA was fragmented to 200-400 bp and bisulfite converted. For library construction, sequencing adapters were ligated, followed by double-strand DNA synthesis and PCR amplification. Next, libraries were sequenced on Illumina HiSeqTM2500 using a pair-end 150-bp protocol rendering >70Gb/sample. Raw data quality assessment was performed, and low-quality reads were removed.

DNA methylation arrays

To assess potential off-target DNA methylation events caused by the dCas9-DNMT3A tool, we utilized the Infinium MethylationEPIC v2.0 Bead-Chip arrays (Illumina Cat #20087706). This platform allows the interrogation of around 935,000 CpG sites per sample at single-nucleotide resolution, covering 99% of the reference sequence (RefSeq) genes. 1 million CTRL or sgIL1RN cells were collected at 0 and 3 days after C/EBPα induction, with 4 biological replicates for each group. Genomic DNA was extracted, bisulfite-converted, and used to hybridize the methylation arrays following the manufacturer's instructions. Raw files (IDAT files) were provided by the Genomics Unit of the Josep Carreras Research Institute.

Chromatin immunoprecipitation (ChIP)

ChIP experiments were performed as previously described(Sardina et al. 2018). Briefly, 30 million cells were cross-linked with 1% formaldehyde in RPMI medium while rotating for 10 minutes at room temperature. To stop fixation, glycine was added to a final concentration of 0.125M and rotated for 5 minutes. Next, collected cells were washed twice with ice-cold PBS and resuspended in cold IP buffer (1 volume SDS buffer (100mM NaCl, 50mM pH8.1 Tris-HCl, 5mM pH8 EDTA, 0.2% NaN3, 0.5% SDS): 0.5 volume Triton dilution buffer (100mM NaCl, 100mM pH8.6 Tris-HCl, 5mM pH8 EDTA, 0.2% NaN3, 5% Triton X-100) supplemented with proteinase inhibitors (Roche Cat #118733580001). Chromatin was sheared to 100-300bp fragments on a Bioruptor pico sonicator (Diagenode) at 4ºC for 13 cycles with 30 sec on and 30 sec off in 15 ml Bioruptor Tubes (Diagenode Cat #C30010017) with 650 mg of beads (Diagenode Cat #C03070001). After sonication, cell lysate was spun down at 20,000xg for 20 min at 4ºC to remove debris and 5% of supernatant was saved as input. Chromatin was conjugated with 10ug of anti-Cas9 antibody (Active Motif Cat #61757) while rotating ON at 4ºC. The next day, 50 ul of Dynabead A/G mix were blocked for 2h at 4ºC with BSA 5mg per ml while rotating and added into antibody-cell lysate mixture for immunoprecipitation for 3h at 4ºC in rotation. Chromatin-antibody-bead complexes were washed three times with ice-cold low salt buffer (50mM pH7.5 HEPES, 140mM NaCl, 1% Trito X-100) and once with ice-cold high salt buffer (50mM pH7.5 HEPES, 500mM NaCl, 1% Triton X-100). Bound protein-DNA complexes were de-crosslinked in elution buffer (1% SDS, 0.1M NaHCO3) by overnight incubation at 65ºC with shaking at 1300 rpm. The next day, the eluted portion was treated with RNAse for 1h at 37ºC and then with

Protein K for 2h at 65ºC. Finally, DNA was purified by phenol:chloroform:isoamyl alcohol (25:24:1) extraction and ethanol precipitated.

For ChIP-qPCR analysis, DNA was diluted 1:10, and relative enrichment was calculated as a percentage of input with the following formula (100*2^(Adjusted input - Ct (IP)). Oligonucleotide sequences are indicated in **Table 5.**

For ChIP-seq, samples were quantified with Agilent 2100 before library preparation. Library preparation and sequencing were performed by the sequencing service provider using a DNABSEQ-G400 sequencer and a SE50 protocol.

Bioinformatic analyses

All sequencing data obtained were mapped onto the human genome assembly hg38 (Ensembl GRCh38) and analyzed with R (4.2.1) using packages from the Bioconductor suite (v3.0)(Huber et al. 2015). For peak calling, regions overlapping the 'Encode blacklist' regions were removed(The ENCODE Project Consortium 2012), as well as mitochondrial reads. Peaks were annotated to genomic features in R with the package ChIPseeker (v1.32.1)(Yu et al. 2015), using Benjamini-Hochberg (BH) FDR corrections. All Gene Ontology (GO) enrichment analyses were performed using the clusterProfiler package (v4.4.4)(Yu et al. 2012). Pathway enrichment analysis was performed with the Reactome Pathway Database Analysis Tool(Milacic et al. 2024). Gene Set Enrichment Analysis (GSEA) was done using MSigDB gene sets(Subramanian et al. 2005), and analyses were performed in R with

the fgsea (v1.30.0)(Korotkevich et al. 2016) and clusterProfiler packages (v4.4.4). Bigwig tracks were generated using DeepTools BamCoverage (3.3.1)(Ramírez et al. 2014). Motif enrichment analyses were performed using the function findMotifsGenome.pl from the package HOMER (v0.2)(Heinz et al. 2010). The integration of DNA methylation and ATAC-seq data was carried out using the bedtools (v2.31.1)(Quinlan and Hall 2010) package. Heatmaps and clustering analyses were performed using the ComplexHeatmap (v2.10.0) package(Complex heatmap visualization - Gu - 2022 - iMeta - Wiley Online Library). The Multidimensional Scaling (MDS) and Principal Component Analysis (PCA) were performed using the limma (v3.52.2)(Ritchie et al. 2015), and factoextra packages (v1.0.7), respectively. Upset plots were generated using the upsetR package (v1.4.0)(Conway et al. 2017). The correlation analyses were performed and plotted with the R package corrplot (v0.92). The RNA-seq MA plots were generated using the R package DESeq2 (v1.36.0)(Love et al. 2014). The remaining plots were generated using the R package ggplot2 (v3.4.2). Genome-wide statistical analyses were performed using a two-tailed student t-test to compare two groups using the R package stats (v4.2.1).

WGBS-seq analysis

Raw sequence reads from WBGS libraries were trimmed to remove poor-quality reads and adapter contamination using the package Trimmomatic (v0.36)(Bolger et al. 2014). The remaining sequences were mapped using Bismark (v0.16.3)(Krueger and Andrews 2011), to the human reference genome GRCh38 in paired-end mode. Reads were then deduplicated, and CpG methylation calls were

extracted from the deduplicated mapping output using the Bismark methylation extractor in paired-end mode. The estimation of DNA methylation levels was calculated by dividing the count of reads identifying a cytosine (C) by the sum of reads identifying either a cytosine (C) or a thymine (T). Only CpGs with coverage equal to or higher than 5X in all tested samples were used for downstream analyses. N = 24,298,869 CpGs analyzed. The genome was split into 1Kb bins using the function makewindows from the bedtools(Quinlan and Hall 2010) package. DNA methylation signal was quantified by calculating the mean methylation on these 1Kb bin regions. Only bins with at least 3 CpGs covered at least 5X in all tested samples were used for downstream analyses. N= 2,807,124 bins analyzed.

Dynamic DNAm bins containing Gene Regulatory Elements (GREs) were identified by overlapping those bins with ATAC-seq peaks, either located at a TSS (promoter) or at an H3K4me1 peak, as previously described(Stik et al. 2020).

Analysis of DNA methylation arrays

IDAT raw data from the MethylationEPIC BeadChip 850k v2.0 microarrays was loaded using R to perform all the analyses, QC, and preprocessing steps using the package minfi (v1.42.0)(Aryee et al. 2014). Probes with low detection p-value (<0.1), probes with a known SNP at the CpG site, and known cross-reactive probes were removed. For the resulting CpGs, beta values were calculated using minfi functions. DMPs were calculated using the limma package (v3.52.2)(Ritchie et al. 2015) in R, adjusting by the Benjamini-Hochberg method. Only DMPs with adjusted p-values (FDR)< 0.05 and a

differential of DNA methylation equal to or greater than 30% ($\Delta\beta \geq 0.3$) were selected for further analyses.

RNA-seq analysis

Reads were mapped using STAR (v2.7.6)(Dobin et al. 2013). Gene expression was quantified using the function featureCounts from the package Subread (v2.0.3)(Liao et al. 2014). Differentially expressed genes were detected using the R package DESeq2 (v1.36.0)(Love et al. 2014), applying FDR<0.05. Transcription factors' activities were inferred from expression values using DoRothEA(Garcia-Alonso et al. 2019).

scRNA-seq analysis

The processed scRNA-seq dataset of monocytes and macrophages (MoMac-VERSE) is publicly available at the FG Lab Resources website (https://gustaveroussy.github.io/FG-Lab/). Information about cross-tissue integration and data processing was described by Mulder and co-workers(Mulder et al. 2021). Data analysis was done in R with the Seurat package (v5.1.0)(Hao et al. 2021). Pre-established clustering counts normalization/scaling, and metadata for paired healthy versus cancer conditions was used for the downstream analysis. For gene signature enrichment (up-regulated vs down-regulated) analysis, only the most significantly differentially expressed genes (log2FC>0.5, FDR<0.05) at each time point were considered. For statistical analysis, healthy versus cancer comparisons were evaluated for cell populations that presented at least 15 cells for each condition. Significant differences in gene expression were calculated using two-

sided Wilcoxon rank-sum tests with the compare_means() function in R ggpubr package (v0.6.0).

ChIP-seq analysis

For the ChIP-seq analysis, reads were trimmed using the TrimGalore package (v0.6.6) to remove adaptors and mapped using Bowtie2 (v2.4.4.1)(Langmead and Salzberg 2012). Duplicated reads were removed with the tool MarkDuplicates from the package Picard (v3.1.0)(Picard Tools - By Broad Institute. html: (https://broadinstitute.github.io/picard/)). Peaks were called using MACS2 (v2.2.5)(Zhang et al. 2008), parameter (-q 0.05). Differential enrichment analysis was performed using the edgeR(Chen et al. 2024), function from the diffBind package (v3.6.5) and filtering by FDR<0.05 and log2FC>2.

RESULTS

RESULTS

CHAPTER 1: Genome-wide correlation studies between DNA methylation and transcription during human myeloid commitment

As mentioned in the Introduction, previous studies have shown the relevance of DNA methylation (DNAm) in immune cell differentiation and determination of their identity. Still, the impact of DNA methylation dynamics at gene regulatory regions (GREs) and their role in gene expression during immune cell fate are not completely understood.

Accordingly, we investigated how changes in DNAm at gene regulatory regions (GREs) impact gene expression during the reprogramming of human leukemic B cells into non-tumorigenic macrophages (Rapino et al. 2013).

1. Whole-genome Bisulfite Sequencing reveals DNA methylation reshaping during human B-cell to macrophage TD

To gain insight into the dynamics of DNAm during myeloid cell fate acquisition, we chose to utilize the highly efficient and homogenous C/EBPα-driven conversion of human B leukemic cells, containing a β-estradiol inducible form of C/EBPα (BlaER cells), into non-tumorigenic induced macrophages (iMacs)(Rapino et al. 2013). The iMacs generated using this protocol closely resemble their natural counterparts as they are fully phagocytic and have inflammasome competency(Rapino et al. 2013; Gaidt et al. 2016; Stik et al. 2020).

Cultured B cells were treated with β-estradiol (E2) and collected at different time points of the cell fate conversion process (0h -B cells-; 24h; 96h and 168h -iMacs-) **(Fig. R1.1a)**. We then generated genome-wide, nucleotide-resolution maps for DNAm by Whole-Genome Bisulfite Sequencing (WGBS-seq) by computing the values of approximately 24 million CpG residues that were covered ≥5X in all the samples.

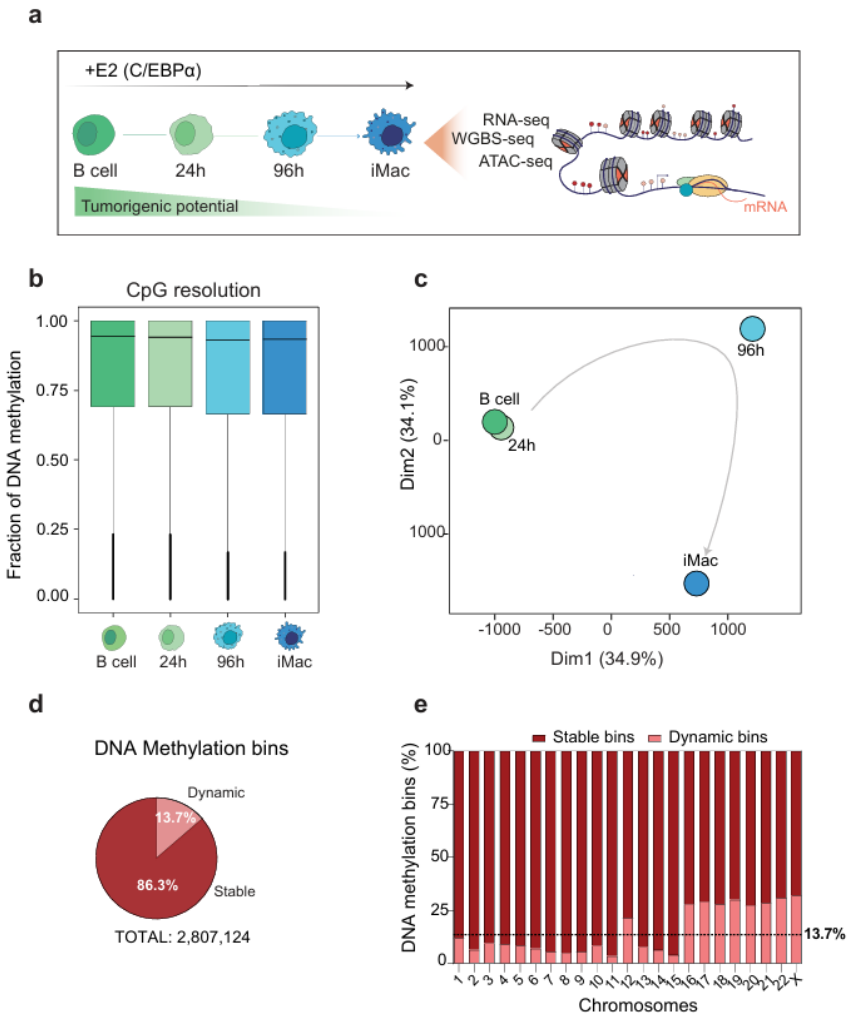

Fig. R1.1. WGBS-seq genome-wide DNA methylation profiling during TD. (a) *Left: Schematic representation of the C/EBPα-mediated TD of human B cell line (B cell) into induced macrophages (iMac). Right: overview of methodology used in the epigenome profiling.* ***(b)*** *Genome-wide DNAm levels at CpG resolution during TD. N (number of CpGs analyzed) = 24,298,869.* ***(c)*** *Multidimensional Scaling (MDS) showing DNAm dynamics at 1kb bins genome-wide during TD* ***(d)*** *Pie chart showing the genome-wide percentage of DNAm stable and dynamic 1kb-bins observed during TD. N (number of bins analyzed) = 2,807,124.* ***(e)*** *Percentage of DNAm stable and dynamic 1kb-bins observed during TD across chromosomes. The dashed line represents the percentage of dynamic bins (13.7%); Right:* *Pie chart showing the genome-wide percentage of DNAm stable and dynamic 1kb-bins observed during TD. N (number of bins analyzed) = 2,807,124.*

We first analyzed the genome-wide DNAm levels at CpG resolution, observing subtle changes from 96h upon TD (**Fig R1.1b**

To better analyse these changes in conjunction with other epigenomic layers, we split the genome into 1kb bins and calculated the mean methylation of these regions, resulting in the analysis of 2 million bins. As shown in **Fig R1.1c**, PCA analysis showed a genome-wide reshaping of DNAm from 96 hours after C/EBPα induction.

Next, to explore the role of DNAm changes during TD we classified bins as stable or dynamic. Bins that were not changing >10% methylation between any time point of TD, and therefore were maintained, were defined as stable. On the contrary, bins that were changing >10% and get redistributed during TD were defined as dynamic. Although most of the bins were stable, 14% of the DNAm signal, which accounts for 384,127 1kb bins, was redistributed during this process **(Fig. R1.1d)**. Interestingly, the redistribution of the DNAm signal did not occur randomly in the genome; instead, it occurred preferentially on specific chromosomes, such as Chromosome X. Approximately 32% of the DNAme signal on ChrX is rewired during the process (2.2-fold over the genomic average) **(Fig. R1.1e)**. Therefore, a

more detailed characterization of those dynamic DNAm changes might be relevant during cellular differentiation.

2. Interplay between DNA demethylation and chromatin accessibility at GREs during transdifferentiation.

To further understand the genomic context where the redistribution of DNAm occurs, we intersected the DNAm dynamic regions detected (**Fig. R1.1d**) with previously published ChIP-seq data collected during the transdifferentiation (TD) process (Stik et al. 2020; Choi et al. 2021). In particular, we analyzed GREs at promoters and enhancers, both defined by chromatin opening (by ATAC-seq). Specifically, to distinguish promoters and enhancers regions, promoters were termed when associated with TSS and enhancers the genomic positions enriched with H3K4me1 mark. As a result, only 8% of all dynamic bins, which accounts for ~ 32,000 1kb bins, were identified as containing Gene Regulatory Elements (GREs).

Since previous studies had shown the relevance of GREs for cell fate decisions (Hon et al. 2014b), we focused all our further DNAm analyses exclusively on them. We next classify dynamic DNAm bins containing GREs into 4 major clusters (C-I to C-IV) based on the timing of their DNAm changes. Interestingly, the clusters exhibited predominantly sequential and mostly transient changes in DNAm (C-I to C-III), except for cluster IV **(Fig. R1.2a)**. Cluster IV, containing approximately one-third of the total number of regions (n= 11,601), showed continuous loss of DNAm from 96 hours onward **(Fig. R1.2a)**.

In line with this observation, only regions included in clusters showing demethylation from 96 hours onwards (C-III and C-IV)

experienced an increase in chromatin accessibility (by ATAC-seq) during the reprogramming process **(Fig. R1.2b)**. Conversely, no chromatin closure was observed in association with the gain of DNAm (cluster I regions) **(Fig.R1.2b).** Thus, suggesting DNAm gain might not regulate chromatin accessibility in this cellular model of myeloid cell fate acquisition.

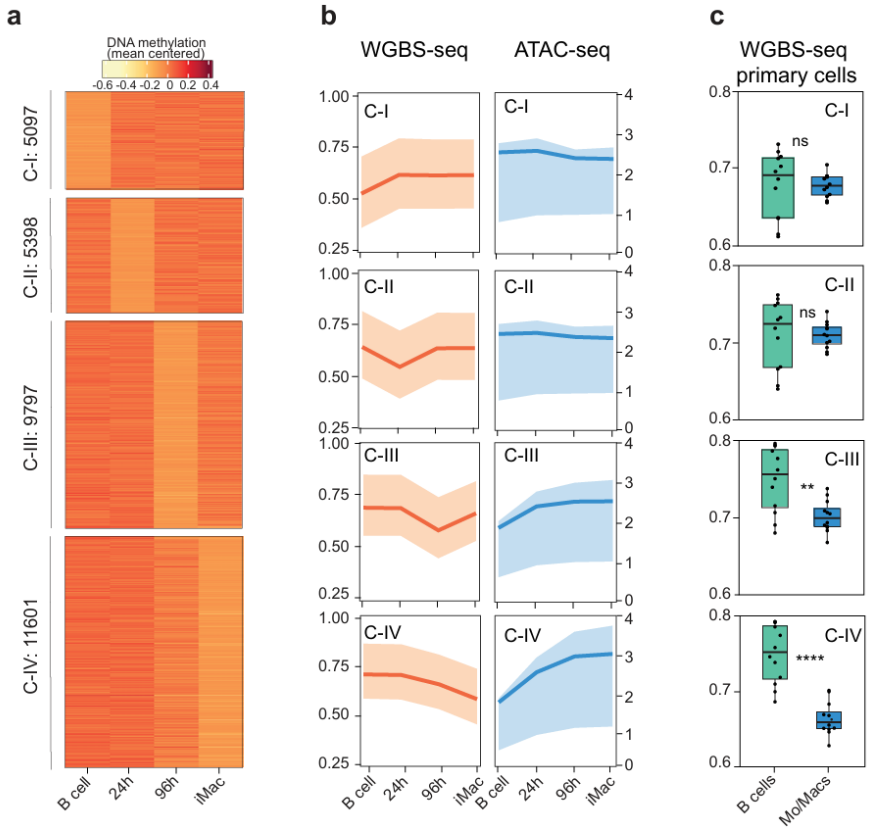

Fig. R1.2. GREs at defined clusters show continuous and transient DNAm and accessibility states during TD and primary human MoMacs. (a) *Clustering of genome-wide DNAm dynamics at 1kb bins showing at least 10% DNAm changes. Bins are defined by containing ATAC+ regions associated with promoters or enhancers during TD.* ***(b)*** *Quantification of DNAm levels (DNAm fraction-) and chromatin accessibility (RPKMs) at the clusters in (a). ATAC-seq data from GSE131620*(Stik et al. 2020; Choi et al. 2021). ***(c)*** *DNAm levels (by WGBS-seq) in primary human B cells (4 B-ALLs, 4 CD38-negative näive B cells, 3 naïve B-cells, 1 precursor B cell) and primary human monocytes n=6 and macrophages n=6 at the clusters in (a). Two-sided Wilcoxon rank-sum test (**p<0.01, ****p<0.0001; n=12). Data collected from the Blueprint Consortium.*

We next sought to determine if the detected changes could also be observed in a human physiological setting. To do this, we compared methylation changes in the 4 cluster regions between primary human B cells and primary human monocytes and macrophages (data from Blueprint consortium). The primary B cells exhibited higher global levels of DNA methylation compared to myeloid cells, consistent with the findings in the cellular model. However, the differences were only statistically significant for the regions associated with C-III and C-IV, indicating that these regions may contain relevant GREs for primary myeloid cells **(Fig. R1.2c).**

3. Macrophage gene regulatory regions lose methylation during transdifferentiation

To investigate if particular GREs were important for myeloid acquisition, we specifically analyze changes in DNAm at chromatin-accessible regions (ATAC-positive) between B cells and iMacs. In iMacs, we observed that most ATAC-positive regions were losing DNAm (7,603), including regulatory regions of well-known myeloid genes such as *ITGAM*, *MAFB* and *TET2*. These DNAm loss regions were preferentially associated with clusters C-III and C-IV **(Fig. R1.3a, b)** from the dynamical clustering in **Fig. R1.3b**. On the other hand, a small proportion of ATAC+ regions were gaining methylation, accounting for 1,858 regions, including regulatory regions of *MECOM, BRD4* or *PAX5* genes, among others. These DNAm gain regions were preferentially associated with clusters C-I and II **(Fig. R1.3a, b)** from the dynamical clustering in **Fig. R1.3b**.

We next examined the genomic distribution of DNAm gain and loss regions to study a possible correlation between DNAm and open

chromatin **(Fig. R1.3c)**. The gain regions mainly overlapped with introns and promoters at similar percentages (35.9% and 29.1%, respectively). Conversely, in the loss regions, there was a preferential enrichment in intronic regions, possibly intragenic enhancers, at the expense of promoters **(Fig.R1.3c).**

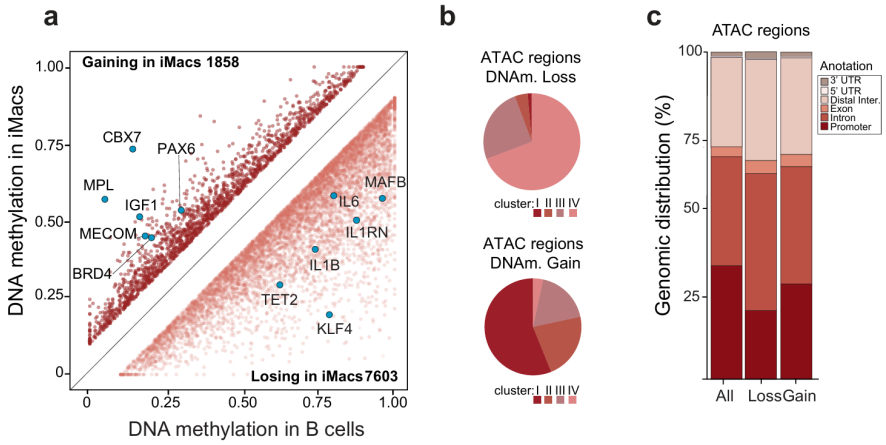

Fig. R1.3. Macrophage GREs (ATAC+) are losing DNA methylation are associated with cluster III and IV (a) *Scatter plot comparing DNAm levels at iMac's (ATAC+ peaks) in iMacs versus in B cells. Dark red dots indicate ATAC+ regions gaining at least 10% (n=1858) of DNAm in iMacs; light red dots indicate ATAC+ regions losing at least 10% (n=7603) of DNAm in iMacs. Blue dots highlight ATAC+ regions of interest.* ***(b)*** *Piecharts depicting the proportion of ATAC+ DNAm loss and gain regions in Fig. R1.2c belonging to the methylation clusters in Fig. R1.2a.**(c)*** *Distribution of ATAC+ DNAm loss and gain regions in iMacs along the different genomic features analyzed (promoters, introns, exons, distal intergenic, 5' UTR and 3'UTR regions). All ATAC+ regions analyzed (All) are shown as a distribution control.*

To uncover biological processes potentially regulated by the DNAm changes described, we performed Gene Ontology (GO) analysis of the genes located at the ATAC-positive DNAm loss and gain regions **(Fig.R1.4a)**. This showed enrichment of terms related to myeloid cells for genes associated with loss regions, including "Myeloid leukocyte migration," "Phagocytosis," and "Positive regulation of cytokine

production," among others. On the other hand, the gain regions were unspecifically associated with terms related to organ development, such as "Axon guidance," "Kidney development," and "Heart morphogenesis," among others **(Fig.R1.4a)**. In line with these findings, Transcription Factor (TF) motif analysis showed significant enrichment of TFs relevant for myeloid cell biology, such as AP1 complex subunits (including Fos, JunB, BATF, Fra1-2, among others) and CEBP factors, in the ATAC-positive DNAm loss regions **(Fig.R1.4b)**. In contrast, the DNAm gain regions displayed a modest enrichment in the motifs of genome architecture TFs, including CTCF and its relative BORIS (also known as CTCFL), along with development related transcription factors such as Hox, Slug, or Snail, among others **(Fig.R1.4b)**.

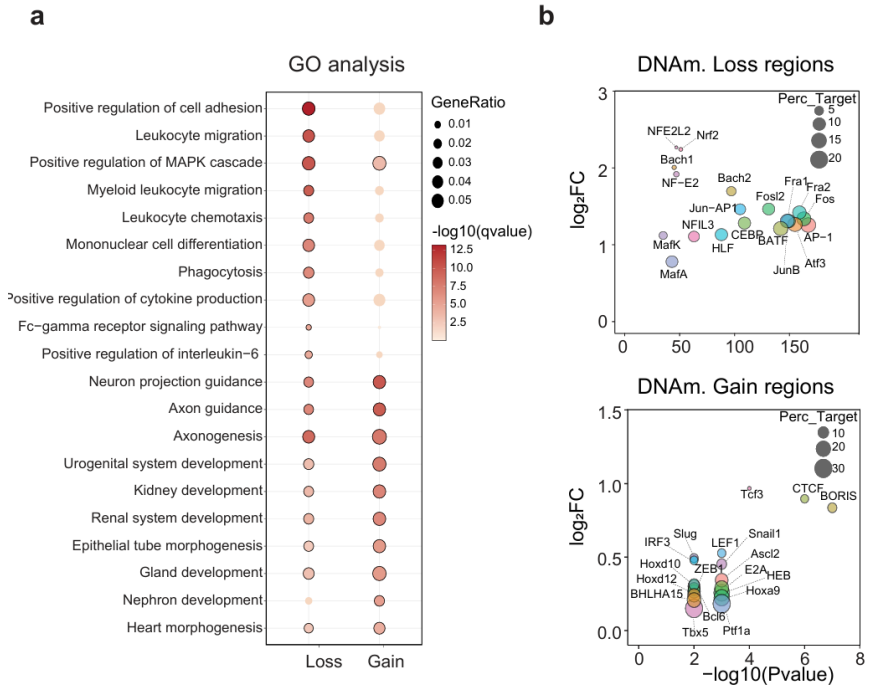

Fig R1.4. DNAm loss regions are associated with inflammatory-related genes and enrichment of AP-1 and C/EBP-myeloid TF (a) *Balloon plot depicting the Gene Ontology (GO) enrichment analysis for the genes associated with the ATAC+ DNAm loss and gain regions in iMacs (related to Fig. R1.3a). 10 significant biological processes (BP)*

terms for each category are plotted. GeneRatio and -log10(qvalue) are shown. Significant terms (qvalue < 0.05) are highlighted with a black stroke ***(b)*** *Bubble plot showing the output of TF enrichment analyses (by HOMER2) at ATAC+ DNAm loss (up) or gain (bottom) regions in iMacs. X-axis reports the –log10(P-value); Y-axis depicts the log2FC; the circle size is related to the percentage of target sequences containing the motif.*

Altogether, this suggests that specific GREs related to myeloid cells are undergoing DNA demethylation and potential chromatin activation during the B-to-macrophage reprogramming. At the same time, GREs unrelated to the cell fate conversion process are gaining DNAm without apparent changes in chromatin activity.

4. Integrative analyses reveal the *IL1RN* promoter as a top event showing a DNA methylation-expression correlation

To gain mechanistic insight into the transcriptional consequences of the DNAm changes observed at GREs, we investigated the interplay between DNAm and gene expression using publicly available RNA-seq data in our cellular model (Stik et al. 2020; Choi et al. 2021). We observed no correlation between the gain of DNAm at ATAC-positive regions and changes in gene expression of their associated genes (R=-0.018; pval=0.64) **(Fig.R1.5a)**. Meanwhile, a significant negative correlation was detected between DNAm loss and gene expression, both at ATAC-positive regions non-associated with promoters (R= -0.132; pval=$7.2x10^{-10}$) **(Fig.R1.5b)** and even stronger correlation when they were overlapping promoters (R= -0.241; pval=$2.2x10^{-16}$) **(Fig.R1.5c)**.

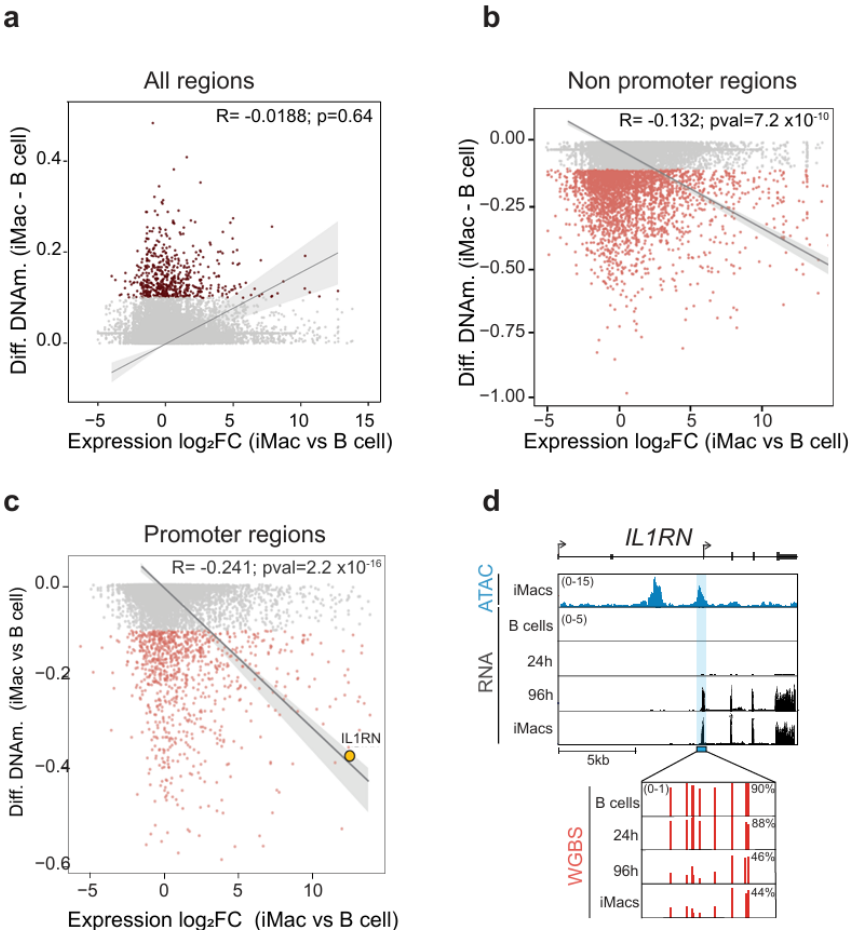

Fig. R1.5. IL1RN promoter undergoes DNA demethylation and gene activation during TD. ***(a)*** *Correlation plot between DNAm and gene expression at iMac's ATAC+ peaks. Grey dots: ATAC+ regions not gaining at least 10% in DNAm. Dark red dots: ATAC+ regions gaining at least 10% in DNAm in iMacs. RNA-seq data from GSE140528*(Stik et al. 2020; Choi et al. 2021). ***(b-c)*** *Correlation plot between DNAm and gene expression at iMac's ATAC+ peaks* ***(b)*** *non-overlapping annotated promoters* ***(c)*** *and overlapping annotated promoters* ***(c)*** *Grey dots: ATAC+ promoter regions not losing at least 10% in DNAm. Light red dots: ATAC+ promoter regions losing at least 10% of DNAm in iMacs. RNA-seq data from GSE140528*(Stik et al. 2020; Choi et al. 2021). ***(d)*** *Genome browser snapshot showing signal for ATAC-seq in iMacs, and RNA-seq during TD at the IL1RN locus. The blue-shaded region represents the promoter of the IL1RN short isoform (ENST00000409930.4).*

The promoter of the Interleukin-1 receptor antagonist (*IL1RN*) gene, which shows a DNAm loss over 40% and an expression increase of more than 1000-fold between iMacs and B cells, emerged as a top correlated event in the analysis **(Fig.R1.5c)**. The *IL1RN* gene, which plays an essential role in inflammatory responses in mature myeloid cells(Gabay et al. 2010), is not expressed and its promoter is fully methylated at the B cell stage **(Fig.R1.5d)**. However, the methylation of the *IL1RN* promoter decreases between 24 and 96 hours, which coincides with the reactivation of the gene **(Fig.R1.5d)**. These changes occur specifically in the promoter of the *IL1RN* short isoform, IL1RN-205 (ENST00000409930.4), which corresponds to the secretory protein variant preferentially expressed in myeloid cells (Gabay et al. 2010).

These analyses suggest that only gene regulatory regions losing DNAm, such as the promoter of the *IL1RN* gene, but not regions gaining it, are correlated with changes in gene expression during transdifferentiation. Notably, as shown in **Fig.R1.2c** these regions are hypomethylated in primary human monocytes and macrophages, indicating that DNAm losses in this context may influence human myeloid cell commitment and inflammatory properties.

CHAPTER 2: Employing dCas9-methylation editing tools to modify the DNA methylation status of the *IL1RN* promoter

1. dCas9-TET1-mediated demethylation of the *IL1RN* promoter is sufficient for its gene reactivation

While the phenotypes associated with the loss of function of major DNAm regulators have been extensively studied(Dawlaty et al. 2014; Charlton et al. 2020), the impact of individual methylation events

on immune phenotypes remains largely unexplored, mainly due to technical limitations(Holtzman and Gersbach 2018). This has been recently challenged with the advent of DNAm editing tools, especially those associated with CRISPR technology as mentioned in the Introduction section(Stricker et al. 2017).

Since the *IL1RN* promoter is hypermethylated and its associated gene is not expressed in B cells **(Fig.R1.5d),** we speculated about the possibility of inducing DNA demethylation specifically at this region to force *IL1RN* expression at the B cell stage. To address this challenge, we stably integrated a previously developed DNA demethylation editing tool (Liu et al. 2016a, 2018b) into our human B leukemic cells **(Fig.R2.1a)**. The editing tool is based on a catalytically dead Cas9 protein tethered with the catalytic domain of the DNA methylcytosine dioxygenase TET1 (dCas9-TET1). B cell clones expressing high levels of the dCas9-TET1 transgene were selected and expanded. Afterward, we transduced dCas9-TET1 clones with lentiviruses simultaneously encoding 4 different sgRNAs that targeted either no sequence within the genome (CTRL cells) or the *IL1RN* promoter (sgIL1RN cells) **(Fig.R2.1a)**.

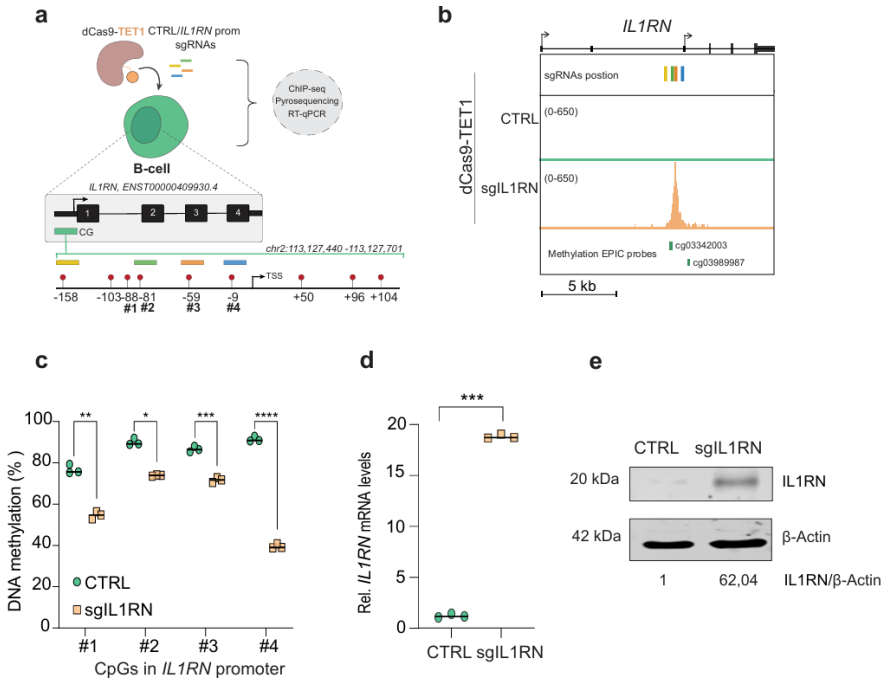

Fig. R2.1. dCas9-TET1 led to IL1RN promoter demethylation and gene reactivation

(a) *Top: schematic diagram illustrating the integration strategy of dCas9-TET1 tool and sgRNAs targeting IL1RN promoter in B cells. Bottom: representation of the sgRNAs targeting regions upstream the TSS of the IL1RN promoter. The sgRNAs are shown in yellow, green, orange, and blue, with the CpG sites as red lollipops. #1 to #4 indicate the CpG residues analyzed in the experiment.* ***(b)*** *Genome browser snapshot showing the dCas9-TET1 binding at the IL1RN promoter region. The location of the 4 sgRNAs targeting the IL1RN promoter are depicted.* ***(c)*** *DNAm levels (by pyrosequencing) at 4 CpG residues located upstream of the IL1RN TSS (as shown in R2.1a) in dCas9-TET1 sgIL1RN and CTRL B cells. One-way ANOVA with Dunnett's post-hoc correction, n=3, mean ± s.e.m., (*p<0.05; **p<0.01, ***p<0.001,****p<0.0001).* ***(d)*** *IL1RN Expression (RT-qPCR) in dCas9-TET1 sgIL1RN and CTRL B cells. Values were normalized against HPRT expression. Unpaired two-tailed Student's t-test, n=3, mean s.e.m., (***p< 0.001).* ***(e)*** *Western blot image of IL1RN protein in dCas9-TET1 sgIL1RN and CTRL B cells. IL1RN levels were normalized to β-Actin levels and expressed as a fold change over shLuc iMacs.*

We first tested by ChIP-seq against the Cas9 protein that the dCas9-TET1 complex was bound to the *IL1RN* promoter. We observed a strong binding in the sgIL1RN B cells compared to CTRL B cells. **(Fig.R2.1b)**. Next, to analyze DNAm changes after targeting with dCas9-TET1 we performed a pyrosequencing analysis at the *IL1RN* promoter region. Notably, dCas9-TET1 recruitment led to the demethylation of CpG residues located upstream of the gene's TSS **(Fig.R2.1c)**. Among them, the largest demethylation (approximately 50% decrease) was observed at the CpG residue located just upstream of the TSS (-9bp) **(Fig.R2.1ca)**. Thus, we could validate dCas9-TET1 editing tool in B cells. Next, we analyzed if *IL1RN* was differentially expressed upon demethylating the region with the dCas9-TET1 tool. Importantly, we detected *IL1RN* gene activation (>15-fold increase in mRNA levels) and protein accumulation (>60-fold increase) in sgIL1RN B cells **(Fig.R2.2d-e)**. Additionally, a preliminary analysis of a recently generated RNA-seq dataset has revealed a distinct transcriptional profile between CTRL and sgILRN cells upon reactivating the *IL1RN* gene with dCas9-TET1. Precisely, we identified roughly 7,000 differentially expressed genes, including 4,039 up-regulated and 2,975 down-regulated genes. Of note, the up-regulated genes were enriched in Gene Ontology terms related to myeloid cells (data not shown).

Thus, dCas9-TET1 editing successfully activated the expression of a myeloid gene in an inappropriate immune cell type (B-lymphoid cells), leading to a modified cell fate change. This allowed us to unveil a causal relationship between the DNAm status of the *IL1RN* promoter, the expression of its gene, and an altered cellular fate.

2. dCas9-DNMT3A binding specificity during TD

As previously shown, the *IL1RN* promoter is demethylated between 24 and 96 hours of the cell fate conversion process, coinciding with the reactivation of its gene **(Fig. R1.5d)**. Therefore, based on the observed causality between DNAm and *IL1RN* expression **(Fig.R2.1c-d)**, we hypothesized that blocking the DNAm loss associated with the transdifferentiation process would alter *IL1RN* gene expression patterns. To tackle this task, we used a previously developed DNAm editing tool (Liu et al. 2016b, 2018b) based on a catalytically dead Cas9 protein tethered with the catalytic domain of the DNA *de novo* methyltransferase DNMT3A (dCas9-DNMT3A). Both, the DNAm editing tool and the sgRNAs were integrated into our human B leukemic cells as previously outlined for the dCas9-TET1 experiment **(Fig.R2.2a)**.

We initially examined the genome-wide binding sites for dCas9-DNMT3A, comparing sgRNA and CTRL cell lines. By ChIP-seq, we observed dCas9-DNMT3A strongly and specifically bound to the *IL1RN* promoter in sgIL1RN B cells, coinciding with the location of the sgRNAs **(Fig. R2.2b)**. However, as expected from previous research using these DNAm editing tools (Galonska et al. 2018; Liu et al. 2018a; Pflueger et al. 2018), we also observed the off-target binding of the dCas9-DNMT3A protein to 852 genomic regions **(Fig. R2.2c)**. Of note, some of the strongest off-target sites ($Log_2FC>3.5$) were identified as overlapping promoters. Therefore, the recruitment of the dCas9-DNMT3A protein may result in the hypermethylation of these promoters and the deregulation of their genes. To explore this possibility, we analyzed the expression and methylation in B cells of all the off-target sites annotated as promoters. Among all the regions analyzed, no

differences in methylation and expression were detected, suggesting minimal off-target effects of dCas9-DNMT3A during TD (**Fig. S1**).

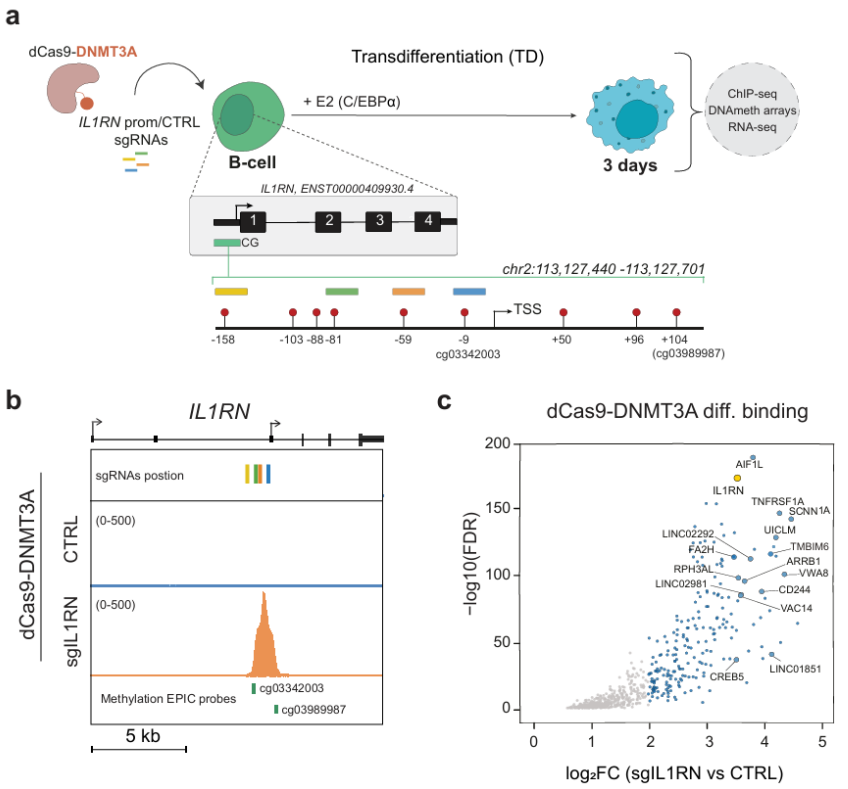

Fig. R2.2. Efficient recruitment of dCas9-DNMT3A at IL1RN promoter by ChIP-seq. ***(a)*** *Top: schematic diagram illustrating the integration strategy of dCas9-DNMT3A tool and sgRNAs targeting IL1RN promoter in B cells. Bottom: as explained in (R2.1a). 2 Infinium MethylationEPIC v2.0 probes are shown in –9 (cg03342003) and +104 (cg03989987) positions.* ***(b)*** *Genome browser snapshot showing the dCas9-DNMT3A binding at the IL1RN promoter region. The location of the 4 sgRNAs targeting the IL1RN promoter and the 2 array probes are depicted.* ***(c)*** *Scatter plot showing differential dCas9-DNMT3A enrichment in sgIL1RN B cells over CTRL B cells. Blue dots indicate regions more enriched in sgIL1RN B cells than CTRL B cells (Log2FC>2, p<0.05, n=853). Large blue dots and the yellow dot (IL1RN prom) (Log2FC>3.5, p<0.05).*

3. dCas9-DNMT3A specifically hypermethylates the *IL1RN* promoter, leading to its downregulation.

We then examined the potential impact of dCas9-DNMT3A on methylation and expression 3 days after C/EBPα activation, when the *IL1RN* promoter has started losing methylation (**Fig. R1.5d**). For this purpose, we did RNA-seq and DNA methylation arrays at 3 days after C/EBPα induction. Differential methylation analysis revealed only 13 CpG residues hypermethylated at sgRNAs cells, with two of them exhibiting the most significant changes in the *IL1RN* promoter itself **(Fig. R2.3.a)**. Additionally, we observed only 3 differentially expressed genes (DEGs), with *IL1RN* showing more than a 4-fold downregulation in sgIL1RN at day 3 of TD **(Fig. R2.3.b)**.

We analyzed in more detail the methylation editing effects caused by dCas9-DNMT3A during TD in the two probes located at the *IL1RN* promoter, cg03342003 and cg03989987. Interestingly, although dCas9-DNMT3A did not prevent the demethylation kinetics of the region, the final levels obtained were significantly higher in sgIL1RN cells than in CTRL cells (~ 70% vs ~ 40%, respectively) **(Fig. R2.3c)**. Moreover, we detected dCas9-DNMT3A hindering the *IL1RN* gene reactivation during TD **(Fig. R2.3d)**.

Overall, the only region differentially occupied by dCas9-DNMT3A, differentially methylated and differentially expressed when comparing sgIL1RN cells and CTRL cells is the *IL1RN* gene **(Fig. R2.3e)**. Moreover, our results highlight the previously described causality between methylation and expression at this gene. Thus, the specificity and accuracy of the dCas9-DNMT3A-mediated DNAm editing were validated.

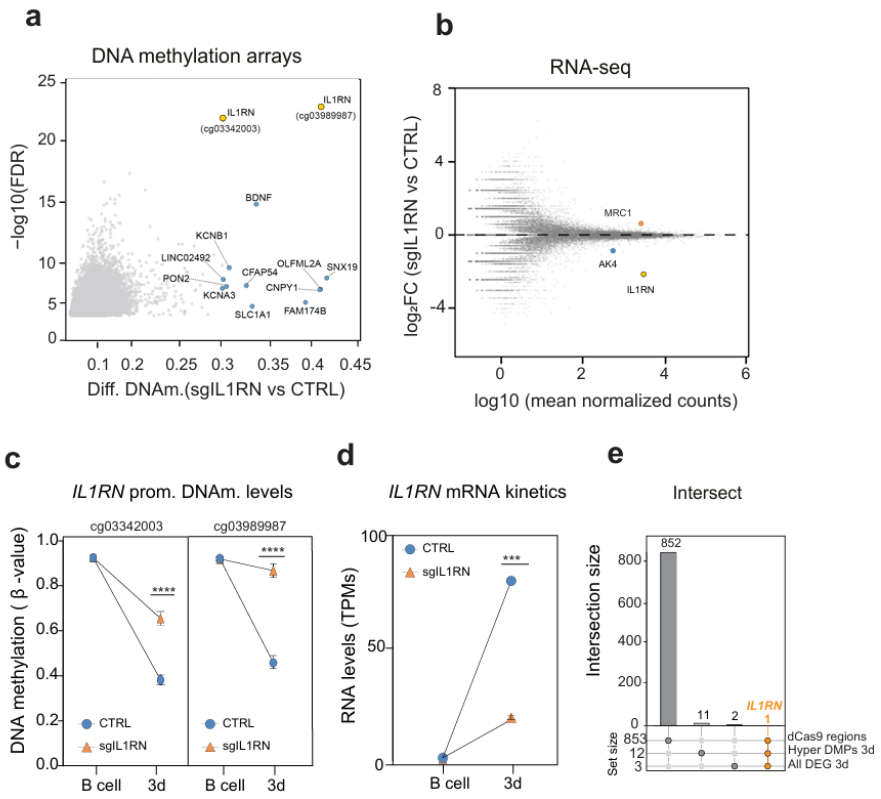

Fig R2.3. Validation of dCas9-DNMT3A editing specificity at IL1RN promoter. ***(a)*** *Scatter plot showing differentially hypermethylated CpGs in sgIL1RN day3 cells compared to CTRL day3 cells. Grey dots indicate hypermethylated CpG positions (FDR < 0.05). Blue and yellow dots indicate hypermethylated CpG positions gaining ≥ 30% of DNAm (Δβ≥0.3, FDR < 0.05, n=13). The yellow dots highlight two differentially hypermethylated CpG positions in the IL1RN prom (probes cg03342003 and cg03989987 from the MethylationEPIC BeadChip 850k v2.0 microarrays)* ***(b)*** *MA plot showing DEGs in sgIL1RN day3 cells compared to CTRL day3 cells. Orange dots indicate upregulated genes (FDR<0.05, n=1). Blue dots and the yellow dot (IL1RN) indicate downregulated genes (FDR<0.05, n=2).* ***(c)*** *Upset plot depicting the intersection of the significantly dCas9-DNMT3A bound regions (in a), the significantly hypermethylated ⍰⍰≥ 0.3 CpG positions (in b), and the significant associated DEGs (in c).* ***(d)*** *DNAm dynamics (array data) of two differentially hypermethylated CpG positions (probes cg03342003 and cg03989987) at the IL1RN prom in sgIL1RN and CTRL cells. Unpaired two-tailed Student's t-test, n=4, mean s.e.m., (****p< 0.0001).* ***(e)*** *IL1RN expression dynamics (by RNA-seq) in sgIL1RN and CTRL cells. Unpaired two-tailed Student's t-test, n=2, mean s.e.m., (***p< 0.001).* ***c)*** *Upset plot depicting the intersection of the significantly dCas9-DNMT3A bound regions (in a), the significantly hypermethylated Δβ≥ 0.3 CpG positions (in b), and the significant associated DEGs (in b).*

CHAPTER 3: dCas9-DNMT3A-mediated hypermethylation of the *IL1RN* promoter leads to impaired human myeloid cell fate acquisition

1. IL1RN epigenome editing alters transcriptional dynamics and phagocytic capacity during transdifferentiation

Previous studies have shown the relevance of the IL-1 pathway in maintaining balanced hematopoiesis between the lymphoid and myeloid lineages in mice. Additionally, both chronic exposure to IL-1β(Higa et al. 2021) and genetic deficiency of *Il1rn*(Villatoro et al. 2023) have been described as leading to hyperactivation of the IL-1 pathway, which causes a bias towards the myeloid lineage. Nevertheless, the exact role of *IL1RN* and the IL-1 pathway in the acquisition of human myeloid cell fate, as well as the molecular mechanisms underlying the myeloid bias following hyperactivation of the IL-1 pathway, are not yet fully understood.

Based on this knowledge, we took advantage of our highly efficient human B-to-macrophage reprogramming system, where *IL1RN* gets upregulated, to study the potential involvement of the IL1 pathway in the acquisition of the human myeloid cell fate.

To that end, we analyzed the transcriptomic profiles (by RNA-seq) of dCas9-DNMT3A CTRL and sgIL1RN cells throughout the transdifferentiation process (B cell, 3 days and 7 days -iMac-). Consistent with our previous observations (**Fig. R2.3 c-d**), minor changes in gene expression were detected at short time points **(Fig. R3.2a)**. This is expected since *IL1RN* expression is detected from day 3

onwards **(Fig. R2.3b and R2-5b)**. Interestingly, at the iMac stage, a distinct transcriptional profile emerged between CTRL and sgILRN cells, with 3,795 differentially expressed genes (DEGs) (FDR<0.05) **(Fig. R3.1a)**. Among these, 1,752 genes were up-regulated, and 2,043 were down-regulated **(Fig. R3.1a)**. In particular, one of the down-regulated genes was *IL1RN* itself, which showed a strong reduction of about 16-fold in its mRNA levels and was largely decreased at the protein level in dCas9-DNMT3A sgIL1RN iMacs **(Fig. R3.1b)**.

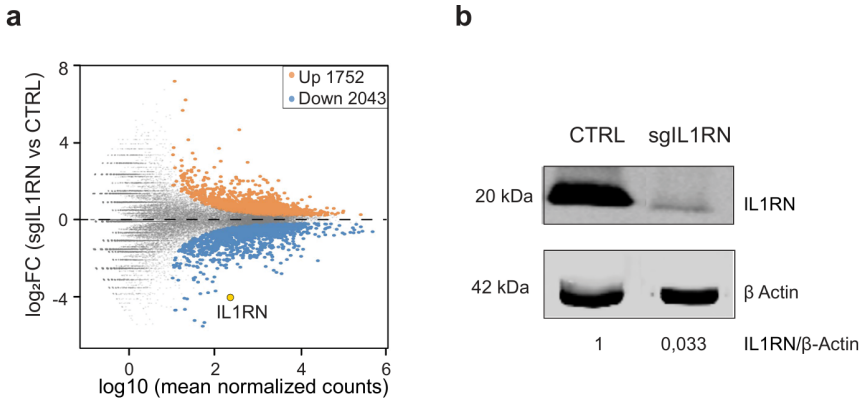

Fig. R3.1. dCas9-DNMT3A (d9-3A) abrogates normal IL1RN activation during B to macrophage TD. (a) *MA plot showing differentially expressed genes (DEGs) in dCas9-DNMT3A sgIL1RN iMacs compared to CTRL iMacs. Orange dots indicate upregulated genes (FDR<0.05). Blue dots and the yellow dot (IL1RN) indicate downregulated genes (FDR<0.05). Left: Representative western blot image of IL1RN protein in dCas9-DNMT3A sgIL1RN and CTRL iMacs. IL1RN levels were normalized to β-Actin levels and expressed as a fold change over CTRL iMacs.*

We next examined the impact of *IL1RN* DNAm editing on the transcriptomic kinetics. For this, DEG between CTRL and sgRNAs cells were clustered into 4 major groups (Transdifferentiation Clusters -TC- 1 to 4) **(Fig. R3.2a)**. This confirmed that differences in gene expression within the clusters between CTRL and sgIL1RN cells were only detectable at the iMac stage **(Fig. R3.2a)**.

In TC1, the *IL1RN* DNAm editing led to an incomplete silencing of genes related to chromosome segregation, such as the well-known *BRCA1* or *CDK1* genes **(Fig. R3.2b-c)**. In TC2, *IL1RN* DNAm editing further enhanced the downregulation of genes involved in the B cell transcriptional program, including the genes coding for the B cell TF *LEF1* and the B cell marker *CD79A*. In TC3, the DNAm editing prevented the decrease in gene expression for a group of transiently upregulated genes related to metabolic processes, including Hexokinase 2 (*HK2*) and Phosphoglycerate kinase 1 (*PGK1*). Finally, in TC4, the DNAm editing hindered the upregulation of genes related to myeloid cell fate and phagocytosis processes, including *ITGAM* and *CD14* **(Fig. R3.2b-c)**. Altogether, these transcriptional analyses suggest that modifying the methylation status of the *IL1RN* promoter could modify the cell fate acquired during the transdifferentiation process, leading to cells with an altered cellular division, metabolism, and myeloid differentiation status.

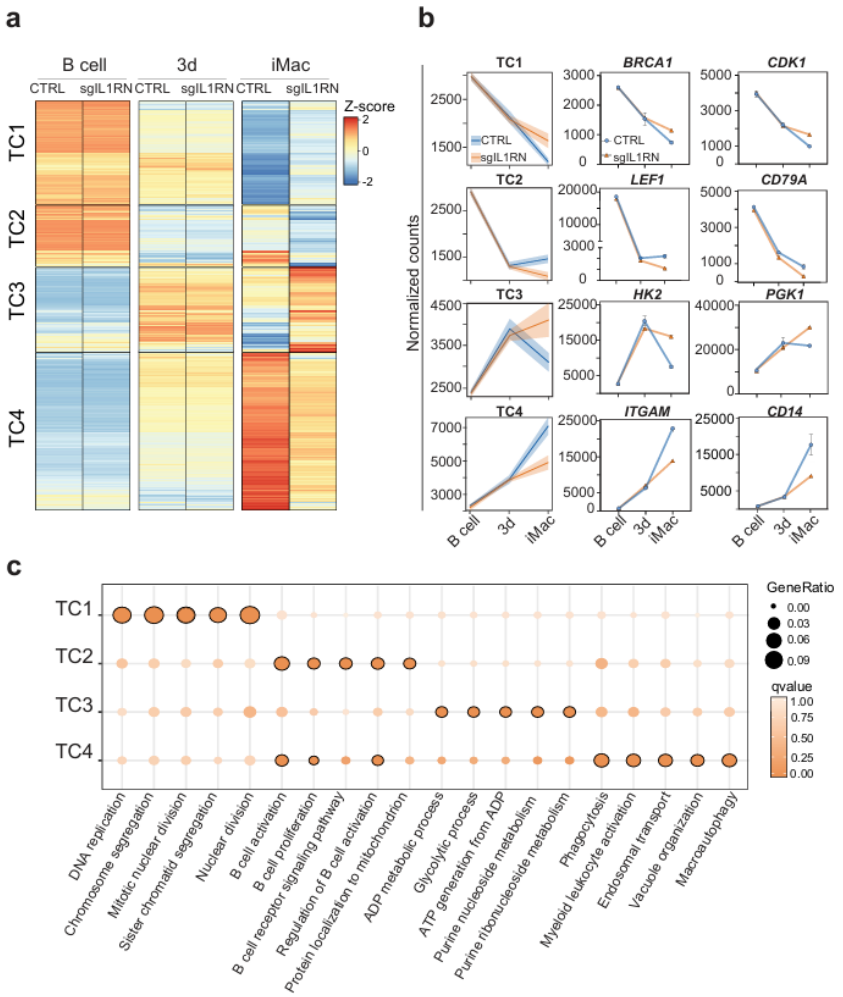

Fig. R3.2. IL1RN-editing altered transcriptional kinetics for genes linked to cell division, B cells and myeloid cells. ***(a)*** *Clustering of the transcriptional dynamics (by RNA-seq) during TD in sgIL1RN and CTRL cells. Average scaled normalized counts (Z-score) of DEG (FDR<0.05) are represented at each timepoint (n=2 biologically independent replicates).* ***(b)*** *Cluster expression tendencies with examples for each cluster in sgIL1RN and CTRL cells.* ***(c)*** *Gene Ontology (GO) enrichment analysis for the genes associated with clusters in R3.1c. The top 5 most significantly BP terms for each cluster are plotted. GeneRatio and qvalue are shown. Significant terms (qvalue < 0.05) are highlighted with a black stroke.*

Given the large transcriptomic changes observed in edited cells, we aimed to investigate if they were associated with altered

cellular phenotypes. To explore this idea, we monitored by FACS through immunostaining of the myeloid surface marker CD11b and CD14. We observed that *IL1RN* DNAm edited iMacs showed reduced levels of CD11b (encoded by *ITGAM*) and CD14 compared to CTRL iMacs **(Fig. R3.3a)**. To further examine the functional properties of edited macrophages, we evaluated their phagocytic capacity. For this purpose, CTRL and sgIL1RN iMacs were incubated with carboxylated beads and examined by FACS 24 hours later. As shown in **Fig. R3.3b**, both iMacs ingested the beads however, sgIL1RN iMacs displayed an enhanced phagocytic capacity (>1,5-fold) compared to CTRL. Uninduced B cells were used as a negative control of the phagocytic essay.

Altogether, these results show that IL1RN is required for myeloid cell fate identity during B cell to iMac TD process.

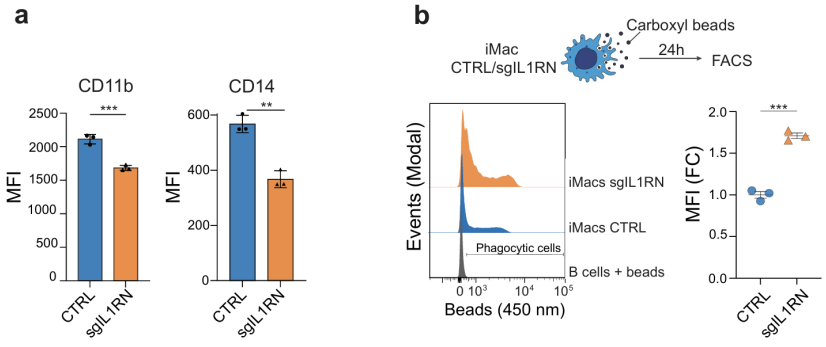

Fig. R3.3. dCas9-DNMT3A epigenome editing leads to decrease expression of myeloid of myeloid markers and altered phagocytic capacity. (a) *Flow cytometric analysis showing the Mean Fluorescence Intensity (MFI) for CD11b and CD14 in sgIL1RN and CTRL iMacs. Unpaired two-tailed Student's t-test, n=3, mean s.e.m., (**p< 0.01; ***p< 0.001).* ***(b)*** *Left: flow cytometry histogram showing the uptake of blue fluorescent beads. Right: Plot showing MFI for the blue beads in sgIL1RN and CTRL iMacs. Unpaired two-tailed Student's t-test, n=3, mean s.e.m., (***p< 0.001)*

2. shRNAs-mediated validation of *IL1RN* involvement in myeloid cell fate acquisition and phagocytic activity.

In another approach to validate IL1RN involvement in myeloid commitment, we employed an orthogonal method based on shRNA-mediated *IL1RN* knockdown. For this purpose, we infected our human B leukemic cells with lentiviruses harboring 2 different shRNAs (1/2) targeting *IL1RN* mRNA and against the firefly luciferase (Luc) as a control. Next, we induced the TD process by treating cells with β-estradiol (E2) **(Fig.R3.4a)**. Notably, both shRNAs efficiently depleted IL1RN at the mRNA and protein levels in iMacs **(Fig. R3.4b-c)**. We next examined some examples of DEGs previously identified in dCas9-DNMT3A edited iMacs to compare if shRNAs were displaying similar expression kinetics. Of note, *IL1RN*-depleted (shIL1RN) iMacs displayed similar changes in gene expression as observed in *IL1RN* DNAm edited iMacs, including increased levels of genes related to cell division (*BRCA1* and *CDK1*) and metabolism (*HK2* and *PGK1*), as well as reduced levels of B- (*LEF1* and *CD79A*) and myeloid- (*ITGAM* and *CD14*) related genes **(Fig.R3.4d)**. Therefore, similar gene expression kinetics were obtained when IL1RN was downregulated, whether by promoter hypermethylation or mRNA degradation.

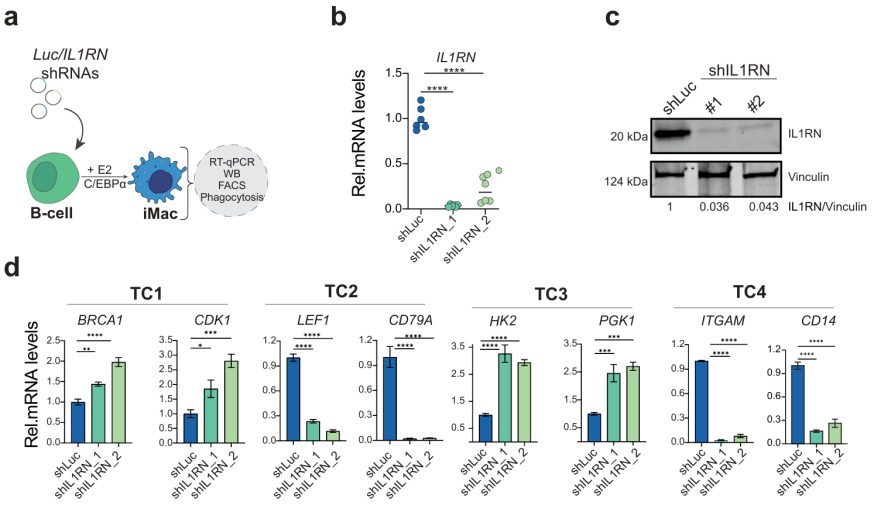

Fig. R3.4. IL1RN-shRNAs generates macrophages with reduced levels of myeloid markers and enhanced phagocytic capacity. ***(a)*** *Schematic of the IL1RN shRNAs experiments during TD. B cells were transduced with lentiviruses encoding shRNAs targeting the luciferase gene (shLuc, control) or the IL1RN gene (shIL1RN).* ***(b)*** *qRT-PCR analysis of IL1RN expression in iMacs harboring shRNAs. Values were normalized against B2M expression. Two-way ANOVA with Dunnett's post-hoc test, n=6, mean ± s.e.m., (****p < 0.0001).* ***(c)*** *Western blot image of IL1RN protein in shIL1RN and shLuc iMacs. IL1RN levels were normalized to vinculin protein levels and expressed as a fold change over shLuc iMacs.* ***(d)*** *qRT-PCR analysis of selected genes from the TD clusters shown in Fig. R3.2b. Values were normalized against B2M expression. Two-way ANOVA with Dunnett's post-hoc test, n=3, mean ± s.e.m., (*p < 0.05; **p < 0.01; ***p < 0.001; ****p < 0.0001).*

Furthermore, the shIL1RN iMacs exhibited as well reduced levels of the myeloid surface markers CD11b and CD14 and enhanced phagocytosis capacity >2-fold compared with control iMacs **(Fig. R3.5 a-b)**. Altogether, we have shown the involvement of *IL1RN* in the establishment of the C/EBPα-driven myeloid cell fate and acquisition of enhanced phagocytic capacity. Thus, our data reveal that the IL1 pathway may be necessary for the proper acquisition of myeloid cell fate during human hematopoiesis.

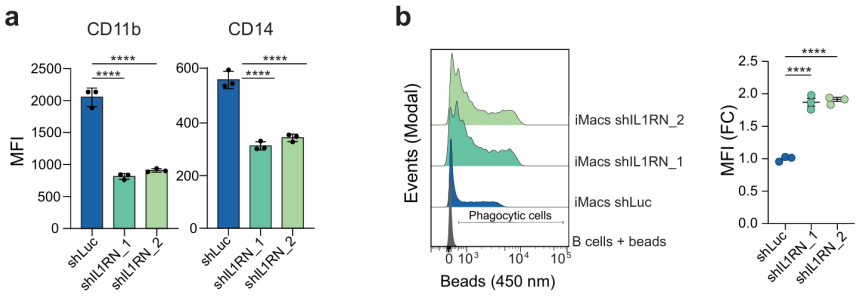

Fig. R3.5. IL1RN-shRNAs generates macrophages with reduced levels of myeloid markers and enhanced phagocytic capacity. (a) *Flow cytometric analysis showing the MFI for CD11b and CD14 in shIL1RN and shLuc iMacs. Two-way ANOVA with Dunnett's post-hoc test, n=3, mean ± s.e.m., (****p < 0.0001).* ***(b)*** *Left: flow cytometry histogram showing beads' fluorescence (Pacific Blue 450 nm) in shIL1RN and shLuc iMacs. B cells are included as a non-phagocytic negative control. Right: Plot showing the normalized MFI for the blue beads in shIL1RN and shLuc iMacs. Two-way ANOVA with Dunnett's post-hoc test, n=3, mean ± s.e.m., (****p < 0.0001).*

3. C/EBPα binds to GREs of IL1 pathway genes during the acquisition of the myeloid cell fate.

Based on our observation of IL1RN's dependency on the correct acquisition of the myeloid cell fate in our cellular model, we analyzed its epigenomic regulation during the process to gain insight into its transcriptional control. For this purpose, we combined various datasets of ChIP-seq, ATAC-seq and RNA-seq previously generated(Stik et al. 2020). We observed that C/EBPα, which drives the transdifferentiation process, binds to the *IL1RN* promoter as early as 24 hours. This binding occurs before the DNA demethylation of the region and the transcriptional activation **(Fig. R1.5d)**, but it temporally coincides with a significant epigenome rewiring, as indicated by increased chromatin accessibility and activation (detected by ATAC-seq and H3K27ac decoration, respectively) at the C/EBPα-bound region **(Fig. R3.6a).**

Additionally, the *IL1B* locus (agonist of IL-1 pathway) was also found to undergo demethylation during the transdifferentiation process **(Fig. R1.3a)**. Precisely, this GRE is a proximal enhancer (PE) of the gene (PE2 at -5.5kb from the TSS) that is bound by C/EBPα along with its promoter, and yet another proximal enhancer (PE1 at -3kb from the TSS) as early as 24h of transdifferentiation (**Fig. R3.6b)**. In B cells, both the promoter and the PE1 of the *IL1B* gene are already accessible and devoid of DNAm (data not shown). However, the binding of C/EBPα to the PE2 occurs in a closed chromatin region that only becomes accessible after its binding, coinciding with the loss of DNAm in the region **(Fig. R3.6d)**.

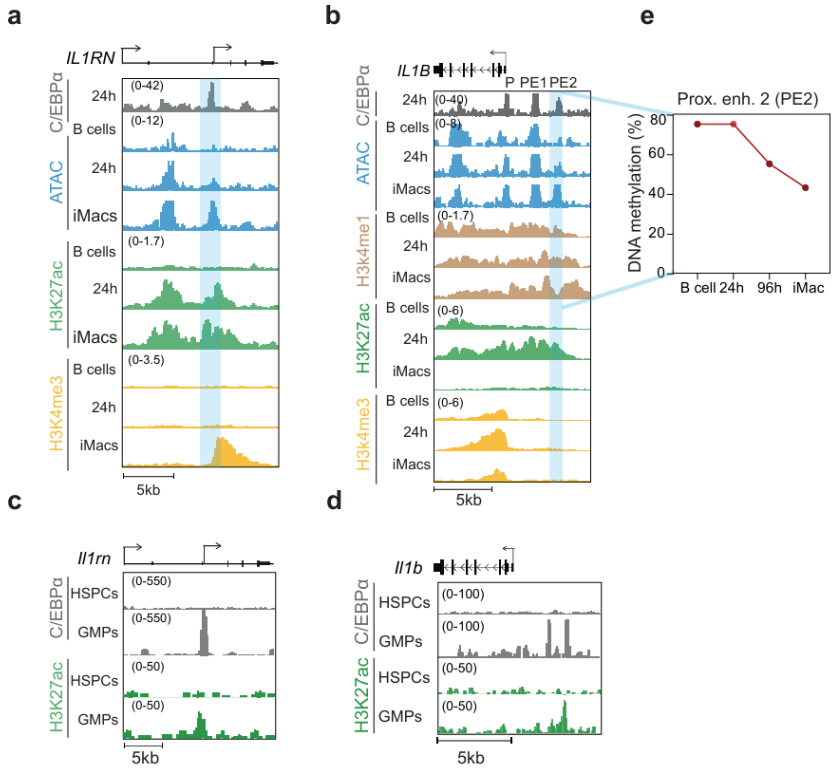

***Fig. R3.6.C/EBPα binds IL-1 related genes during physiological myeloid cell fate. (a-b)** : Genome browser snapshot at the human IL1RN (a) and IL1B (b) locus showing signal for C/EBPα ChIP-seq at 24h and chromatin accessibility (by ATAC-seq), H3K27ac and H3K4me3 ChIP-seq signal. The blue-shaded region indicates the DNA demethylated region at the IL1RN promoter. **(b)** At 24h C/EBPα binds 3 GREs within the IL1B locus: the promoter (P) and 2 proximal enhancers (PE1-2). The blue-shaded highlight indicates a DNA demethylation event at PE2 (as identified in Fig. R3.4b **(c-d):** Genome browser snapshot at the mouse Il1rn (c) and il1b (d) locus showing signal for C/EBPα and H3K27ac ChIP-seq in HSPCs and GMPs. Data were taken from: H3K27ac and H3K4me3 ChIP-seq during TD (ArrayExpress: E-MTAB-9010); C/EBPα ChIP-seq in murine HSPCs and GMPs (GEO: GSE43007)*(Hasseman, et al. C/EBPa is required for long-term self-renewal and lineage priming of Hematopoietic Stem Cells and for the maintenance of Epigenetic Configurations in Multipotens Progenitors. PLOS Genetics (2014).) *H3K27ac ChIP-seq signal in murine HSPCs and GMPs (GEO: GSE59636)*(Lara-Astiaso et al. 2014). **(d)** DNA demethylation kinetics at PE2 GREs during TD.*

The observed DNA demethylation and chromatin activation events at the *IL1RN* and *IL1B* genes upon C/EBPα binding to their GREs strongly suggest that this transcription factor plays an important role in controlling the IL1 pathway activity during the establishment of the myeloid cell fate. To gain mechanistic insight into the physiological process, we studied the transition from mouse hematopoietic stem progenitor cells (HSPCs) to granulocyte-macrophage progenitors (GMPs) driven by C/EBPα(Zhang et al. 1997). Specifically, we only observed chromatin activation at the *Ilrn* and *Il1b* loci at the GMP stage, specifically at the C/EBPα-bound regions, coinciding with the GREs described in the human cellular cell fate model **(Fig. R3.6c-d)**.

Altogether, these analyses reveal a previously unidentified mechanistic role for C/EBPα as a potentially crucial transcriptional regulator of the IL1 pathway during both human and murine myeloid cell fate determination.

CHAPTER 4. IL1RN DNAm editing affects NFKB and IFN early transcription upon IL-1β treatment.

1. dCas9-DNMT3A IL1RN DNAm editing sensitizes iMacs to IL-1β treatment

The observed regulatory mechanism by which C/EBPα binding to GREs of the IL-1 pathway-related genes (*IL1B* and *IL1RN*) coincides with losing DNAm during TD raised the possibility that it reflects an interplay between IL-1β and IL1RN pathways in iMacs that might be relevant during inflammation. As described in the introduction, IL1RN is a negative regulator of the IL1-signaling pathway(Arend et al. 1990). Therefore, we hypothesize that edited (sgIL1RN) iMacs should exhibit an enhanced response to an inflammatory stimulus mediated by IL-1β, the pathway agonist.

To explore this idea, we cultured C/EBPα-induced CTRL and sgIL1RN macrophages with IL-1β for 3 and 16 hours. Then, we extracted RNA for RNA-seq analysis. These two timepoints of IL-1β treatment were selected to compare the early and late inflammatory response (**Fig. R4.1a**). We observed large transcriptomic changes between CTRL and sgIL1RN iMacs at the early phase (0h and 3h) of IL-1β treatment, which diminished following prolonged exposure (16h) **(Fig.R4.1b**). In particular, at 3h, 2229 DEGs (FDR<0.05) were detected after IL-1β treatment, suggesting a different inflammatory response in sgIL1RN iMacs (**Fig.R4.1c**).

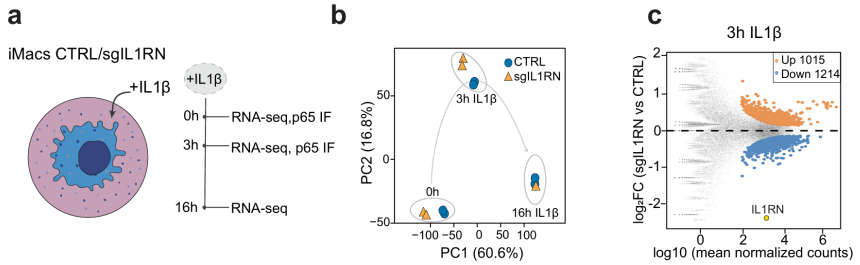

Fig. R4.1. dCas9-DNMT3A IL1RN editing impairs the transcriptional response mediates by IL-1β treatment. ***(a)*** *Schematic of the IL1β treatment experiment.* ***(b)*** *PCA displaying the transcriptomic dynamics of sgIL1RN and CTRL iMacs treated with IL1β.* ***(c)*** *MA plot showing DEGs in sgIL1RN and CTRL iMacs treated with IL1β for 3h. Orange dots indicate upregulated genes (FDR<0.05). Blue dots and the yellow dot (IL1RN) indicate downregulated genes (FDR<0.05).*

2. IL1RN DNAm editing leads to enhanced p65/NF-kB and diminished interferon pathway activation upon IL1β treatment

To further characterize the potential impact of the transcriptional differences observed at 0h and 3h between sgIL1RN and CTRL iMacs, we used DoRothEA (Discriminant Regulon Expression Analysis). DoRothEA is a manually curated human regulon database utilized to estimate the activities of TFs in individual samples based on the expression of their target genes(Garcia-Alonso et al. 2019). The analysis showed higher activity in regulons related to important myeloid TFs such as SPI1 (PU.1) or RUNX1, and the inflammation-related TF RELA/(p65), as well as lower activity in regulons associated with the interferon pathway (STAT2 or IRF9) in sgIL1RN compared to CTRL iMacs, at 3h after IL-1β treatment **(Fig. R4.2a)**.

To validate DoRothEA predictions, we performed immunofluorescence for the NF-kB subunit p65. We observed enhanced p65 nuclear localization in sgIL1RN iMacs at 3h of the IL-1β treatment **(Fig. R4.2b).** Thus, IL1RN editing lead to an enhanced NFKB

nuclear activity in iMacs, raising the possibility that activates a proinflammatory program in sgIL1RN iMacs**.**

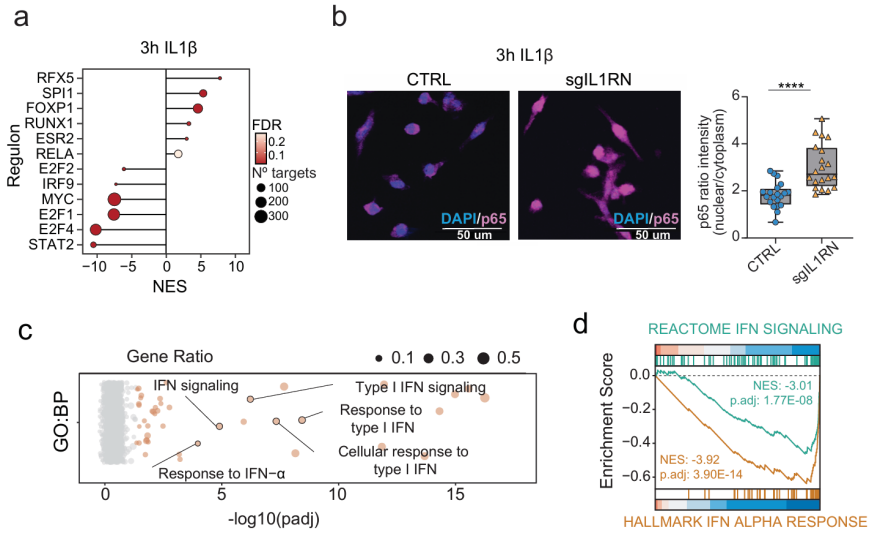

Fig. R4.2. dCas9-DNMT3A IL1RN editing leads to increased NFKB activity and deficient activation of IFN pathway. ***(a)*** *Lollipop plot depicting the TF activity predicted from mRNA expression of target genes with DoRothEA v2.0*(Garcia-Alonso et al. 2019) *in sgIL1RN and CTRL iMacs treated with IL1β for 3h. Lollipop size indicates the total number of genes regulated by each transcriptional regulon.* ***(b)*** *Left: Representative IF showing p65 (red) and DAPI (blue) signals in sgIL1RN and CTRL iMacs treated with IL1β for 3h. Right: quantification of p65 nuclear versus cytoplasmic localization signal in sgIL1RN and CTRL iMacs treated with IL1β for 3h. Unpaired two-tailed Student's t-test, n=20 cells per group, mean s.e.m., (****p< 0.0001).* ***(c)*** *Bubble plot displaying enrichment for BP of the most significantly less enriched genes (log2FC>0.5, FDR<0.05) at 3h of IL1β treatment. Dotted line represents p-adjusted<0.05 threshold. P-adjusted values were calculated by applying the Benjamini-Hochberg correction.* ***(d)*** *Gene Set Enrichment Analysis (GSEA) of the interferon signature at DEG between sgIL1RN and CTRL iMacs treated with IL1β for 3h. P-adjusted values were calculated by applying the Benjamini-Hochberg correction*

In addition, Gene Ontology (GO) and Gene Set Enrichment Analyses (GSEA) for the DEG at 3h showed clear enrichments for biological processes and signaling pathways related to the interferon

response in IL1RN-edited macrophages. Specifically, type I IFN signaling was the process more enriched in the downregulated genes at 3h of IL-1β treatment **(Fig. R4.2c-d).**

Therefore, these analyses suggest that methylation editing at the *IL1RN* promoter alters the activation balance between two key inflammatory pathways: the NF-kB pathway and the Interferon pathway.

3. IL1RN-editing leads to altered transcriptional kinetics in response to IL-1β treatment

To further characterize the transcriptional response of *IL1RN* DNAm iMacs upon IL-1β treatment we identified genes that were differentially expressed between sgILRN and CTRL iMacs during IL1β-treatment and categorized them into 4 major clusters (IL1βI-Clusters -IC- 1 to 4). Interestingly, regardless of the initial transcriptional status or the early response to IL1β treatment, genes in all clusters exhibited no differences after 16 hours of IL1β treatment **(Fig. R4.3a)**.

An unsupervised gene ontology analysis of these clusters showed terms related to lipopolysaccharide response or phagocytosis, as exemplified by *CD14* showing impaired downregulation in IC1 **(Fig. R4.3b-c)**. In IC2, DNAm editing induced a strong and transient gene upregulation at 3h of IL1β -treatment of genes related to metabolic biological processes, such as the mitochondrially encoded ATP synthase 6, *MT-ATP6***.** IC3 contains genes that exhibit reduced expression at 0h and impaired upregulation at 3h. These genes are enriched in viral response biological processes, exemplified by the interferon-induced gene 2'-5'-oligoadenylate synthetase 3 (*OAS3*)**.** Finally, IC4 contains genes involved in DNA recombination, such as

IL7R, which show reduced expression in IL1RN DNAm-edited cells at 0h and reach CTRL levels at 3h of IL1β treatment (**Fig. R4.3b-c).**

Taken together, we have shown that altering the methylation status of the IL1RN promoter affects how cells react to IL-1β-driven inflammatory stimuli. This alteration disrupts the balance between the activation of the NF-kB and Interferon signaling pathways over time following exposure to IL-1β, potentially resulting in modified cellular responses.

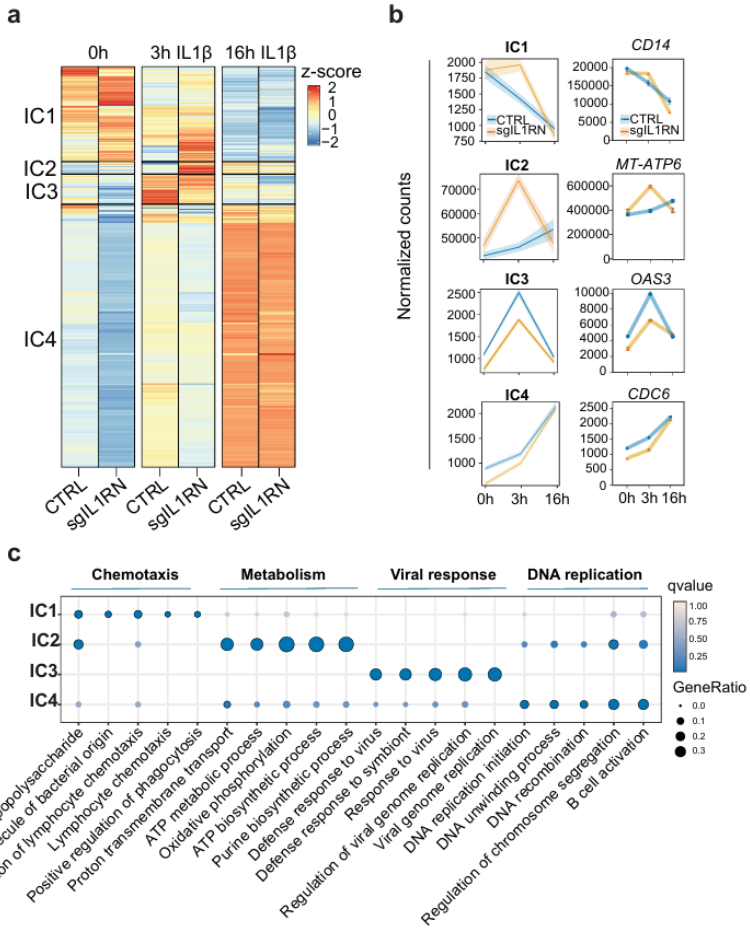

Fig. R4.3. Characterization of the gene expression kinetics of CTRL and sgRNAs iMacs during IL-1β treatment. (a) *Clustering of the transcriptional dynamics (by RNA-seq) observed during the IL1β -treatment in sgIL1RN and CTRL iMacs. Average scaled normalized counts of differentially expressed genes (FDR<0.05) are represented at each timepoint (n=2 biologically independent replicates). Black lines show splitting by k-means clustering. IL1β-treatment Clusters (IC1-4).* ***(b)*** *Left: quantification of RNA signal at the IL1β-treatment clusters (IC1-4) in h. Right: expression dynamics in sgIL1RN and CTRL iMacs of representative genes from the clusters.* ***(c)*** *Balloon plot depicting the Gene Ontology (GO) enrichment analysis for the genes associated with clusters in h. The top 5 most significantly over-represented biological processes (BP) terms for each cluster are plotted. Ratio of genes of interest over all unique genes (GeneRatio) and qvalue are shown. Significant terms (qvalue < 0.05) are highlighted with a black stroke.*

4. Single-cell RNA-seq analyses identified an ISG-monocyte signature in the IL1RN-downregulated genes

To understand the physiological relevance of the observed differential transcriptional response to the IL-1β treatment between sgIL1RN and CTRL iMacs, we examined a publicly available dataset that displays the transcriptional profiles of 17 different monocyte and macrophage identities at single-cell resolution and integrating 41 studies from healthy and pathologic tissues (MoMac-VERSE) (Mulder et al. 2021) **(Fig. S2)**.

We combined our bulk RNA-seq with the MoMac-VERSE scRNA-seq data to identify specific monocyte/macrophage subpopulations that might be affected by the IL1RN editing. The first step was to study which clusters across all the populations displayed high levels of *IL1RN* to determine which cellular identities might depend on its function. Our analysis revealed that *IL1RN* was preferentially expressed in the CD16-negative monocyte (CD16- Mon., 12), IL1B monocyte (IL1B Mon., 15), and Interferon Stimulating Gene monocyte (ISG Mon., 4) identities **(Fig. R4.4)**.

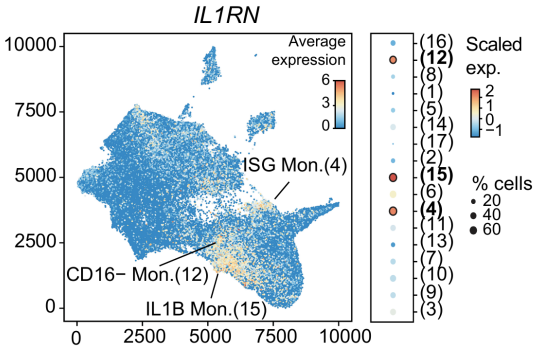

Fig. R4.4. High dimensional maps of IL1RN expression across scRNA-seq MoMac-Verse. *UMAP and balloon plots showing IL1RN expression across the MoMac-Verse. The cellular identities showing the highest IL1RN levels are highlighted in bold and depicted in the UMAP.*

Then, we assessed the expression of the 3h-DEGs (FDR<0.05) detected between sgIL1RN and CTRL iMacs (**Fig. R4.1c)** across the 17 identities contained in the MoMac-VERSE scRNA-seq dataset. Notably, the upregulated genes, which are more expressed in the sgIL1RN macrophages, are mainly expressed in CD16-negative monocytes (CD16- Mon., 8) and HEIS1 macrophages (HEIS1 Mac., 2) **(Fig. R4.5)**. On the other hand, the downregulated genes, which are more expressed in CTRL macrophages, are preferentially expressed in ISG-Mon (4) **(Fig. R4.5)**.

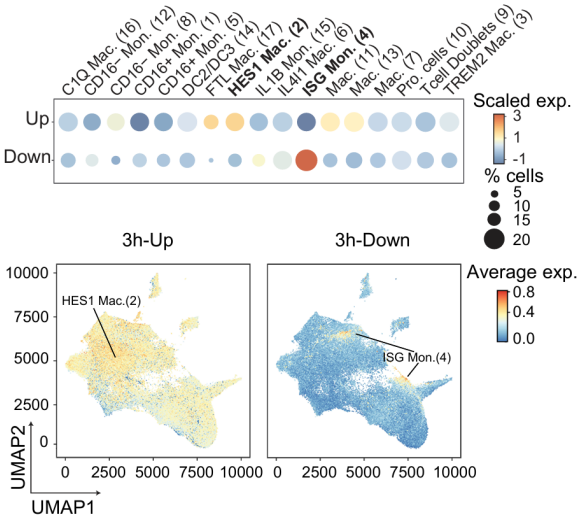

Fig. R4.5. scRNA-seq identifies ISG Monocyte subpopulation in the downregulated genes after 3h IL-1β treatment. *Up: Balloon plot showing scaled expression of the 3h-up and 3h-down gene signatures (in R4.1c). Down: UMAP plots showing the average expression of the gene signatures. Highest expression levels of the signatures are highlighted in bold and depicted in the UMAPs.*

In conclusion, we have identified ISG monocytes as the primary monocyte-macrophage population that may be more significantly affected by the disruption of *IL1RN* levels. Moreover, our analysis indicates the differential transcriptional response to IL-1β in *IL1RN*-depleted cells may have physiological relevance and provides evidence supporting the idea that *IL1RN* methylation editing alters myeloid cell fate activation.

CHAPTER 5. *IL1RN* promoter DNAm alters the macrophage capacity to support cancer growth.

Given the observed transcriptomic alteration at the early phase of IL-1β treatment, we wondered whether iMacs cytokine production might be affected. To explore this idea, CTRL and sgIL1RN iMacs were treated for 24-hours with IL-1β. Next, we collected the supernatant of CTRL and sgIL1RN iMacs to quantify cytokine secretion **(Fig. R5.1a)**. As shown in **Fig. R5.1b,** sgIL1RN iMacs displayed a distinct cytokine secretory profile after 24-hour IL1β-treatment, showing minor changes in the untreated state (not shown). From a panel of 10 inflammatory and anti-inflammatory cytokines, we observed significantly increased levels of well-known proinflammatory cytokines, including IL-1β, IL-6, and the interferon gamma-induced protein 10 (IP10) in sgIL1RN iMacs **(Fig. R5.1b)**. All of them showed an average increase of at least 2-fold in their levels, with the highest differential accumulation observed for IL-6 (>3.5-fold). Strikingly, the impact of the DNAm editing on *IL1RN* was also detectable at the cytokine level, with edited cells displaying a >2-fold decrease in secreted IL1RN levels **(Fig. R5.1b)**.

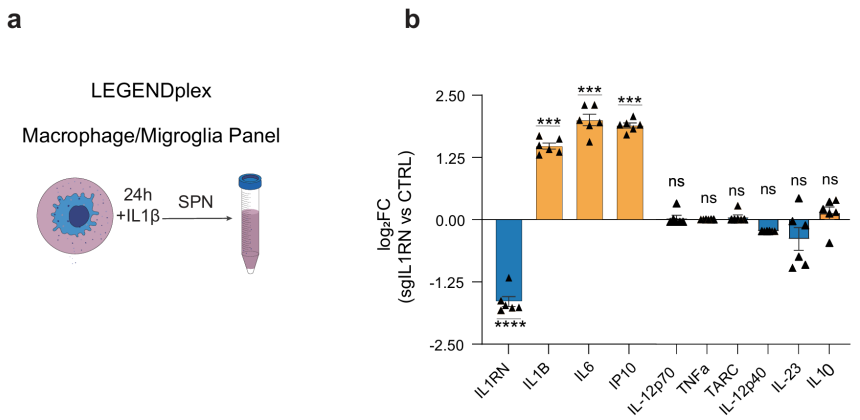

Fig. R5.1. ***(a)*** *Schematics of the experimentation performed to quantify cytokine secretion from the cultured SPN upon 24h of IL1β treatment* ***(b)*** *Normalized levels of secreted cytokines in dCas9-DNMT3A sgIL1RN iMacs treated for 24h with IL-1β. One-way ANOVA with Dunnett's post-hoc correction, n=6, mean, not significant (p>0.05) (***p < 0.001; ****p < 0.0001).*

Since macrophages in the tumor microenvironment impact cancer development by producing different sets of cytokines(Ma et al. 2022), the distinct cytokine profile secreted by the *IL1RN*-edited macrophages might modulate cancer cell growth. To address this hypothesis, we investigated the expression of *IL1RN* in both healthy and cancer cells from 12 different tissues across the 17 cellular identities in the MoMac-Verse dataset (**Fig S2**). Then, we narrowed down our analysis to the colon, liver, and lung because they had enough healthy and cancer cells, particularly for the ISG Mon (4) cellular identity, to carry out statistical analyses. By doing so, we identified *IL1RN* as differentially expressed between healthy and cancer cells in the lung and colon, but not in the liver **(Fig. R5.2)**. Likewise, genes encoding for the other cytokines differentially secreted by the sgIL1RN macrophages (*IL1B*, *IL6*, and *CXCL10* -IP10-) were also significantly upregulated in cancer compared to healthy ISG Mon (4) in the lung and colon **(Fig. R5.2).** Therefore, suggesting ISG Mon (4) displaying elevated levels of

these pro-inflammatory genes might be involved in modulating colon and lung cancer growth in the tumor microenvironment.

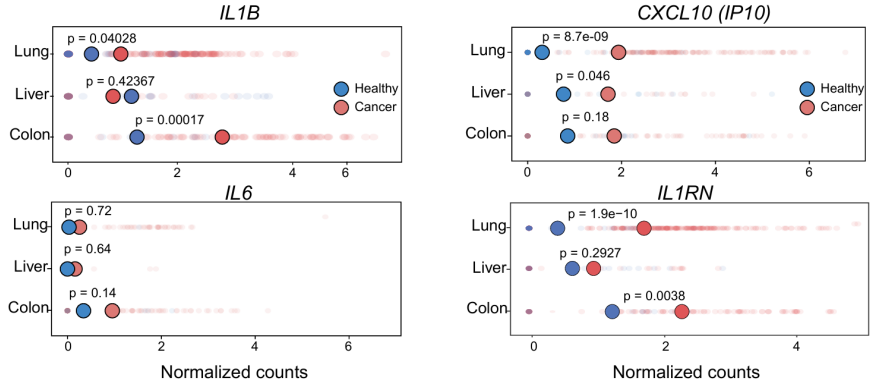

***Fig.R5.2**. Balloon plots showing IL1B, IL6, CXCL10 (IP10) and IL1RN normalized expression levels in healthy and cancer ISG-monocytes from tissues with available data from the MoMac-Verse scRNA-seq dataset. Average expression values for each group are shown as a circle with a black stroke. P-values were calculated using a two-sided Wilcoxon rank-sum test.*

To assess the possibility that elevated levels of IL-1β, IL-6 and IP10 might modulate cancer growth, we collected the supernatant of CTRL and sgIL1RN iMac after 24-hour IL1β-treatment **(Fig. R5.3)**. Then, we labeled cells from different cancer origins (HCT116: colon cancer and Cal-12t: non-small cell lung carcinoma) with the proliferation dye Carboxyfluorescein Succinimidyl Ester (CFSE) and cultured them using the supernatant previously collected from the CTRL and sgIL1RN iMacs. We observed that cells from both cancer origins, when grown in the IL-1β, IL-6, IP10-rich supernatant of the sgIL1RN iMacs, retain an average of 30% less of the CFSE signal 4 days after staining **(Fig. R5.3)**. This means that the differential cytokine profile secreted by the *IL1RN* DNAm edited cells favors the proliferation of these cancer cells. In summary, these analyses identified increased expression of pro-

inflammatory cytokine genes (*IL1B*, *IL6*, and *CXCL10*) by the ISG monocytes in the colon and lung tumor microenvironments. Interestingly, cell growth in cancer cells from these origins can be modulated when cultured in the pro-inflammatory environment produced by *IL1RN* methylation-edited cells treated with IL-1β.

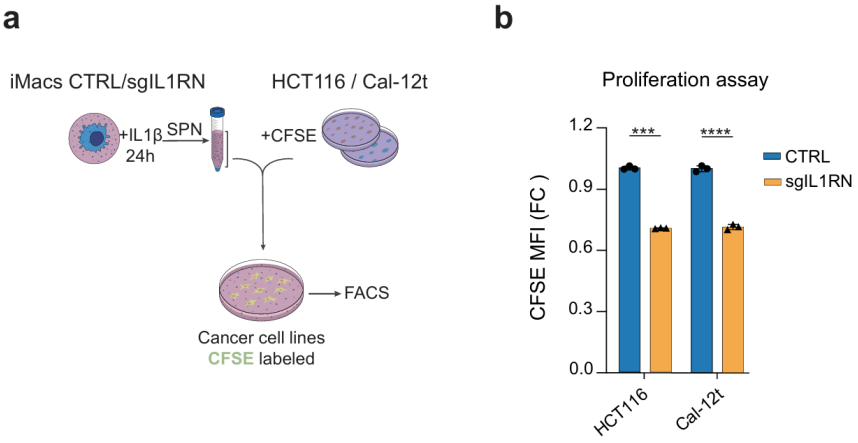

Fig. R5.3. ***(a)*** *Proliferation assay (by CFSE retention) assessing the impact of the differential cytokines produced by the sgIL1RN iMacs in the proliferation of HCT116 and Cal12-t cancer cell lines. Up: Schematic of the experimental setup.* ***(b)*** *Plot showing the normalized Mean Fluorescence Intensity (MFI) for the CFSE signal (4 days after staining) in cancer cells exposed to the supernatant of sgIL1RN or the supernatant of CTRL iMacs. Unpaired two-tailed Student's t-test, n=20 cells per group, mean s.e.m., (***p < 0.001; ****p< 0.0001).*

DISCUSSION

DISCUSSION

In this study, we have combined the highly efficient and homogenous reprogramming of B cells into macrophages and CRISPR/dCas9 DNAm editing tools to address whether DNAm and expression have a causal relationship. In addition, by using this approach, we have demonstrated that altering the methylation status of the *IL1RN* promoter region is sufficient to trigger significant changes in gene expression, leading to distinct myeloid cell fate outcomes and responses to inflammatory signals, which impact the behavior of these cells in functional and pathological contexts.

CHAPTER 1: Genome-wide correlation studies between DNAm and transcription during human myeloid commitment

1. WGBS-seq reveals a DNAm reshaping during transdifferentiation

In the first part of the study, we characterized the genome-wide DNA methylome during the highly efficient conversion of leukemic B cells into non-tumorigenic macrophages by WGBS-seq (**Fig. R1.1a**). We observed a genome-wide progressive loss of DNAm as early as 96h during transdifferentiation (**Fig. R1.1c)**. Previous studies have found early redistribution of 5mC during the conversion of B cells into induced pluripotent stem cells (Sardina et al. 2018), suggesting that rapid changes in DNAm might be a common mechanism in efficient cellular reprogramming. By analysing the dynamics of DNAm, we observed that the changing regions were unequally distributed along the different chromosomes, with the largest changes occurring on ChrX (**Fig. R1.1e**). Notably, about 32% of the DNAm signal on ChrX is rewired during this

process, representing a 2.3-fold increase compared to the genomic average changes (13,7%). Specifically, in this chromosome, 2 out of 3 regions change their DNAm by losing signal in the induced macrophage state. As our B cells are derived from the RCH-ACV female B-ALL cell line (Jack et al. 1986), the significant changes observed in ChrX may indicate either a partial reactivation of the inactive ChrX during the cell fate conversion or abnormal hypermethylation of the active ChrX in B cells. On the one hand, it has been described that immune cells may not maintain the inactivation of ChrX as efficiently as other somatic cells (Wang et al. 2016; Syrett et al. 2017, 2019). This could lead to the overactivation of immune-related genes abundantly located on this chromosome, ultimately contributing to the development of autoimmune diseases that have a higher incidence in female individuals(Forsyth et al. 2024).

On the other hand, hypermethylation of ChrX and reduced levels of the master regulator of ChrX dynamics, Xist, have been described as mechanisms that promote progression in breast and blood cancers(Yildirim et al. 2013; Richart et al. 2022). Therefore, the loss of DNAm at ChrX may contribute to the loss of tumorigenicity associated with the B-to-macrophage transdifferentiation process.

Our data of DNA methylation and chromatin accessible regions (ATAC+) showed DNA demethylation at GREs during B-cell to iMac TD and primary human MoMacs (**Fig R1.2a,c**). Interestingly, only regions that experience continuous DNAm loss (7,603) showed increased chromatin accessibility (**Fig R1.2b**). Of note, based on gene ontology analysis we could determine that those GREs were relevant for myeloid processes (**Fig R1.3a-b and R1.4a)**. They included key transcription factors such as *KLF4* or *MAFB and*, DNA methylation-related enzymes

including *TET2* **(Fig. R1.3a)**. Previous findings have shown the involvement of KLF4 (Di Stefano et al. 2016), MAFB (Morante-Palacios et al. 2022a) and TET2 (Sardina et al. 2018; Lazarenkov and Sardina 2022; Kallin et al. 2012) in immune-related cell fate decisions, therefore validating the relevance of the methylation changes observed at these loci.

One of the mechanisms that could be driving these changes is the interplay between C/EBPα and Tet2. During C/EBPα-driven B-to-iPSC reprogramming, C/EBPα binding leads to the upregulation of Tet2, which subsequently binds to regulatory regions of pluripotency and myeloid genes, inducing their active demethylation and chromatin activation (Di Stefano et al. 2016; Sardina et al. 2018). Thus, showing that C/EBPα acts in concert with TET2 to reactivate pluripotency and myeloid genes. Therefore, we speculate that these proteins might be equally important for the DNA demethylation observed during C/EBPα-induced human B-cell to Macrophage conversion. To test this hypothesis, we should perform loss-of-function of *TET2* and interrogate which GREs become hypermethylated and experience a loss of 5hmC mark upon TET2 depletion. Moreover, we would need to identify if those regions are direct chromatin targets of TET2 by chromatin immunoprecipitation (ChIP) during TD. However, this last approach is challenging due to low-quality TET2 available commercial antibodies and the fact that this enzyme does not bind to the DNA. Therefore, it needs to be recruited always to the chromatin through partner proteins.

On the contrary, a small proportion of regions (1,858) that underwent methylation gains were no associated with the state of chromatin either closure or opening (**Fig R1.2b**). Moreover, those regions seem to be irrelevant for TD process with TF associated to

genome architecture (CTCF) and development (Hox, Snail). In fact, if we had applied a more stringent threshold for methylation changes (20% in contrast to 10%), we would have end with a smaller subset of gain regions.

Additionally, we also found demethylation occurring at GREs associated with inflammation-related genes such as the cytokine-coding genes *IL1B*, *IL1RN* and *IL6* **(Fig. R1.3a)**. Importantly, the IL6 pathway was found crucial for establishing proper pluripotency during the conversion of mouse embryonic fibroblasts (Takahashi and Yamanaka 2006; Mosteiro et al. 2016), or murine pre-B cells (Di Stefano et al. 2014; Plana-Carmona et al. 2022), into induced pluripotent stem cells (iPSCs). However, it was found to be dispensable for myeloid acquisition during the conversion of murine pre-B cells into induced macrophages (Plana-Carmona et al. 2022; Xie et al.). However, our current cellular model, starting from human B leukemic cells differs from the mouse transdifferentiation system and therefore IL-6 inflammatory pathway might be related to species requirements. Based on this, a previous work found differential IL-1β secretion between mouse and human monocytes after LPS treatment pointing out a different role in inflammasome activation (Gaidt et al. 2016).

Conversely to the IL6 pathway, the IL1 pathway has not been studied in the context of experimentally induced cell fate conversions. Therefore, we would need to interrogate IL-1 pathway and determine if its relevant for the acquired myeloid cell fate and explore its role in inflammation.

2. Interleukin 1 Receptor Antagonist (IL1RN) promoter as the top event showing DNA methylation-expression correlation

The link between DNAm and gene expression has been widely studied, with many reports showing a negative correlation between DNAm levels and gene expression, especially at promoter sites(Jones and Baylin 2002). However, reports describing causal relationships between DNAm, expression, and cellular phenotypes are scarce(Stricker et al. 2017). Here, we have utilized the highly efficient and homogenous reprogramming of B cells into macrophages to conduct an integrative analysis of DNAm and transcriptional dynamics by using RNA-seq.

Our findings revealed correlative changes, specifically in gene regulatory regions (ATAC+) experiencing a loss of DNAm. Specifically, a strong correlation was found between promoter regions losing methylation and gene reactivation compared to non-promoter regions **(Fig. R1.5 b-c)**. These changes were associated with genes related to myeloid cell fate and inflammation, such as the promoter of the Interleukin-1 receptor antagonist (*IL1RN*) gene **(Fig. R1.3c)**. However, when exploring the interplay between gain of DNAm (at ATAC+ regions) and gene expression changes, no significant correlation was observed **(Fig. R1.3a)**. These last results are conflicted with the stablished dogma for the interplay between DNAm and gene repression. Of note, we analyzed all open chromatin regions, not exclusively promoters, which may have impacted the obtained results. Nonetheless, recent evidence has shown that DNAm can cause transcriptional activation by counteracting the polycomb-mediated deposition of H3K27me3 during early embryogenesis (Monteagudo-Sánchez et al. 2024).

This is in line with previous genome-wide studies that have revealed context-specific transcriptional responses associated with DNAm gain at promoter regions, including increased gene expression (De Mendoza et al. 2022). The diverse responses may be influenced by the varying sensitivity of different transcription factor families to the presence of DNAm at their specific recognition sites in the genome.

Further analysis of the correlation between gene expression and DNAm loss reveals complex relationships. For instance, we detected some regions that were losing methylation during TD while its gene was getting inactivated **(Fig. R1.3c)**. One possible explanation is that the expression of those genes might not be controlled by DNA methylation of its promoter region. It has been shown that distant gene regulatory regions, such enhancers, can control expression of those genes (Hon et al. 2014c). Additionally, other epigenetic mechanisms like chromatin modifications might play a role, suggesting that we need to integrate more layers to understand their cooperativity and mechanism of gene regulation (Villaseñor and Baubec 2021).

Nevertheless, the aforementioned correlations have some limitations. Firstly, we have associated the differential methylation position to its closest gene. Although this approach is the gold standard it does not consider that some CpGs might have effects on distal genes.

To address this, an interesting experiment would be to assess the 3D structure of the chromatin to better define gene regulatory contacts. Of note, we can take advantage of public available Hi-C data (Stik et al. 2020) in our cellular model to interrogate possible interactions of the detected GREs and analyse the impact of DNAm in those contacts. However, although it will provide crucial information,

we would be limited by the heterogeneity of the data since our methods of WGBS-seq and RNA-seq are examining the bulk-population. Therefore, other approaches like scNMT-seq (single-cells nucleosome, methylation and transcription sequencing) would allow simultaneous profiling of the distinct epigenetic layers to better understand gene regulation (Argelaguet et al. 2019; Achinger-Kawecka et al. 2024). Moreover, a more precise technology based on single-molecule footprinting has been used to investigate the function of DNAm, accessibility and TF binding at cis-regulatory elements (Kreibich et al. 2023).

Despite there is more work to be done, our findings provide a better understanding of DNAm changes at GREs. We have validated the correlation between DNAm loss, such as the promoter of the *IL1RN* gene, with gene activation during TD. In addition, our data reveal that DNAm gain is not associated with changes at gene expression.

CHAPTER 2: Employing dCas9-methylation editing tools to modify the DNA methylation status of the IL1RN promoter

1. dCas9-TET1-mediated demethylation of the *IL1RN* promoter is sufficient for altering B cell fate

Since we aimed to uncover the causality between DNA methylation and gene expression, we targeted *IL1RN* promoter region with CRISPR/dCas9 DNAm editing tools.

The combination of four gRNAs with dCas9-TET1 fusion protein demonstrated specific binding and efficient demethylation of *IL1RN* gene promoter in B cells **(Fig. R2.1a-c)**. The strongest decrease in DNA methylation was observed in CpG #4 located upstream the TSS.

However, a small region, containing 4 CpGs, was analyzed in the *IL1RN* promoter **(Fig. R2.1c)**. Therefore, other techniques such as WGBS-seq or amplicon bisulfite sequencing are needed to better characterize the demethylation effect that dCas9-TET1 is inducing. Additionally, since TET1-mediated demethylation occurs through 5hmC, it would be interesting to measure methylation intermediates and investigate their effect on gene regulation. Importantly, 5hmC has been described as an essential mechanism for the correct cell fate decisions during normal and malignant development (Klug et al. 2013).

When investigating changes at gene expression upon dCas9-TET1 editing, we observed *IL1RN* gene activation and protein accumulation **(Fig. R2.1d-e)**. These findings suggest that *IL1RN* expression is directly regulated by its promoter methylation status. However, a methylation loss is insufficient to trigger transcription since this process requires the active engagement of chromatin factors. Therefore, to fully uncover the mechanism underlying the dCas9-TET1 mediated transcriptional activation, detailed profiling of changes in transcription factor occupancy and histone mark deposition is needed.

Comparing the transcriptomic profile of dCas9-TET1 sgIL1RN B cells with a public dataset generated during normal TD, we observed that our edited B cells cluster together with intermediate timepoints of the transdifferentiation and apart from the non-edited cells. Thus, suggesting we can initiate the B-to-macrophage conversion by just demethylating the *IL1RN* promoter. However, more experiments are needed to better elucidate the acquired phenotype of the edited B cells. For instance, we would need to check a panel of B-cell and myeloid surface markers by FACS to better defined the new acquired identity. Additionally, we still need to characterize further the dCas9-TET1 ChIP-

seq data to rule out the possibility that part of the transcriptomic changes observed are due to the reactivation of off-target genes.

A key question that remains open is the maintenance of the dCas9-TET1 mediated DNAm throughout cell division. On the one hand, we could expect a long-term effects since the lentiviral delivery ensures genome insertion and, therefore, constitutive expression of the dCas9-TET1, in contrast to transient expression methods. Nevertheless, based on previous research, it remains a challenge to maintain the gene reactivation effect during cell division as it requires permanent recruitment of dCas9 to the target region. In addition, endogenous cellular machinery such as *de novo* methyltransferase activity can interfere with dCas9-TET1 mediated effect (Sapozhnikov and Szyf 2021). To reach more potent and stable gene activation, recent studies have combined different strategies by fusing TET1 enzyme with transcription activators (CRISPRon) (Nuñez et al. 2021).

Taken together, our data suggest that IL1RN activation is dependent of DNA demethylation and is sufficient to modify the cellular transcriptome of B cells.

2. Validation of dCas9-DNMT3A editing specificity at IL1RN promoter

Previous studies have used CRISPRi and CRISPRa screens to discover genes or epigenetic regulators that regulate cellular processes, such as survival (Sanson et al. 2018) and differentiation(Liu et al. 2018a). However, these strategies are challenging when studying low-dividing cells like macrophages. Additionally, few studies have addressed the function of DNA modifications such as DNAm role during cell fate transitions (Liu et al. 2016a; Holtzman and Gersbach 2018).

In the present study, we have employed dCas9-DNM3A tool to specifically deposit 5-methylcytosine residues in the *IL1RN* promoter during the conversion of leukemic B cells into non-tumorigenic macrophages **(Fig. R2.2a)**. Firstly, we checked Cas9 binding to the target region to address potential off-targets by ChIP-seq. Genome-wide differential binding analysis revealed 853 off-target sites with IL1RN as one of the top candidates **(Fig. R2.2b-c)**. It is worth mentioning that this unspecificity was previously reported using these DNAm editing tools (Galonska et al. 2018; Liu et al. 2018a; Pflueger et al. 2018). In Liu's work they observed higher levels of the epigenetic construct were correlated with of non-specific binding of dCas9, pointing out the importance of modulating dCas9 levels to diminish the off-target effect (Liu et al. 2018a). In addition, they detected a positive correlation between gene expression and more levels of dCas9 vector. Based on this, we selected clones with the highest levels of dCas9 to achieve efficient *IL1RN* silencing.

Although we could detect dCas9-DNMT3A off-target binding sites no changes in DNA methylation or expression levels were found **(Fig. R2.3a-b)**. Moreover, when intersecting ChIP-seq, RNA-seq and methylation array data we detected *IL1RN* as the only gene bound by dCas9-DNMT3A, hypermethylated and downregulated **(Fig. R2.1e)**. Thus, we could validate the dCas9-DNMT3A editing specificity at the IL1RN promoter.

Finally, to rule out that the binding of the complexes might influence gene expression regardless of their catalytic activity, we should perform similar experiments with the catalytically dead epigenetic effectors (dTET and dDNMT3A) to assess the specific impact

of the chromatin modifiers in comparison with the wild-type form (Sapozhnikov and Szyf 2021).

CHAPTER 3: dCas9-DNMT3A-mediated hypermethylation of the *IL1RN* promoter leads to impaired human myeloid cell fate acquisition

1. IL1RN epigenome editing alters transcriptional dynamics and phagocytic capacity during transdifferentiation

As reviewed in the Introduction, previous studies have shown the relevance of the IL-1 pathway in myeloid malignancies (Higa et al. 2021; Villatoro et al. 2023; Park et al. 2024). However, the molecular mechanism involved in the observed myeloid bias upon loss of *IL1RN* are still unclear.

Here, dCas9-DNMT3A achieved targeted DNA hypermethylation to *IL1RN* promoter which was sufficient to abrogate *IL1RN* reactivation during TD. However, we did not achieve a complete blockage of DNA demethylation during TD (**Fig R2.3c**). One possible explanation would be that TET2 mediated DNA demethylation is competing with dCas9-DNMT3A effects. Of note, public available data of C/EBPα ChIP-seq confirmed its binding to the region as early as 24h upon TD induction (data not shown), just prior of the observed DNA demethylation (**Fig R1.5c**). Moreover, another work identified NF-KB TF binding to *IL1RN* promoter (Vento-Tormo et al. 2017). Interestingly, C/EBPα and NFKB TF have been described to interact with TET2 and demethylate myeloid genes (Sardina et al. 2018; Morante-Palacios et al. 2022b; De La Calle-Fabregat et al. 2024). Therefore, the data suggest that the balance between TET2 and the dCas9-DNMT3A effects might be involved in the incomplete blocked of the DNA demethylation in the

IL1RN promoter during TD in sgIL1RN edited cells. Another possible explanation would be that the steric interference of other proteins might affect dCas9-DNMT3A targeting the *IL1RN* region.

Our RNA expression analysis revealed large transcriptomic changes in sgIL1RN at day 7, while minor alterations were observed at short time points **(Fig. R3.1a)**. These results are in line with the progressive accumulation of *IL1RN* during TD **(Fig. R1.5d).** In addition, we observed a shift in the myeloid cell fate based on the reduced levels of CD14 and CD11b markers. Notably, HSCs exposed to IL-1β show differential expression of myeloid markers such as CD11b, M-CSFR, and CD18, therefore suggesting that we might be somehow mimicking these results by downregulating the pathway antagonist. Moreover, we also observed the sgIL1RN iMacs displayed an enhanced phagocytic capacity **(Fig. R3.3),** again indicating an altered myeloid status.

Despite the general link between macrophages and phagocytosis, further analyses are needed to better determine the polarized phenotypes (M1 or M2) of sgI1LRN iMacs. For instance, the analysis of cell surface protein expressions such as CD86, CD80, CD206, and CD163 would help us to better determine the cellular phenotype. In addition, metabolic assays to determine the use of glycolysis, mitochondrial oxidative phosphorylation or fatty acid oxidation would be fundamental (Wculek et al. 2023). In this regard, a recent study provides insights into the mechanism by which M2 AML-associated macrophages with altered phagocytic capacity enhanced fatty acid oxidation contribute to leukemia invasiveness (Weinhäuser et al. 2023).

Altogether, the observed altered myeloid phenotype is consistent with the imbalanced production of blood cells observed in mice chronically exposed to IL-1β(Higa et al. 2021) or those with an *Il1rn* deficiency(Villatoro et al. 2023). In both studies, HSCs exposed show differential expression of myeloid markers such as CD11b, M-CSFR and CD18.

Therefore, by affecting *IL1RN* expression by methylating its promoter could impact the acquisition of human myeloid cell fate during TD.

2. C/EBPα binds IL-1-pathway GREs during physiological myeloid cell fate

As discussed earlier, we identified GREs associated with the IL1 pathway-related genes (*IL1B* and *IL1RN*) that were losing DNAm during human B-to-macrophage TD **(Fig. R1.3a)**. Interestingly, these IL1 pathway-related GREs losing DNAm coincide with C/EBPα TF binding sites **(Fig. R3.6a-b)**. We also found that during the homeostatic differentiation of murine HSPCs to GMPs C/EBPα binds to the IL-1-related GREs **(Fig R3.6c-d)**.

Therefore, we hypothesize that C/EBPα binding to the *IL1B* and *IL1RN* promoter potentially triggers their DNA demethylation and chromatin activation, finally leading to their increased transcriptional activity (**Fig R3.6a-b)**. This is in line with the previously described role of C/EBPα as a pioneer transcription factor engaging a broad range of chromatin modifiers(Di Stefano et al. 2016) (Grebien et al. 2015), including TET2(Sardina et al. 2018). To test this, we would need to target *IL1B* and *IL1RN* with dCas9-DNMT3A and check if we can alter C/EBPα binding upon methylating its regulatory regions. Another approach to

confirm if C/EBPα transcriptionally regulates these regions would be to specifically mutate the binding domain of C/EBPα.

Overall, our results indicate that C/EBPα could be a critical transcriptional regulator of the IL-1 pathway during physiological myeloid establishment.

CHAPTER 4. IL1RN DNAm editing increases the responsiveness of iMacs to IL-1β treatment.

In mature myeloid cells, the IL1 pathway is crucial in responding to inflammatory stimuli(Gabay et al. 2010). Overactivity in this pathway leads to various immune disorders that can be managed by treating patients with a recombinant form of IL1RN known as anakinra(Cavalli and Dinarello 2018; Huet et al. 2020). One such immune disorder is the Deficiency of the Interleukin-1-Receptor Antagonist (DIRA), a rare but severe autoinflammatory disease characterized by mutations in the *IL1RN* gene(Aksentijevich et al. 2009). However, in most IL-1-related autoinflammatory conditions, such as cryopyrin-associated periodic syndromes (CAPS), no mutations exist in the *IL1RN* or *IL1B* genes. Rather, hyperactivation of the pathway in CAPS may be caused by abnormal methylation at these gene's promoters. Notably, this molecular condition is correctable by anti-IL-1b treatment(Vento-Tormo et al. 2017). Thus, it suggests that inflammatory responses involved in certain pathological conditions might be fine-tuned through the methylation status of the *IL1RN* gene.

We have proven this possibility using a DNAm editing tool to induce hypermethylation of the *IL1RN* promoter in a physiologically relevant macrophage cellular model. We observed hyperactivation of

the p65/NF-kB pathway in both untreated and 3-hour treated IL-1β iMacs, along with a deficient interferon pathway activation by immunofluorescence and gene expression data **(Fig R4.1 a-d)**. In line with these observations, DNAm profiling at the IL1RN or IL1β loci could be an early biomarker of IL1-related autoinflammatory conditions.

The IL-1 pathway and the interferon pathway counter-regulate each other, playing a crucial role in maintaining innate inflammatory balance in both homeostasis and infection(Mayer-Barber and Yan 2017). The impact of the Type I IFN pathway on the IL-1 pathway has been extensively researched (Gjerstorff 2023). However, little is known about the reciprocal cross-regulation molecular mechanisms(Mayer-Barber and Yan 2017)-(Mayer-Barber et al. 2014). In fact, recent work in the context of Mycobacterium tuberculosis infections in the lungs indicated that type I IFN responses antagonizes IL-1 pathway by inducing IL-10 and IL-1RN anti-inflammatory cytokines secretion - (Mayer-Barber et al. 2014).

Therefore, our *IL1RN*-depleted macrophages displaying an altered IFN activation in response to IL-1β might be instrumental in providing insight into the interplay of both key inflammatory pathways. Of note, we would need to interrogate the targets of p65 (NF-KB pathway) or STAT1/2 and IRF9 (IFN pathway) by chromatin immunoprecipitation assays upon IL1RN DNAm. This, will help us to understand the mechanistic insight of the genes that might be regulated by IL1RN DNAm status. Additionally, we could check protein post-translational modifications (including phosphorylation) to better determine pathway activity upon IL1RN DNAm editing.

Our results suggest that *IL1RN* promoter methylation affects myeloid differentiation that sensitizes the cells to respond differently to IL1β stimulation (**Fig.R4.3a-c**). However, we cannot rule out how fast DNAm can epigenetically regulate cellular response. For instance, Tet2 can be recruited to chromatin in fast response to oxidative stress to protect against abnormal DNAm (Zhang et al. 2017; Lazarenkov and Sardina 2022). To address this open question, we would need to alter DNAm at the terminal differentiation state of iMacs and then perform the treatment with IL-1β. This would need optimization as these cells are non-proliferative and difficult to transfect or infect (Moradian et al. 2020).

CHAPTER 5. IL1RN promoter DNAm alters the macrophage capacity to support cancer growth.

Our single-cell RNA-seq analysis identified CTRL iMacs that transcriptionally resemble the Interferon Stimulated Gene-Monocytes (ISG-Mon, 4) population in comparison with sgIL1RN cells that were more associated with the HEIS1 phenotype **(Fig. R4.5).** Therefore, IL1RN DNAm editing can modulate the acquisition of the ISG signature. Of note, the ISG-monocyte signature has been associated with lung pathological conditions. For instance, a positive correlation was detected between the percentage of ISG-monocytes in the lungs and the severity of the COVID-19 disease (Mulder et al. 2021).

Taken together, profiling DNA methylation and gene expression of *IL1RN* in COVID-19 patients might be relevant in the future. Hence, correlation studies between patients' prognosis and IL1RN levels can shed light on the disease's epigenetic mechanisms.

There are growing evidences suggesting that macrophages can both sense the signals to regulate immune responses by secreting cytokines and direct cell-cell interaction. For this, we applied a immunoassay approach to explore changes in the secretome upon IL1β treatment for 24h. We showed that sgIL1RN iMacs secrete higher levels of pro-inflammatory cytokines such as IL-1β and IL-6 while IL1RN anti-inflammatory cytokine was less secreted **(Fig. R5.1).** Notably, CXCL10 (IP-10), a cytokine secreted in response to IFN-γ, was more secreted when compared to CTRL iMacs. Thus, this suggests that IL1RN DNAm edited iMacs produce different cytokines that might modulate cellular responses in the tumor microenvironment.

In the context of cancer, our study identified lung and colon cancer-associated ISG monocytes displaying higher levels of pro-inflammatory genes than their healthy counterparts **(Fig. R5.2**). This suggests that ISG monocytes may play a role in regulating cancer growth within the tumor microenvironment. Interestingly, lung and colon cancer cells exhibited altered growth when cultured in the proinflammatory environment generated by the sgIL1RN macrophages **(Fig. R5.3)**. This aligns with the inflammation's known role in modulating cancer development (Grivennikov et al. 2010). However, these assays did not consider the crosstalk with other immune cells in the tumor microenvironment. To circumvent this limitation and to gain more physiological insight, we want to explore the role of the proinflammatory milieu in modulating CD8+ T-cell suppressive capacity in the context of solid tumors. Remarkably, CD8+ T cells are crucial in cold tumors where the absence of effector T cells difficult the tumor elimination (Bonaventura et al. 2019). Therefore, we want to check cytotoxic CD8+ T-cells proliferation and investigate if pro-

inflammatory sgIL1RN iMacs can affect the suppressive ability of CD8+ T-cells. Of note, in the tumor niche pro-inflammatory tumor associated macrophages can induce immune activation (Ma et al. 2022). Taken together, we hypothesize that our sgIL1RN cells would be more effective in suppressing T cells when coculture.

How can we utilize IL1RN DNAm editing for in vivo therapeutic purposes?

While major drug agencies have already approved a CRISPR/Cas9-based DNA editing treatment (FDA Approves First Gene Therapies to Treat Patients with Sickle Cell Disease), therapies for editing the epigenome are being delayed due to initial off-target effects and challenges in accurate delivery into the targeted cells (Villiger et al. 2024b). Despite these limitations, preclinical studies show promise in using DNAm editors, for instance, in reversing disease-associated abnormal DNAm events in neurological conditions (Liu et al. 2018a; Qian et al. 2023b). Notably, a recent breakthrough in epigenome therapy achieved permanent silencing of a gene involved in cholesterol homeostasis directly in the mouse liver (Cappelluti et al. 2024b). Therefore, based on recent technological developments, an epigenome editing therapy to modulate the DNAm levels of the *IL1RN* promoter in human myeloid cells might be a reality in the mid-term. For this, we first need to deliver dCas9-TET1 or dCas9-DNMT3A plasmids into primary cells. Since primary cells are challenging to transduce and have limited growth potential *in vitro*, we might use patient-derived xenografts (PDXs) for the initial mouse in vivo experiments.

Based on our findings, such therapy might be instrumental in fine-tuning the activity of the IL1 pathway in a broad range of human

conditions, from controlling autoinflammatory processes to modulating the growth of leukemia or solid cancers.

CONCLUSIONS

CONCLUSIONS

The conclusions obtained from this doctoral thesis can be summarized as follows:

1. WGBS-seq reveals an early genome-wide DNA methylation reshaping and loci-specific demethylation at ATAC-positive regions during human B cell to macrophage transdifferentiation (TD).

2. Gene regulatory elements (GREs) that experience DNA demethylation and gain accessibility during TD are related to myeloid genes, while the regions that gain DNA methylation are unrelated to cell fate conversion.

3. Interleukin-1 Receptor Antagonist (IL1RN) promoter has been identified as the best DNA methylation-expression correlated event during TD.

4. CRISPR dCas9-TET1-mediated methylation editing allows for establishing direct causality between the loss of DNA methylation at the IL1RN promoter and the upregulation of both IL1RN mRNA and protein in B cells.

5. Targeted DNA demethylation of the *IL1RN* promoter by dCas9-TET1 upregulates myeloid genes and influences the transcriptomic profile of B cells, poising them to a macrophage-like state.

6. An efficient DNA hypermethylation of the *IL1RN* promoter is achieved by using dCas9-DNMT3A editing tool, leading to impaired transcriptional kinetics at late stages of the TD process.

7. dCas9-DNMT3A-mediated hypermethylation of the *IL1RN* promoter leads to an altered myeloid cell fate characterized by reduced levels of CD11b and CD14 and enhanced phagocytic capacity.

8. C/EBPα TF binds to GREs of the IL-1 pathway prior to DNA demethylation during acquisition both human and murine myeloid cell fate the determination.

9. *IL1RN* DNAm editing modifies the early transcriptional response to IL-1β, leading to enhanced p65/NF-kB and diminished interferon pathway activation affecting genes related to phagocytosis, metabolism, and viral response

10. The ISG-monocyte transcriptional signature is largely perturbed upon *IL1RN* disruption.

11. The ISG-monocyte subpopulation is associated with distinct transcriptomic profile in colon and lung cancer when compared to healthy patients' datasets

12. dCas9-DNMT3A *IL1RN* DNAm editing enhances the realese of pro-inflammatory cytokines, leading to the establishment of secretome with a distinctive capacity to support cancer growth.

APPENDIX

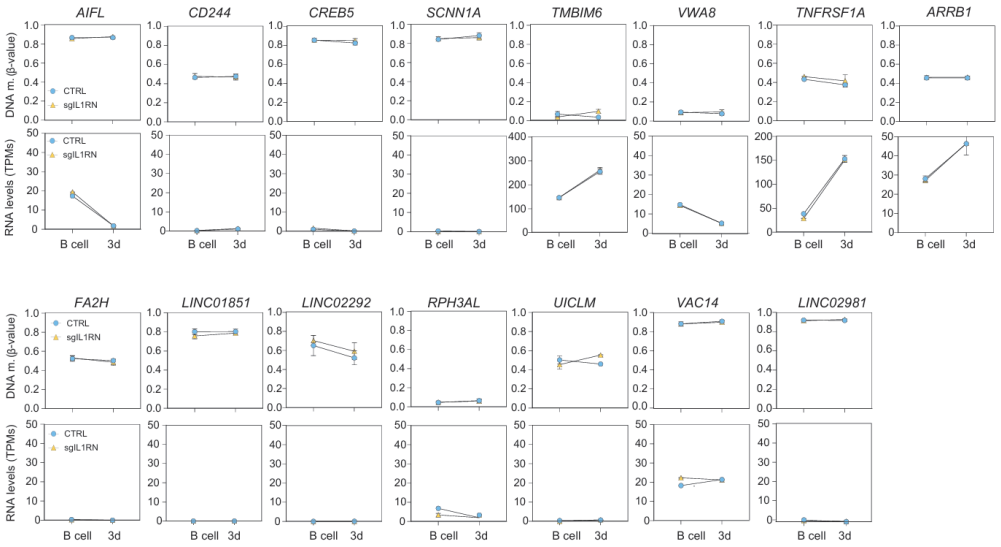

Fig S1. Plots showing the DNAm (upper panels) and transcriptional (bottom panels) dynamics of top dCas9-DNMT3A bound regions (FC>3.5, p<0.05) identified in Fig R2.2. Unpaired two-tailed Student's t-test, n=4 (DNAm) n=2 (RNA-seq) per group, mean ± s.e.m, not significant (p>0.05). Infinium MethylationEPIC BeadChip 850k v2.0 probes used to calculate DNAm levels for each plot are depicted in **Supplementary Table 1**.

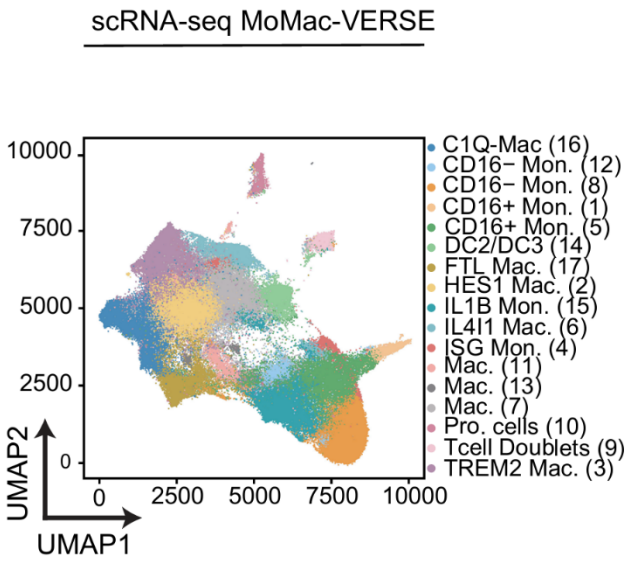

Fig S2. Uniform Manifold Approximation and Projection (UMAP) plot depicting the cellular identities contained in the MoMac-Verse scRNA-seq dataset.Related to **Fig R4.4**.

Supplementary Table 1: EPIC array probes used in Fig S1.

Gene name	EPIC array probes
AIFL	cg1431702, cg14351708, cg26572165
CD244	cg17283691, cg13143320
CREB5	cg07660664
SCNN1A	cg17727262
TMBIM6	cg20081348
VWA8	cg07584516
TNFRSF1A	cg00574580, cg23039316
ARRB1	cg20581146
FA2H	cg11572506
LINC01851	cg01136754
LINC02292	cg2077388
RPH3AL	cg08770870, cg10440639,cg11940040,cg23246911
UICLM	cg101434416, cg12525096
VAC14	cg02529145, cg02643387, cg14813551
LINC02981	cg23096130

Supplementary Table 2: Oligonucleotides used to construct sgRNAs targeting with dCas9 methylation editing tool**.**

	Forward (5' to 3')	Reverse (5' to 3')
lLsgRNA_H1	TCCCACTCCATTGCGACACTTAGTG	CACTAAGTGTCGCAATGGAG
lLsgRNA_mU6	TTGTTTGCTTCTCGCAGTGGGGCAGGG	CCCTGCCCCACTGCGAGAAG
lLsgRNA_hU6	CACCGAGCTTGGGTGAGTGACTATT	AATAGTCACTCACCCAAGCT
lLsgRNA_7SK	CCTCGCCACAACTCTGGGCCCGCAA	TTGCGGGCCCAGAGTTGTGG

CTRLsgRNA_H1	TCCCACCTAAGGTTAAGTCGCCCTC	AAACGATTCCAATTCAGCGGGAGT
CTRLsgRNA_mU6	TTGTTTGGCCCCCGGGGGAAAAATTT	AAACCCGGGGGCCCCCTTTTTAAACAA
CTRLsgRNA_ hU6	CACCGTAGTACTTTCAAGAGTCCA	AAACTATCATGAAAGTTCTCAGGTC
CTRLsgRNA_7SK	CCTCGCACTACCAGAGCTAACTCA	AAACCGTGATGGTCTCGATTGAGT

Supplementary Table 3: Primers used for RT-qPCR to determine the expression levels in sgIL1RN and sgCTRL cells.

	Forward (5' to 3')	**Reverse (5' to 3')**
IL1RN	IDT Cat #228354241	CTGCATTGTTTTGCCAGTGT
HPRT	GACCAGTCAACAGGGGACAT	CTGCATTGTTTTGCCAGTGT
B2M	AGGCTATCCAGCGTACTCCA	TCAATGTCGGATGGATGAAA
BRCA1	CTGCTCTGGGTAAAGTTCATTGG	TAAAGGACACTGTGAAGGCCC
CDK1	CACTTGGCTTCAAAGCTGGC	TGGGTATGGTAGATCCCGGC
LEF1	ATTCTTGGCAGAAGGTGGCA	GCAGCTGTCATTCTTGGACC
CD79A	CCTTAGTCATATTCCCCCAG	TTTAGAGGGAAGAAGAGTGG

HK2	GCTCAACCATGACCAAGTGC	AACTCTCCGTGTTCTGTCCC
PGK1	CTGGGCAAGGATGTTCTGTT	CACATGAAAGCGGAGGTTCT
ITGAM	GGGGTCTCCACTAAATATCTC	CTGACCTGATATTGATGCTG
CD14	GATTACATAAACTGTCAGAGGC	TCCATGGTCGATAAGTCTTC

Supplementary Table 4. List of genomic regions of the CpGs located at *IL1RN* promoter analyzed by pyrosequencing. CpG code corresponds at **Fig R2.1c.**

CpG code	**Genomic position hg38**
#1	chr2:113,127,510-113,127,511
#2	chr2:113,127,517-113,127,518
#3	chr2:113,127,539-113,127,540
#4	chr2:113,127,589-113,127,590

Primers used in this study for the PCR amplification of *IL1RN* promoter after bisulfite conversion for pyrosequencing analysis.

	Forward (5' to 3')	**Reverse-bio (5' to 3')**	**Region (5' to 3') hg38**
IL1RN promoter	AGTGGGGTTGAAAGTGACAAC	CAGAATGGAAATCTGCAGAGGCCTC	chr2:113,127,448-113,127,645

Primers used in this study for sequencing by pyrosequencing and assess the methylation levels of target CpG sites.

	Forward (5' to 3')
S1 IL1RN	GAAATGCGAGGAGGGTATTTCCGCTTCTCG
S2 IL1RN	CGCTTCTCGCAGTGGGGCAGGGTGGCAGACGC

REFERENCES

1. Abudayyeh OO, Gootenberg JS, Konermann S, Joung J, Slaymaker IM, Cox DBT, et al. C2c2 is a single-component programmable RNA-guided RNA-targeting CRISPR effector. Science. 2016 Aug 5;353(6299):aaf5573.

2. Achinger-Kawecka J, Stirzaker C, Portman N, Campbell E, Chia KM, Du Q, et al. The potential of epigenetic therapy to target the 3D epigenome in endocrine-resistant breast cancer. Nat Struct Mol Biol. 2024 Mar;31(3):498–512.

3. Ågerstam H, Karlsson C, Hansen N, Sandén C, Askmyr M, Von Palffy S, et al. Antibodies targeting human IL1RAP (IL1R3) show therapeutic effects in xenograft models of acute myeloid leukemia. Proc Natl Acad Sci. 2015 Aug 25;112(34):10786–91.

4. Agostini L, Martinon F, Burns K, McDermott MF, Hawkins PN. NALP3 Forms an IL-1␣-Processing Inflammasome with Increased Activity in Muckle-Wells Autoinflammatory Disorder. 2004;

5. Aksentijevich I, Dancey P, Laxer R, Pham TH, Sandler NG, Turner ML, et al. An Autoinflammatory Disease with Deficiency of the Interleukin-1–Receptor Antagonist. N Engl J Med. 2009;

6. Allis CD, Jenuwein T. The molecular hallmarks of epigenetic control. Nat Rev Genet. 2016 Aug;17(8):487–500.

7. Álvarez-Errico D, Vento-Tormo R, Sieweke M, Ballestar E. Epigenetic control of myeloid cell differentiation, identity and function. Nat Rev Immunol. 2015 Jan;15(1):7–17.

8. Amabile A, Migliara A, Capasso P, Biffi M, Cittaro D, Naldini L, et al. Inheritable Silencing of Endogenous Genes by Hit-and-Run Targeted Epigenetic Editing. Cell. 2016 Sep;167(1):219-232.e14.

9. Anzalone AV, Randolph PB, Davis JR, Sousa AA, Koblan LW, Levy JM, et al. Search-and-replace genome editing without double-strand breaks or donor DNA. Nature. 2019 Dec;576(7785):149–57.

10. Arend WP, Joslin FG, Massoni RJ. Effects of immune complexes on production by human monocytes of interleukin 1 or an interleukin 1 inhibitor. J Immunol. 1985 Jun 1;134(6):3868–75.

11. Arend WP, Welgus HG, Thompson RC, Eisenberg SP. Biological properties of recombinant human monocyte-derived interleukin 1 receptor antagonist. J Clin Invest. 1990 May 1;85(5):1694–7.

12. Argelaguet R, Clark SJ, Mohammed H, Stapel LC, Krueger C, Kapourani CA, et al. Multi-omics profiling of mouse gastrulation at single cell resolution. Nature. 2019 Oct 24;576(7787):487–91.

13. Aryee MJ, Jaffe AE, Corrada-Bravo H, Ladd-Acosta C, Feinberg AP, Hansen KD, et al. Minfi: a flexible and comprehensive Bioconductor package for the analysis of Infinium DNA methylation microarrays. Bioinformatics. 2014 May 15;30(10):1363–9.

14. Babaian A, Romanish MT, Gagnier L, Kuo LY, Karimi MM, Steidl C, et al. Onco-exaptation of an endogenous retroviral LTR drives IRF5 expression in Hodgkin lymphoma. Oncogene. 2016 May 12;35(19):2542–6.

15. Bauer U, Daujat S, Nielsen SJ, Nightingale K, Kouzarides T. Methylation at arginine 17 of histone H3 is linked to gene activation. EMBO Rep. 2002 Jan;3(1):39–44.

16. Baylin SB, Jones PA. Epigenetic Determinants of Cancer. Cold Spring Harb Perspect Biol. 2016 Sep 1;8(9):a019505.

17. Berdasco M, Esteller M. Clinical epigenetics: seizing opportunities for translation. Nat Rev Genet. 2019 Feb;20(2):109–27.

18. Bernstein BE, Mikkelsen TS, Xie X, Kamal M, Huebert DJ, Cuff J, et al. A bivalent chromatin structure marks key developmental genes in embryonic stem cells. Cell. 2006 Apr 21;125(2):315–26.

19. Bird A. DNA methylation patterns and epigenetic memory. Genes Dev. 2002 Jan 1;16(1):6–21.

20. Bird AP. CpG-rich islands and the function of DNA methylation. Nature. 1986 May 15;321(6067):209–13.

21. Blériot C, Chakarov S, Ginhoux F. Determinants of Resident Tissue Macrophage Identity and Function. Immunity. 2020 Jun;52(6):957–70.

22. Bogdanović O, Smits AH, de la Calle Mustienes E, Tena JJ, Ford E, Williams R, et al. Active DNA demethylation at enhancers during the vertebrate phylotypic period. Nat Genet. 2016 Apr;48(4):417–26.

23. Bogdanović O, Veenstra GJC. DNA methylation and methyl-CpG binding proteins: developmental requirements and function. Chromosoma. 2009 Oct;118(5):549–65.

24. Bolger AM, Lohse M, Usadel B. Trimmomatic: a flexible trimmer for Illumina sequence data. Bioinformatics. 2014 Aug 1;30(15):2114–20.

25. Bonaventura P, Shekarian T, Alcazer V, Valladeau-Guilemond J, Valsesia-Wittmann S, Amigorena S, et al. Cold Tumors: A Therapeutic Challenge for Immunotherapy. Front Immunol. 2019 Feb 8;10:168.

26. Boyer LA, Plath K, Zeitlinger J, Brambrink T, Medeiros LA, Lee TI, et al. Polycomb complexes repress developmental regulators in murine embryonic stem cells. Nature. 2006 May 18;441(7091):349–53.

27. Broderick L, Hoffman HM. IL-1 and autoinflammatory disease: biology, pathogenesis and therapeutic targeting. Nat Rev Rheumatol. 2022 Aug;18(8):448–63.

28. Bussmann LH, Schubert A, Vu Manh TP, De Andres L, Desbordes SC, Parra M, et al. A Robust and Highly Efficient Immune Cell Reprogramming System. Cell Stem Cell. 2009 Nov;5(5):554–66.

29. Caiado F, Kovtonyuk LV, Gonullu NG, Fullin J, Boettcher S, Manz MG. Aging drives *Tet2 +/−* clonal hematopoiesis via IL-1 signaling. Blood. 2023 Feb 23;141(8):886–903.

30. Cappelluti MA, Mollica Poeta V, Valsoni S, Quarato P, Merlin S, Merelli I, et al. Durable and efficient gene silencing in vivo by hit-and-run epigenome editing. Nature. 2024a Mar 14;627(8003):416–23.

31. Cauchois R, Koubi M, Delarbre D, Manet C, Carvelli J, Blasco VB, et al. Early IL-1 receptor blockade in severe inflammatory respiratory failure complicating COVID-19. Proc Natl Acad Sci. 2020 Aug 11;117(32):18951–3.

32. Cavalli G, Dinarello CA. Anakinra Therapy for Non-cancer Inflammatory Diseases. Front Pharmacol. 2018 Nov 6;9:1157.

33. Challen GA, Sun D, Jeong M, Luo M, Jelinek J, Berg JS, et al. Dnmt3a is essential for hematopoietic stem cell differentiation. Nat Genet. 2012 Jan;44(1):23–31.

34. Chaplin DD. Overview of the immune response. J Allergy Clin Immunol. 2010 Feb;125(2 Suppl 2):S3-23.

35. Charlton J, Jung EJ, Mattei AL, Bailly N, Liao J, Martin EJ, et al. TETs compete with DNMT3 activity in pluripotent cells at thousands of methylated somatic enhancers. Nat Genet. 2020 Aug;52(8):819–27.

36. Chatterjee P, Jakimo N, Jacobson JM. Minimal PAM specificity of a highly similar SpCas9 ortholog. Sci Adv. 2018 Oct 24;4(10):eaau0766.

37. Chavez A, Scheiman J, Vora S, Pruitt BW, Tuttle M, P R Iyer E, et al. Highly efficient Cas9-mediated transcriptional programming. Nat Methods. 2015 Apr;12(4):326–8.

38. Chen S, Saeed AFUH, Liu Q, Jiang Q, Xu H, Xiao GG, et al. Macrophages in immunoregulation and therapeutics. Signal Transduct Target Ther. 2023 May 22;8(1):207.

39. Chen Y, Chen L, Lun ATL, Baldoni PL, Smyth GK. edgeR 4.0: powerful differential analysis of sequencing data with expanded functionality and improved support for small counts and larger datasets [Internet]. 2024 [cited 2024 Jul 8]. Available from: http://biorxiv.org/lookup/doi/10.1101/2024.01.21.576131

40. Choi J, Lysakovskaia K, Stik G, Demel C, Söding J, Tian TV, et al. Evidence for additive and synergistic action of mammalian enhancers during cell fate determination. eLife. 2021 Mar 26;10:e65381.

41. Choudhury SR, Cui Y, Lubecka K, Stefanska B, Irudayaraj J. CRISPR-dCas9 mediated TET1 targeting for selective DNA demethylation at *BRCA1* promoter. Oncotarget. 2016 Jul 19;7(29):46545–56.

42. Coates CJ, Kaminski JM, Summers JB, Segal DJ, Miller AD, Kolb AF. Site-directed genome modification: derivatives of DNA-modifying enzymes as targeting tools. Trends Biotechnol. 2005 Aug 1;23(8):407–19.

43. Colantuoni M, Jofra Hernandez R, Pettinato E, Basso-Ricci L, Magnani L, Andolfi G, et al. Constitutive IL-1RA production by modified immune cells protects against IL-1–mediated inflammatory disorders. Sci Transl Med. 2023 May 31;15(698):eade3856.

44. Complex heatmap visualization - Gu - 2022 - iMeta - Wiley Online Library. [cited 2024 May 17]. Available from: https://onlinelibrary.wiley.com/doi/full/10.1002/imt2.43

45. Conway JR, Lex A, Gehlenborg N. UpSetR: an R package for the visualization of intersecting sets and their properties. Hancock J, editor. Bioinformatics. 2017 Sep 15;33(18):2938–40.

46. Dahl R, Walsh JC, Lancki D, Laslo P, Iyer SR, Singh H, et al. Regulation of macrophage and neutrophil cell fates by the PU.1:C/EBPα ratio and granulocyte colony-stimulating factor. Nat Immunol. 2003 Oct;4(10):1029–36.

47. Dai HQ, Wang BA, Yang L, Chen JJ, Zhu GC, Sun ML, et al. TET-mediated DNA demethylation controls gastrulation by regulating Lefty–Nodal signalling. Nature. 2016 Oct;538(7626):528–32.

48. Davis RL, Weintraub H, Lassar AB. Expression of a single transfected cDNA converts fibroblasts to myoblasts. Cell. 1987 Dec 24;51(6):987–1000.

49. Dawlaty MM, Breiling A, Le T, Barrasa MI, Raddatz G, Gao Q, et al. Loss of Tet Enzymes Compromises Proper Differentiation of Embryonic Stem Cells. Dev Cell. 2014 Apr;29(1):102–11.

50. De La Calle-Fabregat C, Calafell-Segura J, Gardet M, Dunsmore G, Mulder K, Ciudad L, et al. NF-κB and TET2 promote macrophage reprogramming in hypoxia that overrides the immunosuppressive effects of the tumor microenvironment. Sci Adv. 2024 Sep 20;10(38):eadq5226.

51. De Mendoza A, Nguyen TV, Ford E, Poppe D, Buckberry S, Pflueger J, et al. Large-scale manipulation of promoter DNA methylation reveals context-specific transcriptional responses and stability. Genome Biol. 2022 Jul 26;23(1):163.

52. DeNardo DG, Ruffell B. Macrophages as regulators of tumour immunity and immunotherapy. Nat Rev Immunol. 2019 Jun;19(6):369–82.

53. Di Stefano B, Collombet S, Jakobsen JS, Wierer M, Sardina JL, Lackner A, et al. C/EBPα creates elite cells for iPSC reprogramming by upregulating Klf4 and increasing the levels of Lsd1 and Brd4. Nat Cell Biol. 2016 Apr;18(4):371–81.

54. Di Stefano B, Sardina JL, Van Oevelen C, Collombet S, Kallin EM, Vicent GP, et al. C/EBPα poises B cells for rapid reprogramming into induced pluripotent stem cells. Nature. 2014 Feb 13;506(7487):235–9.

55. Dinarello CA. The IL-1 family of cytokines and receptors in rheumatic diseases. Nat Rev Rheumatol. 2019 Oct;15(10):612–32.

56. Dinarello CA, Goldin NP, Wolff SM. Demonstration and characterization of two distinct human leukocytic pyrogens. J Exp Med. 1974 Jun 1;139(6):1369–81.

57. Dobin A, Davis CA, Schlesinger F, Drenkow J, Zaleski C, Jha S, et al. STAR: ultrafast universal RNA-seq aligner. Bioinformatics. 2013 Jan 1;29(1):15–21.

58. Doi A, Park IH, Wen B, Murakami P, Aryee MJ, Irizarry R, et al. Differential methylation of tissue- and cancer-specific CpG island shores distinguishes human induced pluripotent stem cells, embryonic stem cells and fibroblasts. Nat Genet. 2009 Dec;41(12):1350–3.

59. Elliott EI, Sutterwala FS. Monocytes Take Their Own Path to IL-1β. Immunity. 2016 Apr;44(4):713–5.

60. Engler C, Kandzia R, Marillonnet S. A One Pot, One Step, Precision Cloning Method with High Throughput Capability. El-Shemy HA, editor. PLoS ONE. 2008 Nov 5;3(11):e3647.

61. Engler C, Marillonnet S. Golden Gate Cloning. In: Valla S, Lale R, editors. DNA Cloning and Assembly Methods [Internet]. Totowa, NJ: Humana Press; 2014 [cited 2024 Jul 8]. p. 119–31. (Methods in

Molecular Biology; vol. 1116). Available from: https://link.springer.com/10.1007/978-1-62703-764-8_9

62. Falkenberg KJ, Johnstone RW. Histone deacetylases and their inhibitors in cancer, neurological diseases and immune disorders. Nat Rev Drug Discov. 2014 Sep;13(9):673–91.

63. FDA Approves First Gene Therapies to Treat Patients with Sickle Cell Disease.

64. Figueroa ME, Abdel-Wahab O, Lu C, Ward PS, Patel J, Shih A, et al. Leukemic IDH1 and IDH2 Mutations Result in a Hypermethylation Phenotype, Disrupt TET2 Function, and Impair Hematopoietic Differentiation. Cancer Cell. 2010 Dec;18(6):553–67.

65. Fitzpatrick GV, Soloway PD, Higgins MJ. Regional loss of imprinting and growth deficiency in mice with a targeted deletion of KvDMR1. Nat Genet. 2002 Nov;32(3):426–31.

66. Forsyth KS, Jiwrajka N, Lovell CD, Toothacre NE, Anguera MC. The conneXion between sex and immune responses. Nat Rev Immunol. 2024 Jul;24(7):487–502.

67. Gabay C, Lamacchia C, Palmer G. IL-1 pathways in inflammation and human diseases. Nat Rev Rheumatol. 2010 Apr;6(4):232–41.

68. Gabay C, Palmer G. Mutations in the IL1RN locus lead to autoinflammation. Nat Rev Rheumatol. 2009 Sep;5(9):480–2.

69. Gaidt MM, Ebert TS, Chauhan D, Schmidt T, Schmid-Burgk JL, Rapino F, et al. Human Monocytes Engage an Alternative Inflammasome Pathway. Immunity. 2016 Apr;44(4):833–46.

70. Galonska C, Charlton J, Mattei AL, Donaghey J, Clement K, Gu H, et al. Genome-wide tracking of dCas9-methyltransferase footprints. Nat Commun. 2018 Feb 9;9(1):597.

71. Garcia-Alonso L, Holland CH, Ibrahim MM, Turei D, Saez-Rodriguez J. Benchmark and integration of resources for the estimation of human transcription factor activities. Genome Res. 2019 Aug;29(8):1363–75.

72. Garlanda C, Mantovani A. Interleukin-1 in tumor progression, therapy, and prevention. Cancer Cell. 2021 Aug;39(8):1023–7.

73. Geissmann F, Manz MG, Jung S, Sieweke MH, Merad M, Ley K. Development of monocytes, macrophages, and dendritic cells. Science. 2010 Feb 5;327(5966):656–61.

74. Gemberling MP, Siklenka K, Rodriguez E, Tonn-Eisinger KR, Barrera A, Liu F, et al. Transgenic mice for in vivo epigenome editing with CRISPR-based systems. Nat Methods. 2021 Aug;18(8):965–74.

75. Gilbert LA, Horlbeck MA, Adamson B, Villalta JE, Chen Y, Whitehead EH, et al. Genome-Scale CRISPR-Mediated Control of Gene Repression and Activation. Cell. 2014 Oct 23;159(3):647–61.

76. Gilbert LA, Larson MH, Morsut L, Liu Z, Brar GA, Torres SE, et al. CRISPR-mediated modular RNA-guided regulation of transcription in eukaryotes. Cell. 2013 Jul 18;154(2):442–51.

77. Ginhoux F, Jung S. Monocytes and macrophages: developmental pathways and tissue homeostasis. Nat Rev Immunol. 2014 Jun;14(6):392–404.

78. Gjerstorff MF. Crosstalk between interferon and interleukin-1 antiviral signaling in cancer cells: implications for immune evasion and therapeutic resistance. Front Immunol. 2023 Jun 8;14:1219870.

79. Goldberg AD, Allis CD, Bernstein E. Epigenetics: A Landscape Takes Shape. Cell. 2007 Feb 23;128(4):635–8.

80. Gordon S, Taylor PR. Monocyte and macrophage heterogeneity. Nat Rev Immunol. 2005 Dec 1;5(12):953–64.

81. Graf T. Historical Origins of Transdifferentiation and Reprogramming. Cell Stem Cell. 2011 Dec;9(6):504–16.

82. Grebien F, Vedadi M, Getlik M, Giambruno R, Grover A, Avellino R, et al. Pharmacological targeting of the Wdr5-MLL interaction in C/EBPα N-terminal leukemia. Nat Chem Biol. 2015 Aug;11(8):571–8.

83. Greenberg MVC, Bourc'his D. The diverse roles of DNA methylation in mammalian development and disease. Nat Rev Mol Cell Biol. 2019 Oct;20(10):590–607.

84. Greve G, Andrieux G, Schlosser P, Blagitko-Dorfs N, Rehman UU, Ma T, et al. In vivo kinetics of early, non-random methylome and transcriptome changes induced by DNA-hypomethylating treatment in primary AML blasts. Leukemia. 2023 May;37(5):1018–27.

85. Grivennikov SI, Greten FR, Karin M. Immunity, Inflammation, and Cancer. Cell. 2010 Mar;140(6):883–99.

86. Hao Y, Hao S, Andersen-Nissen E, Mauck WM, Zheng S, Butler A, et al. Integrated analysis of multimodal single-cell data. Cell. 2021 Jun;184(13):3573-3587.e29.

87. Hasseman, et al. C/EBPa is required for long-term self-renewal and lineage priming of Hematopoietic Stem Cells and for the maintenance of Epigenetic Configurations in Multipotens Progenitors. PLOS Genetics (2014).

88. Hawkins PN, Lachmann HJ, McDermott MF. Interleukin-1-receptor antagonist in the Muckle-Wells syndrome. N Engl J Med. 2003 Jun 19;348(25):2583–4.

89. He YF, Li BZ, Li Z, Liu P, Wang Y, Tang Q, et al. Tet-Mediated Formation of 5-Carboxylcytosine and Its Excision by TDG in Mammalian DNA. Science. 2011 Sep 2;333(6047):1303–7.

90. Heinz S, Benner C, Spann N, Bertolino E, Lin YC, Laslo P, et al. Simple Combinations of Lineage-Determining Transcription Factors Prime cis-Regulatory Elements Required for Macrophage and B Cell Identities. Mol Cell. 2010 May;38(4):576–89.

91. Heinz S, Romanoski CE, Benner C, Glass CK. The selection and function of cell type-specific enhancers. Nat Rev Mol Cell Biol. 2015 Mar;16(3):144–54.

92. Higa KC, Goodspeed A, Chavez JS, De Dominici M, Danis E, Zaberezhnyy V, et al. Chronic interleukin-1 exposure triggers selection for *Cebpa* -knockout multipotent hematopoietic progenitors. J Exp Med. 2021 Jun 7;218(6):e20200560.

93. Hilton IB, D'Ippolito AM, Vockley CM, Thakore PI, Crawford GE, Reddy TE, et al. Epigenome editing by a CRISPR-Cas9-based acetyltransferase activates genes from promoters and enhancers. Nat Biotechnol. 2015 May;33(5):510–7.

94. Hoffman HM, Mueller JL, Broide DH, Wanderer AA, Kolodner RD. Mutation of a new gene encoding a putative pyrin-like protein causes familial cold autoinflammatory syndrome and Muckle–Wells syndrome. Nat Genet. 2001 Nov;29(3):301–5.

95. Holtzman L, Gersbach CA. Editing the Epigenome: Reshaping the Genomic Landscape. Annu Rev Genomics Hum Genet. 2018 Aug 31;19(1):43–71.

96. Hon GC, Song CX, Du T, Jin F, Selvaraj S, Lee AY, et al. 5mC oxidation by Tet2 modulates enhancer activity and timing of transcriptome reprogramming during differentiation. Mol Cell. 2014a Oct 23;56(2):286–97.

97. Huang HT, Figueroa ME. Epigenetic deregulation in myeloid malignancies. Blood. 2021 Aug 26;138(8):613–24.

98. Huber W, Carey VJ, Gentleman R, Anders S, Carlson M, Carvalho BS, et al. Orchestrating high-throughput genomic analysis with Bioconductor. Nat Methods. 2015 Feb;12(2):115–21.

99. Huet T, Beaussier H, Voisin O, Jouveshomme S, Dauriat G, Lazareth I, et al. Anakinra for severe forms of COVID-19: a cohort study. Lancet Rheumatol. 2020 Jul;2(7):e393–400.

100. Hussmann JA, Ling J, Ravisankar P, Yan J, Cirincione A, Xu A, et al. Mapping the genetic landscape of DNA double-strand break repair. Cell. 2021 Oct 28;184(22):5653-5669.e25.

101. Ito S, Shen L, Dai Q, Wu SC, Collins LB, Swenberg JA, et al. Tet Proteins Can Convert 5-Methylcytosine to 5-Formylcytosine and 5-Carboxylcytosine. Science. 2011 Sep 2;333(6047):1300–3.

102. Iwasaki H, Somoza C, Shigematsu H, Duprez EA, Iwasaki-Arai J, Mizuno S ichi, et al. Distinctive and indispensable roles of PU.1 in maintenance of hematopoietic stem cells and their differentiation. Blood. 2005 Sep 1;106(5):1590–600.

103. Jack I, Seshadri R, Garson M, Michael P, Callen D, Zola H, et al. RCH-ACV: A lymphoblastic leukemia cell line with chromosome translocation 1;19 and trisomy 8. Cancer Genet Cytogenet. 1986 Jan 15;19(3):261–9.

104. Jacobsen SEW, Nerlov C. Haematopoiesis in the era of advanced single-cell technologies. Nat Cell Biol. 2019 Jan;21(1):2–8.

105. Jiang F, Doudna JA. CRISPR-Cas9 Structures and Mechanisms. Annu Rev Biophys. 2017 May 22;46:505–29.

106. Jinek M, Chylinski K, Fonfara I, Hauer M, Doudna JA, Charpentier E. A programmable dual-RNA-guided DNA endonuclease in adaptive bacterial immunity. Science. 2012 Aug 17;337(6096):816–21.

107. Jones PA. Functions of DNA methylation: islands, start sites, gene bodies and beyond. Nat Rev Genet. 2012 Jul;13(7):484–92.

108. Jones PA, Baylin SB. The fundamental role of epigenetic events in cancer. Nat Rev Genet. 2002 Jun;3(6):415–28.

109. Kabadi AM, Ousterout DG, Hilton IB, Gersbach CA. Multiplex CRISPR/Cas9-based genome engineering from a single lentiviral vector. Nucleic Acids Res. 2014 Oct 29;42(19):e147–e147.

110. Kallin EM, Rodríguez-Ubreva J, Christensen J, Cimmino L, Aifantis I, Helin K, et al. Tet2 Facilitates the Derepression of Myeloid Target Genes during CEBPα-Induced Transdifferentiation of Pre-B Cells. Mol Cell. 2012 Oct;48(2):266–76.

111. Kaluscha S, Domcke S, Wirbelauer C, Stadler MB, Durdu S, Burger L, et al. Evidence that direct inhibition of transcription factor binding is the prevailing mode of gene and repeat repression by DNA methylation. Nat Genet. 2022 Dec;54(12):1895–906.

112. Kelly TK, Miranda TB, Liang G, Berman BP, Lin JC, Tanay A, et al. H2A.Z maintenance during mitosis reveals nucleosome shifting on mitotically silenced genes. Mol Cell. 2010 Sep 24;39(6):901–11.

113. Klann TS, Black JB, Chellappan M, Safi A, Song L, Hilton IB, et al. CRISPR–Cas9 epigenome editing enables high-throughput screening for functional regulatory elements in the human genome. Nat Biotechnol. 2017 Jun;35(6):561–8.

114. Klug A, Rhodes D. Zinc fingers: a novel protein fold for nucleic acid recognition. Cold Spring Harb Symp Quant Biol. 1987;52:473–82.

115. Klug M, Schmidhofer S, Gebhard C, Andreesen R, Rehli M. 5-Hydroxymethylcytosine is an essential intermediate of active DNA demethylation processes in primary human monocytes. Genome Biol. 2013 May 26;14(5):R46.

116. Ko M, Huang Y, Jankowska AM, Pape UJ, Tahiliani M, Bandukwala HS, et al. Impaired hydroxylation of 5-methylcytosine in myeloid cancers with mutant TET2. Nature. 2010 Dec;468(7325):839–43.

117. Kohn DB, Booth C, Kang EM, Pai SY, Shaw KL, Santilli G, et al. Lentiviral gene therapy for X-linked chronic granulomatous disease. Nat Med. 2020 Feb;26(2):200–6.

118. Kojima S, Shiochi N, Sato K, Yamaura M, Ito T, Yamamura N, et al. Epigenome editing reveals core DNA methylation for imprinting control in the *Dlk1-Dio3* imprinted domain. Nucleic Acids Res. 2022 May 20;50(9):5080–94.

119. Konermann S, Brigham MD, Trevino AE, Joung J, Abudayyeh OO, Barcena C, et al. Genome-scale transcriptional activation by an engineered CRISPR-Cas9 complex. Nature. 2015 Jan 29;517(7536):583–8.

120. Korotkevich G, Sukhov V, Budin N, Shpak B, Artyomov MN, Sergushichev A. Fast gene set enrichment analysis [Internet]. 2016 [cited 2024 Aug 16]. Available from: http://biorxiv.org/lookup/doi/10.1101/060012

121. Kreibich E, Kleinendorst R, Barzaghi G, Kaspar S, Krebs AR. Single-molecule footprinting identifies context-dependent regulation of enhancers by DNA methylation. Mol Cell. 2023 Mar;83(5):787-802.e9.

122. Krueger F, Andrews SR. Bismark: a flexible aligner and methylation caller for Bisulfite-Seq applications. Bioinformatics. 2011 Jun 1;27(11):1571–2.

123. Kulessa H, Frampton J, Graf T. GATA-1 reprograms avian myelomonocytic cell lines into eosinophils, thromboblasts, and erythroblasts. Genes Dev. 1995 May 15;9(10):1250–62.

124. Kyriazopoulou E, Poulakou G, Milionis H, Metallidis S, Adamis G, Tsiakos K, et al. Early treatment of COVID-19 with anakinra guided by soluble urokinase plasminogen receptor plasma levels: a double-blind, randomized controlled phase 3 trial. Nat Med. 2021 Oct;27(10):1752–60.

125. Lacey DC, Achuthan A, Fleetwood AJ, Dinh H, Roiniotis J, Scholz GM, et al. Defining GM-CSF– and Macrophage-CSF–Dependent Macrophage Responses by In Vitro Models. J Immunol. 2012 Jun 1;188(11):5752–65.

126. Laganiere J, Kells AP, Lai JT, Guschin D, Paschon DE, Meng X, et al. An Engineered Zinc Finger Protein Activator of the Endogenous Glial Cell Line-Derived Neurotrophic Factor Gene Provides Functional Neuroprotection in a Rat Model of Parkinson's Disease. J Neurosci. 2010 Dec 8;30(49):16469–74.

127. Langmead B, Salzberg SL. Fast gapped-read alignment with Bowtie 2. Nat Methods. 2012 Apr;9(4):357–9.

128. Lara-Astiaso D, Weiner A, Lorenzo-Vivas E, Zaretsky I, Jaitin DA, David E, et al. Chromatin state dynamics during blood formation. Science. 2014 Aug 22;345(6199):943–9.

129. Lawrence T, Natoli G. Transcriptional regulation of macrophage polarization: enabling diversity with identity. Nat Rev Immunol. 2011 Nov;11(11):750–61.

130. Lazarenkov A, Sardina JL. Dissecting TET2 Regulatory Networks in Blood Differentiation and Cancer. Cancers. 2022 Feb 6;14(3):830.

131. Li B, Carey M, Workman JL. The Role of Chromatin during Transcription. Cell. 2007 Feb;128(4):707–19.

132. Li E, Bestor TH, Jaenisch R. Targeted mutation of the DNA methyltransferase gene results in embryonic lethality. Cell. 1992 Jun 12;69(6):915–26.

133. Li Z, Cai X, Cai CL, Wang J, Zhang W, Petersen BE, et al. Deletion of Tet2 in mice leads to dysregulated hematopoietic stem cells and subsequent development of myeloid malignancies. Blood. 2011 Oct 27;118(17):4509–18.

134. Liao HK, Hatanaka F, Araoka T, Reddy P, Wu MZ, Sui Y, et al. In Vivo Target Gene Activation via CRISPR/Cas9-Mediated Trans-epigenetic Modulation. Cell. 2017 Dec;171(7):1495-1507.e15.

135. Liao J, Karnik R, Gu H, Ziller MJ, Clement K, Tsankov AM, et al. Targeted disruption of DNMT1, DNMT3A and DNMT3B in human embryonic stem cells. Nat Genet. 2015 May;47(5):469–78.

136. Liao Y, Smyth GK, Shi W. featureCounts: an efficient general purpose program for assigning sequence reads to genomic features. Bioinformatics. 2014 Apr 1;30(7):923–30.

137. Liu R, Zhao E, Yu H, Yuan C, Abbas MN, Cui H. Methylation across the central dogma in health and diseases: new therapeutic strategies. Signal Transduct Target Ther. 2023 Aug 25;8(1):310.

138. Liu XS, Wu H, Ji X, Stelzer Y, Wu X, Czauderna S, et al. Editing DNA Methylation in the Mammalian Genome. Cell. 2016a Sep;167(1):233-247.e17.

139. Liu XS, Wu H, Krzisch M, Wu X, Graef J, Muffat J, et al. Rescue of Fragile X Syndrome Neurons by DNA Methylation Editing of the FMR1 Gene. Cell. 2018a Feb;172(5):979-992.e6.

140. Lopez-Millan B, Rubio-Gayarre A, Vinyoles M, Trincado JL, Fraga MF, Fernandez-Fuentes N, et al. NG2 is a target gene of MLL-AF4 and underlies glucocorticoid resistance in MLL-r B-ALL by regulating NR3C1 expression. Blood J. 2024 Aug 2;blood.2023022050.

141. Love MI, Huber W, Anders S. Moderated estimation of fold change and dispersion for RNA-seq data with DESeq2. Genome Biol. 2014 Dec;15(12):550.

142. Ma RY, Black A, Qian BZ. Macrophage diversity in cancer revisited in the era of single-cell omics. Trends Immunol. 2022 Jul;43(7):546–63.

143. Makarova KS, Wolf YI, Alkhnbashi OS, Costa F, Shah SA, Saunders SJ, et al. An updated evolutionary classification of CRISPR-Cas systems. Nat Rev Microbiol. 2015 Nov;13(11):722–36.

144. Mali P, Yang L, Esvelt KM, Aach J, Guell M, DiCarlo JE, et al. RNA-guided human genome engineering via Cas9. Science. 2013 Feb 15;339(6121):823–6.

145. Marshall JS, Warrington R, Watson W, Kim HL. An introduction to immunology and immunopathology. Allergy Asthma Clin Immunol. 2018 Sep;14(S2):49.

146. Matharu N, Rattanasopha S, Tamura S, Maliskova L, Wang Y, Bernard A, et al. CRISPR-mediated activation of a promoter or enhancer rescues obesity caused by haploinsufficiency. Science. 2019 Jan 18;363(6424):eaau0629.

147. Maunakea AK, Nagarajan RP, Bilenky M, Ballinger TJ, D'Souza C, Fouse SD, et al. Conserved role of intragenic DNA methylation in regulating alternative promoters. Nature. 2010 Jul;466(7303):253–7.

148. Maurano MT, Wang H, John S, Shafer A, Canfield T, Lee K, et al. Role of DNA Methylation in Modulating Transcription Factor Occupancy. Cell Rep. 2015 Aug;12(7):1184–95.

149. Mayer-Barber KD, Andrade BB, Oland SD, Amaral EP, Barber DL, Gonzales J, et al. Host-directed therapy of tuberculosis based on interleukin-1 and type I interferon crosstalk. Nature. 2014 Jul 3;511(7507):99–103.

150. Mayer-Barber KD, Yan B. Clash of the Cytokine Titans: counter-regulation of interleukin-1 and type I interferon-mediated inflammatory responses. Cell Mol Immunol. 2017 Jan;14(1):22–35.

151. McCutcheon SR, Rohm D, Iglesias N, Gersbach CA. Epigenome editing technologies for discovery and medicine. Nat Biotechnol. 2024 Aug;42(8):1199–217.

152. Metchnikoff E. Lectures on the comparative pathology of inflammation delivered at the Pasteur Institute in 1891. Рипол Классик; 1893.

153. Milacic M, Beavers D, Conley P, Gong C, Gillespie M, Griss J, et al. The Reactome Pathway Knowledgebase 2024. Nucleic Acids Res. 2024 Jan 5;52(D1):D672–8.

154. Millán-Zambrano G, Burton A, Bannister AJ, Schneider R. Histone post-translational modifications — cause and consequence of genome function. Nat Rev Genet. 2022 Sep;23(9):563–80.

155. Miller LS, O'Connell RM, Gutierrez MA, Pietras EM, Shahangian A, Gross CE, et al. MyD88 Mediates Neutrophil Recruitment Initiated by IL-1R but Not TLR2 Activation in Immunity against Staphylococcus aureus. Immunity. 2006 Jan;24(1):79–91.

156. Miyanari Y, Ziegler-Birling C, Torres-Padilla ME. Live visualization of chromatin dynamics with fluorescent TALEs. Nat Struct Mol Biol. 2013 Nov;20(11):1321–4.

157. Mojica FJM, Díez-Villaseñor C, García-Martínez J, Almendros C. Short motif sequences determine the targets of the prokaryotic CRISPR defence system. Microbiology. 2009 Mar 1;155(3):733–40.

158. Monk M, Boubelik M, Lehnert S. Temporal and regional changes in DNA methylation in the embryonic, extraembryonic and germ cell lineages during mouse embryo development. Development. 1987 Mar 1;99(3):371–82.

159. Monteagudo-Sánchez A, Richard Albert J, Scarpa M, Noordermeer D, Greenberg MVC. The impact of the embryonic DNA methylation program on CTCF-mediated genome regulation. Nucleic Acids Res. 2024 Aug 24;gkae724.

160. Moradian H, Roch T, Lendlein A, Gossen M. mRNA Transfection-Induced Activation of Primary Human Monocytes and Macrophages: Dependence on Carrier System and Nucleotide Modification. Sci Rep. 2020 Mar 6;10(1):4181.

161. Moran-Crusio K, Reavie L, Shih A, Abdel-Wahab O, Ndiaye-Lobry D, Lobry C, et al. Tet2 loss leads to increased hematopoietic stem cell self-renewal and myeloid transformation. Cancer Cell. 2011 Jul 12;20(1):11–24.

162. Morante-Palacios O, Ciudad L, Micheroli R, de la Calle-Fabregat C, Li T, Barbisan G, et al. Coordinated glucocorticoid receptor and MAFB action induces tolerogenesis and epigenome remodeling in dendritic cells. Nucleic Acids Res. 2022a Jan 11;50(1):108–26.

163. Morante-Palacios O, Godoy-Tena G, Calafell-Segura J, Ciudad L, Martínez-Cáceres EM, Sardina JL, et al. Vitamin C enhances NF-κB-

driven epigenomic reprogramming and boosts the immunogenic properties of dendritic cells. Nucleic Acids Res. 2022b Oct 28;50(19):10981–94.

164. Moreno AM, Alemán F, Catroli GF, Hunt M, Hu M, Dailamy A, et al. Long-lasting analgesia via targeted in situ repression of $Na_V 1.7$ in mice. Sci Transl Med. 2021 Mar 10;13(584):eaay9056.

165. Morita S, Noguchi H, Horii T, Nakabayashi K, Kimura M, Okamura K, et al. Targeted DNA demethylation in vivo using dCas9–peptide repeat and scFv–TET1 catalytic domain fusions. Nat Biotechnol. 2016 Oct;34(10):1060–5.

166. Mosser DM, Hamidzadeh K, Goncalves R. Macrophages and the maintenance of homeostasis. Cell Mol Immunol. 2021 Mar;18(3):579–87.

167. Mosteiro L, Pantoja C, Alcazar N, Marión RM, Chondronasiou D, Rovira M, et al. Tissue damage and senescence provide critical signals for cellular reprogramming in vivo. Science. 2016 Nov 25;354(6315):aaf4445.

168. Mulder K, Patel AA, Kong WT, Piot C, Halitzki E, Dunsmore G, et al. Cross-tissue single-cell landscape of human monocytes and macrophages in health and disease. Immunity. 2021 Aug;54(8):1883-1900.e5.

169. Nakamura M, Gao Y, Dominguez AA, Qi LS. CRISPR technologies for precise epigenome editing. Nat Cell Biol. 2021 Jan;23(1):11–22.

170. Newby GA, Yen JS, Woodard KJ, Mayuranathan T, Lazzarotto CR, Li Y, et al. Base editing of haematopoietic stem cells rescues sickle cell disease in mice. Nature. 2021 Jul 8;595(7866):295–302.

171. Nuñez JK, Chen J, Pommier GC, Cogan JZ, Replogle JM, Adriaens C, et al. Genome-wide programmable transcriptional memory by CRISPR-based epigenome editing. Cell. 2021 Apr 29;184(9):2503-2519.e17.

172. O'Geen H, Bates SL, Carter SS, Nisson KA, Halmai J, Fink KD, et al. Ezh2-dCas9 and KRAB-dCas9 enable engineering of epigenetic memory in a context-dependent manner. Epigenetics Chromatin. 2019 May 3;12(1):26.

173. O'Geen H, Tomkova M, Combs JA, Tilley EK, Segal DJ. Determinants of heritable gene silencing for KRAB-dCas9 + DNMT3 and Ezh2-dCas9 + DNMT3 hit-and-run epigenome editing. Nucleic Acids Res. 2022 Apr 8;50(6):3239–53.

174. Okano M, Bell DW, Haber DA, Li E. DNA Methyltransferases Dnmt3a and Dnmt3b Are Essential for De Novo Methylation and Mammalian Development. Cell. 1999 Oct;99(3):247–57.

175. Ooi SKT, Qiu C, Bernstein E, Li K, Jia D, Yang Z, et al. DNMT3L connects unmethylated lysine 4 of histone H3 to de novo methylation of DNA. Nature. 2007 Aug;448(7154):714–7.

176. Ostrander EL, Kramer AC, Mallaney C, Celik H, Koh WK, Fairchild J, et al. Divergent Effects of Dnmt3a and Tet2 Mutations on Hematopoietic Progenitor Cell Fitness. Stem Cell Rep. 2020 Apr;14(4):551–60.

177. Pachano T, Sánchez-Gaya V, Ealo T, Mariner-Faulí M, Bleckwehl T, Asenjo HG, et al. Orphan CpG islands amplify poised enhancer regulatory activity and determine target gene responsiveness. Nat Genet. 2021 Jul;53(7):1036–49.

178. Park MD, Le Berichel J, Hamon P, Wilk CM, Belabed M, Yatim N, et al. Hematopoietic aging promotes cancer by fueling IL-1α–driven emergency myelopoiesis. Science. 2024 Sep 5;eadn0327.

179. Patel JP, Gönen M, Figueroa ME, Fernandez H, Sun Z, Racevskis J, et al. Prognostic relevance of integrated genetic profiling in acute myeloid leukemia. N Engl J Med. 2012 Mar 22;366(12):1079–89.

180. Perez-Pinera P, Ousterout DG, Brown MT, Gersbach CA. Gene targeting to the ROSA26 locus directed by engineered zinc finger nucleases. Nucleic Acids Res. 2012 Apr;40(8):3741–52.

181. Pflueger C, Tan D, Swain T, Nguyen T, Pflueger J, Nefzger C, et al. A modular dCas9-SunTag DNMT3A epigenome editing system overcomes pervasive off-target activity of direct fusion dCas9-DNMT3A constructs. Genome Res. 2018 Aug;28(8):1193–206.

182. Picard Tools - By Broad Institute. html: (https://broadinstitute.github.io/picard/).

183. Pillai K, Pillai J, Ling J. Analysis of Anakinra Therapy for the Deficiency of Interleukin-1 Receptor Antagonist through Clinical Evidence. J Clin Med. 2024 Feb 10;13(4):1026.

184. Pinho S, Frenette PS. Haematopoietic stem cell activity and interactions with the niche. Nat Rev Mol Cell Biol. 2019 May;20(5):303–20.

185. Plana-Carmona M, Stik G, Bulteau R, Segura-Morales C, Alcázar N, Wyatt CDR, et al. The trophectoderm acts as a niche for the inner cell mass through C/EBPα-regulated IL-6 signaling. Stem Cell Rep. 2022 Sep;17(9):1991–2004.

186. Policarpi C, Dabin J, Hackett JA. Epigenetic editing: Dissecting chromatin function in context. BioEssays. 2021 May;43(5):2000316.

187. Policarpi C, Munafò M, Tsagkris S, Carlini V, Hackett JA. Systematic epigenome editing captures the context-dependent instructive function of chromatin modifications. Nat Genet. 2024 Jun;56(6):1168–80.

188. Polstein LR, Perez-Pinera P, Kocak DD, Vockley CM, Bledsoe P, Song L, et al. Genome-wide specificity of DNA binding, gene regulation, and chromatin remodeling by TALE- and CRISPR/Cas9-based transcriptional activators. Genome Res. 2015 Aug;25(8):1158–69.

189. Prieto C, López-Millán B, Roca-Ho H, Stam RW, Romero-Moya D, Rodríguez-Baena FJ, et al. NG2 antigen is involved in leukemia invasiveness and central nervous system infiltration in MLL-rearranged infant B-ALL. Leukemia. 2018 Mar;32(3):633–44.

190. Prince HM, Bishton MJ, Harrison SJ. Clinical Studies of Histone Deacetylase Inhibitors. Clin Cancer Res. 2009 Jun 15;15(12):3958–69.

191. Pulecio J, Verma N, Mejía-Ramírez E, Huangfu D, Raya A. CRISPR/Cas9-Based Engineering of the Epigenome. Cell Stem Cell. 2017 Oct;21(4):431–47.

192. Qian J, Guan X, Xie B, Xu C, Niu J, Tang X, et al. Multiplex epigenome editing of MECP2 to rescue Rett syndrome neurons. Sci Transl Med. 2023a;.

193. Qian J, Guan X, Xie B, Xu C, Niu J, Tang X, et al. Multiplex epigenome editing of MECP2 to rescue Rett syndrome neurons. Sci Transl Med. 2023b;.

194. Quinlan AR, Hall IM. BEDTools: a flexible suite of utilities for comparing genomic features. Bioinformatics. 2010 Mar 15;26(6):841–2.

195. Ramírez F, Dündar F, Diehl S, Grüning BA, Manke T. deepTools: a flexible platform for exploring deep-sequencing data. Nucleic Acids Res. 2014 Jul 1;42(W1):W187–91.

196. Rapino F, Robles EF, Richter-Larrea JA, Kallin EM, Martinez-Climent JA, Graf T. C/EBPα Induces Highly Efficient Macrophage Transdifferentiation of B Lymphoma and Leukemia Cell Lines and Impairs Their Tumorigenicity. Cell Rep. 2013 Apr;3(4):1153–63.

197. Rasmussen KD, Berest I, Keβler S, Nishimura K, Simón-Carrasco L, Vassiliou GS, et al. TET2 binding to enhancers facilitates transcription factor recruitment in hematopoietic cells. Genome Res. 2019 Apr;29(4):564–75.

198. Reik W, Surani MA. Germline and Pluripotent Stem Cells. Cold Spring Harb Perspect Biol. 2015 Nov;7(11):a019422.

199. Ren R. Mechanisms of BCR–ABL in the pathogenesis of chronic myelogenous leukaemia. Nat Rev Cancer. 2005 Mar;5(3):172–83.

200. Richart L, Picod-Chedotel ML, Wassef M, Macario M, Aflaki S, Salvador MA, et al. XIST loss impairs mammary stem cell differentiation and increases tumorigenicity through Mediator hyperactivation. Cell. 2022 Jun;185(12):2164-2183.e25.

201. Rideout WM, Coetzee GA, Olumi AF, Jones PA. 5-Methylcytosine as an endogenous mutagen in the human LDL receptor and p53 genes. Science. 1990 Sep 14;249(4974):1288–90.

202. Rieger MA, Schroeder T. Hematopoiesis. Cold Spring Harb Perspect Biol. 2012 Dec 1;4(12):a008250.

203. Ritchie ME, Phipson B, Wu D, Hu Y, Law CW, Shi W, et al. limma powers differential expression analyses for RNA-sequencing and microarray studies. Nucleic Acids Res. 2015 Apr 20;43(7):e47–e47.

204. Robb L. Cytokine receptors and hematopoietic differentiation. Oncogene. 2007 Oct 15;26(47):6715–23.

205. Rodriguez RM, Suarez-Alvarez B, Lavín JL, Ascensión AM, Gonzalez M, Lozano JJ, et al. Signal Integration and Transcriptional Regulation of the Inflammatory Response Mediated by the GM-/M-CSF Signaling Axis in Human Monocytes. Cell Rep. 2019 Oct;29(4):860-872.e5.

206. Rohm D, Black JB, McCutcheon SR, Barrera A, Morone DJ, Nuttle X, et al. Activation of the imprinted Prader-Willi Syndrome locus by CRISPR-based epigenome editing [Internet]. 2024 [cited 2024 May 7]. Available from: http://biorxiv.org/lookup/doi/10.1101/2024.03.03.583177

207. Rönnerblad M, Andersson R, Olofsson T, Douagi I, Karimi M, Lehmann S, et al. Analysis of the DNA methylome and transcriptome in granulopoiesis reveals timed changes and dynamic enhancer methylation. Blood. 2014 Apr 24;123(17):e79-89.

208. Roth GV, Gengaro IR, Qi LS. Precision epigenetic editing: Technological advances, enduring challenges, and therapeutic applications. Cell Chem Biol. 2024 Aug;31(8):1422–46.

209. Roy R, Ramamoorthy S, Shapiro BD, Kaileh M, Hernandez D, Sarantopoulou D, et al. DNA methylation signatures reveal that distinct combinations of transcription factors specify human immune cell epigenetic identity. Immunity. 2021 Nov;54(11):2465-2480.e5.

210. Russler-Germain DA, Spencer DH, Young MA, Lamprecht TL, Miller CA, Fulton R, et al. The R882H DNMT3A mutation associated with AML dominantly inhibits wild-type DNMT3A by blocking its ability to form active tetramers. Cancer Cell. 2014 Apr 14;25(4):442–54.

211. Sanin DE, Ge Y, Marinkovic E, Kabat AM, Castoldi A, Caputa G, et al. A common framework of monocyte-derived macrophage activation. Sci Immunol. 2022 Apr 15;7(70):eabl7482.

212. Sanjana NE, Cong L, Zhou Y, Cunniff MM, Feng G, Zhang F. A Transcription Activator-Like Effector (TALE) Toolbox for Genome Engineering. Nat Protoc. 2012 Jan 5;7(1):171–92.

213. Sanson KR, Hanna RE, Hegde M, Donovan KF, Strand C, Sullender ME, et al. Optimized libraries for CRISPR-Cas9 genetic screens with multiple modalities. Nat Commun. 2018 Dec 21;9(1):5416.

214. Sapozhnikov DM, Szyf M. Unraveling the functional role of DNA demethylation at specific promoters by targeted steric blockage of DNA methyltransferase with CRISPR/dCas9. Nat Commun. 2021 Sep 29;12(1):5711.

215. Sardina JL, Collombet S, Tian TV, Gómez A, Di Stefano B, Berenguer C, et al. Transcription Factors Drive Tet2-Mediated Enhancer Demethylation to Reprogram Cell Fate. Cell Stem Cell. 2018 Nov;23(5):727-741.e9.

216. Sasaki H, Matsui Y. Epigenetic events in mammalian germ-cell development: reprogramming and beyond. Nat Rev Genet. 2008 Feb;9(2):129–40.

217. Saunderson EA, Encabo HH, Devis J, Rouault-Pierre K, Piganeau M, Bell CG, et al. CRISPR/dCas9 DNA methylation editing is heritable during human hematopoiesis and shapes immune progeny. Proc Natl Acad Sci. 2023 Aug 22;120(34):e2300224120.

218. Shukla R, Upton KR, Muñoz-Lopez M, Gerhardt DJ, Fisher ME, Nguyen T, et al. Endogenous retrotransposition activates oncogenic

pathways in hepatocellular carcinoma. Cell. 2013 Mar 28;153(1):101–11.

219. Sims JE, March CJ, Cosman D, Widmer MB, MacDonald HR, McMahan CJ, et al. cDNA expression cloning of the IL-1 receptor, a member of the immunoglobulin superfamily. Science. 1988 Jul 29;241(4865):585–9.

220. Spencer DH, Russler-Germain DA, Ketkar S, Helton NM, Lamprecht TL, Fulton RS, et al. CpG Island Hypermethylation Mediated by DNMT3A Is a Consequence of AML Progression. Cell. 2017 Feb 23;168(5):801-816.e13.

221. Stadler MB, Murr R, Burger L, Ivanek R, Lienert F, Schöler A, et al. DNA-binding factors shape the mouse methylome at distal regulatory regions. Nature. 2011 Dec;480(7378):490–5.

222. Stik G, Vidal E, Barrero M, Cuartero S, Vila-Casadesús M, Mendieta-Esteban J, et al. CTCF is dispensable for immune cell transdifferentiation but facilitates an acute inflammatory response. Nat Genet. 2020 Jul;52(7):655–61.

223. Stricker SH, Köferle A, Beck S. From profiles to function in epigenomics. Nat Rev Genet. 2017 Jan;18(1):51–66.

224. Subramanian A, Tamayo P, Mootha VK, Mukherjee S, Ebert BL, Gillette MA, et al. Gene set enrichment analysis: A knowledge-based approach for interpreting genome-wide expression profiles. Proc Natl Acad Sci. 2005 Oct 25;102(43):15545–50.

225. Syrett CM, Sindhava V, Hodawadekar S, Myles A, Liang G, Zhang Y, et al. Loss of Xist RNA from the inactive X during B cell development is restored in a dynamic YY1-dependent two-step process in activated B cells. Chadwick BP, editor. PLOS Genet. 2017 Oct 9;13(10):e1007050.

226. Syrett CM, Sindhava V, Sierra I, Dubin AH, Atchison M, Anguera MC. Diversity of Epigenetic Features of the Inactive X-Chromosome in NK Cells, Dendritic Cells, and Macrophages. Front Immunol. 2019 Jan 8;9:3087.

227. Tahiliani M, Koh KP, Shen Y, Pastor WA, Bandukwala H, Brudno Y, et al. Conversion of 5-methylcytosine to 5-hydroxymethylcytosine in mammalian DNA by MLL partner TET1. Science. 2009 May 15;324(5929):930–5.

228. Tahtinen S, Tong AJ, Himmels P, Oh J, Paler-Martinez A, Kim L, et al. IL-1 and IL-1ra are key regulators of the inflammatory response to RNA vaccines. Nat Immunol. 2022 Apr;23(4):532–42.

229. Takahashi K, Yamanaka S. Induction of Pluripotent Stem Cells from Mouse Embryonic and Adult Fibroblast Cultures by Defined Factors. Cell. 2006 Aug;126(4):663–76.

230. Tanenbaum ME, Gilbert LA, Qi LS, Weissman JS, Vale RD. A protein tagging system for signal amplification in gene expression and fluorescence imaging. Cell. 2014 Oct 23;159(3):635–46.

231. Tarjan DR, Flavahan WA, Bernstein BE. Epigenome editing strategies for the functional annotation of CTCF insulators. Nat Commun. 2019 Sep 18;10(1):4258.

232. Tejedor JR, Bueno C, Vinyoles M, Petazzi P, Agraz-Doblas A, Cobo I, et al. Integrative methylome-transcriptome analysis unravels cancer cell vulnerabilities in infant MLL-rearranged B cell acute lymphoblastic leukemia. J Clin Invest. 2021 Jul 1;131(13):e138833.

233. Tejedor JR, Peñarroya A, Gancedo-Verdejo J, Santamarina-Ojeda P, Pérez RF, López-Tamargo S, et al. CRISPR/dCAS9-mediated DNA demethylation screen identifies functional epigenetic

determinants of colorectal cancer. Clin Epigenetics. 2023 Aug 24;15(1):133.

234. Thakore PI, Kwon JB, Nelson CE, Rouse DC, Gemberling MP, Oliver ML, et al. RNA-guided transcriptional silencing in vivo with S. aureus CRISPR-Cas9 repressors. Nat Commun. 2018 Apr 26;9(1):1674.

235. The ENCODE Project Consortium. An integrated encyclopedia of DNA elements in the human genome. Nature. 2012 Sep;489(7414):57–74.

236. Toyota M, Kopecky KJ, Toyota MO, Jair KW, Willman CL, Issa JP. Methylation profiling in acute myeloid leukemia. Blood. 2001 May 1;97(9):2823–9.

237. Tulstrup M, Soerensen M, Hansen JW, Gillberg L, Needhamsen M, Kaastrup K, et al. TET2 mutations are associated with hypermethylation at key regulatory enhancers in normal and malignant hematopoiesis. Nat Commun. 2021 Oct 18;12(1):6061.

238. Vavouri T, Lehner B. Human genes with CpG island promoters have a distinct transcription-associated chromatin organization. Genome Biol. 2012;13(11):R110.

239. Vento-Tormo R, Álvarez-Errico D, Garcia-Gomez A, Hernández-Rodríguez J, Buján S, Basagaña M, et al. DNA demethylation of inflammasome-associated genes is enhanced in patients with cryopyrin-associated periodic syndromes. J Allergy Clin Immunol. 2017 Jan;139(1):202-211.e6.

240. Villaseñor R, Baubec T. Regulatory mechanisms governing chromatin organization and function. Curr Opin Cell Biol. 2021 Jun;70:10–7.

241. Villatoro A, Cuminetti V, Bernal A, Torroja C, Cossío I, Benguría A, et al. Endogenous IL-1 receptor antagonist restricts healthy and malignant myeloproliferation. Nat Commun. 2023 Jan 3;14(1):12.

242. Villiger L, Joung J, Koblan L, Weissman J, Abudayyeh OO, Gootenberg JS. CRISPR technologies for genome, epigenome and transcriptome editing. Nat Rev Mol Cell Biol. 2024a Feb 2;1–24.

243. Vivier E, Malissen B. Innate and adaptive immunity: specificities and signaling hierarchies revisited. Nat Immunol. 2005 Jan 1;6(1):17–21.

244. Waddington CH. The epigenotype. 1942. Int J Epidemiol. 2012 Feb;41(1):10–3.

245. Walsh CP, Chaillet JR, Bestor TH. Transcription of IAP endogenous retroviruses is constrained by cytosine methylation. Nat Genet. 1998 Oct;20(2):116–7.

246. Wang J, Syrett CM, Kramer MC, Basu A, Atchison ML, Anguera MC. Unusual maintenance of X chromosome inactivation predisposes female lymphocytes for increased expression from the inactive X. Proc Natl Acad Sci [Internet]. 2016 Apr 5 [cited 2024 Jul 2];113(14). Available from: https://pnas.org/doi/full/10.1073/pnas.1520113113

247. Wang L, Ozark PA, Smith ER, Zhao Z, Marshall SA, Rendleman EJ, et al. TET2 coactivates gene expression through demethylation of enhancers. Sci Adv. 2018 Nov 2;4(11):eaau6986.

248. Wang S. Targeting M2-like tumor-associated macrophages is a potential therapeutic approach to overcome antitumor drug resistance. Npj Precis Oncol. 2024;

249. Wculek SK, Heras-Murillo I, Mastrangelo A, Mañanes D, Galán M, Miguel V, et al. Oxidative phosphorylation selectively orchestrates

tissue macrophage homeostasis. Immunity. 2023 Mar 14;56(3):516-530.e9.

250. Weinhäuser I, Pereira-Martins DA, Almeida LY, Hilberink JR, Silveira DRA, Quek L, et al. M2 macrophages drive leukemic transformation by imposing resistance to phagocytosis and improving mitochondrial metabolism. Sci Adv. 2023 Apr 14;9(15):eadf8522.

251. Wienholz BL, Kareta MS, Moarefi AH, Gordon CA, Ginno PA, Chédin F. DNMT3L modulates significant and distinct flanking sequence preference for DNA methylation by DNMT3A and DNMT3B in vivo. PLoS Genet. 2010 Sep 9;6(9):e1001106.

252. Wu X, Zhang Y. TET-mediated active DNA demethylation: mechanism, function and beyond. Nat Rev Genet. 2017 Sep;18(9):517–34.

253. Xie H, Ye M, Feng R, Graf T. Stepwise Reprogramming of B Cells into Macrophages.

254. Xie M, Lu C, Wang J, McLellan MD, Johnson KJ, Wendl MC, et al. Age-related mutations associated with clonal hematopoietic expansion and malignancies. Nat Med. 2014 Dec;20(12):1472–8.

255. Xu X, Tao Y, Gao X, Zhang L, Li X, Zou W, et al. A CRISPR-based approach for targeted DNA demethylation. Cell Discov. 2016 May 3;2(1):16009.

256. Yang L, Rodriguez B, Mayle A, Park HJ, Lin X, Luo M, et al. DNMT3A Loss Drives Enhancer Hypomethylation in FLT3-ITD-Associated Leukemias. Cancer Cell. 2016 Jun 13;29(6):922–34.

257. Yildirim E, Kirby JE, Brown DE, Mercier FE, Sadreyev RI, Scadden DT, et al. Xist RNA Is a Potent Suppressor of Hematologic Cancer in Mice. Cell. 2013 Feb;152(4):727–42.

258. Yin Y, Morgunova E, Jolma A, Kaasinen E, Sahu B, Khund-Sayeed S, et al. Impact of cytosine methylation on DNA binding specificities of human transcription factors. Science. 2017 May 5;356(6337):eaaj2239.

259. Yu G, Wang LG, Han Y, He QY. clusterProfiler: an R Package for Comparing Biological Themes Among Gene Clusters. OMICS J Integr Biol. 2012 May;16(5):284–7.

260. Yu G, Wang LG, He QY. ChIPseeker: an R/Bioconductor package for ChIP peak annotation, comparison and visualization. Bioinformatics. 2015 Jul 15;31(14):2382–3.

261. Zetsche B, Gootenberg JS, Abudayyeh OO, Slaymaker IM, Makarova KS, Essletzbichler P, et al. Cpf1 is a single RNA-guided endonuclease of a class 2 CRISPR-Cas system. Cell. 2015 Oct 22;163(3):759–71.

262. Zhang B, Ho YW, Huang Q, Maeda T, Lin A, Lee S uk, et al. Altered Microenvironmental Regulation of Leukemic and Normal Stem Cells in Chronic Myelogenous Leukemia. Cancer Cell. 2012 Apr;21(4):577–92.

263. Zhang DE, Zhang P, Wang ND, Hetherington CJ, Darlington GJ, Tenen DG. Absence of granulocyte colony-stimulating factor signaling and neutrophil development in CCAAT enhancer binding protein ␣-deficient mice. Proc Natl Acad Sci USA. 1997;

264. Zhang P, Iwasaki-Arai J, Iwasaki H, Fenyus ML, Dayaram T, Owens BM, et al. Enhancement of hematopoietic stem cell repopulating capacity and self-renewal in the absence of the transcription factor C/EBP alpha. Immunity. 2004 Dec;21(6):853–63.

265. Zhang Y, Jurkowska R, Soeroes S, Rajavelu A, Dhayalan A, Bock I, et al. Chromatin methylation activity of Dnmt3a and Dnmt3a/3L is guided by interaction of the ADD domain with the histone H3 tail. Nucleic Acids Res. 2010 Jul;38(13):4246–53.

266. Zhang Y, Liu T, Meyer CA, Eeckhoute J, Johnson DS, Bernstein BE, et al. Model-based Analysis of ChIP-Seq (MACS). Genome Biol. 2008 Nov;9(9):R137.

267. Zhang YW, Wang Z, Xie W, Cai Y, Xia L, Easwaran H, et al. Acetylation Enhances TET2 Function in Protecting against Abnormal DNA Methylation during Oxidative Stress. Mol Cell. 2017 Jan 19;65(2):323–35.